

GOODYEAR AEROSPACE CORPORATION

AKRON 15, OHIO

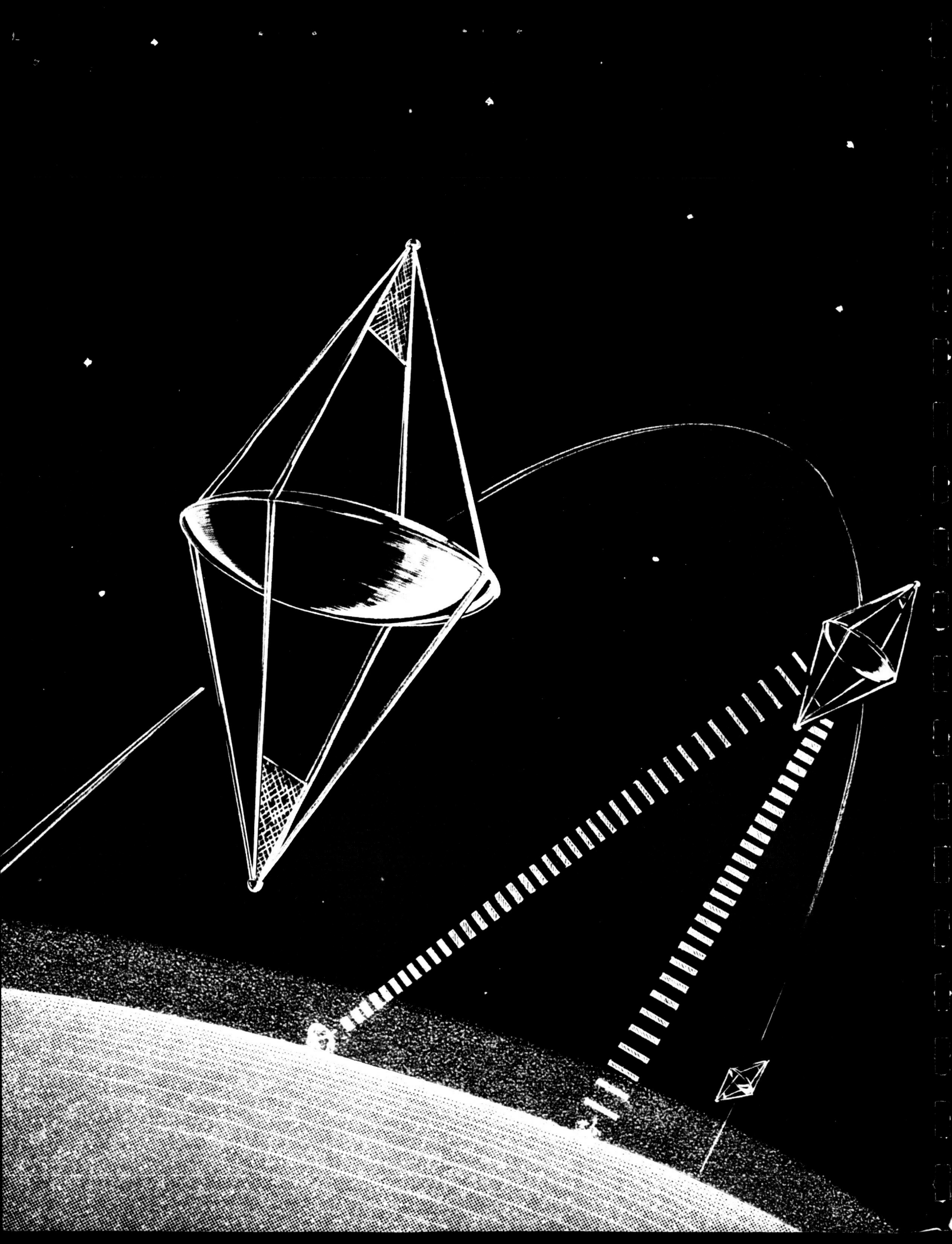
STUDY OF A PASSIVE COMMUNICATION,
GRAVITY-GRADIENT STABILIZED,
LENTICULAR SATELLITE

Interim Summary Report

GER 11893

January 1965

National Aeronautics and Space Administration
Langley Research Center
Langley Station, Hampton, Virginia



ABSTRACT

GER 11893

The feasibility of applying orbit position control and station-keeping to a gravity-gradient stabilized, lenticular, passive communications satellite has been demonstrated. The satellite mobility is realized by the action of direct solar pressure and thermal reradiation forces on surfaces having different optical characteristics. Several methods for rotating the satellite to align the proper surface with respect to the sun were evaluated.

FOREWORD

This report summarizes the preliminary design and feasibility studies conducted by Goodyear Aerospace Corporation (GAC) of a gravity gradient stabilized lenticular satellite with station keeping capability for use in a passive communication satellite system. These studies were conducted on Contract NAS 1-3114 from July 1963 through December 1964. The technical objectives and contract requirements were changed by various amendments during this period to broaden the study scope in technical problem areas and recommend new R and D efforts. Documents for the minute technical details in the specialty areas are referenced in this report.

The work was administered by the Applied Materials and Physics Division of LRC with Mr. D. C. Grana from the Spacecraft Applications Section acting as project engineer assisted by Mr. J. Humble of the Flight Vehicles and Systems Division, Spacecraft Structures Section. F. J. Stimler of the Space Systems Division was the GAC project engineer, with H. E. Henjum associate project engineer. The work was conducted as a cooperative effort by personnel from several divisions within GAC for the various specialties listed below:

| | |
|-------------------------------|---|
| Design | R. R. Carman and H. W. Barrett |
| Materials Development | R. W. Nordlie and W. B. Cross |
| Orientation and Stabilization | A. C. Buxton, D. E. Campbell, and K. Losch |
| Structural Analysis | E. Rottmayer and J. D. Marketos |
| Fabrication | D. R. Thompson |
| Planning | J. B. Boughton |
| Contract Administration | A. F. Tinker |

A companion study, under the administration of AMPD of LRC with Mr. John E. Cooper from the Space Vehicle Branch as project engineer (NAS 1-3131), was conducted by Aerospace Division of Westinghouse Electric Corporation, Baltimore, Maryland with Mr. Sid J. Worley as project engineer. Technical review meetings were conducted by NASA-LRC, Good-year Aerospace (Amendment 6), and Westinghouse (Amendment 2) during the period of July through December 1964. The cooperation experienced and the coordination of these two programs proved beneficial, clarifying mutual objectives and expediting understanding of the technical problems.

TABLE OF CONTENTS

| Section | | Page |
|---------|---|------|
| | FOREWORD | iii |
| I | INTRODUCTION | 1 |
| II | TECHNICAL DISCUSSION | 3 |
| | A. Design Considerations | 3 |
| | 1. Preliminary Lenticular Satellite Configuration | 3 |
| | 2. Lenticular Satellite with Solar Sailing | 5 |
| | 3. Solar Sail Configurations | 7 |
| | 4. Materials Considerations | 8 |
| | 5. Satellite Depressurization System | 14 |
| | 6. RF Performance Review | 15 |
| | 7. Summary | 18 |
| | B. Orientation and Stabilization | 19 |
| | 1. General Requirements | 19 |
| | 2. Initial Gravity Gradient Capture | 22 |
| | 3. Gravity Gradient Damping | 27 |
| | 4. Yaw Control Methods | 30 |
| | C. Structural Analysis. | 34 |
| | 1. General | 34 |
| | 2. Asymmetrical Configuration Study | 34 |
| | 3. Preliminary Loads. | 35 |
| | 4. Yaw Control | 36 |
| | 5. Tumbling | 37 |
| | 6. Structural Damping | 37 |
| | 7. Deployment | 38 |
| | 8. Weight Study. | 39 |
| | 9. Summary | 40 |
| III | CONCLUSIONS AND RECOMMENDATIONS | 41 |
| | REFERENCES. | 43 |
| | TABLES | 45 |
| | ILLUSTRATIONS. | 55 |

LIST OF TABLES

| Table | | Page |
|-------|--|------|
| I | Satellite Evaluation Summary | 45 |
| II | Summary of Film-Wire Mesh Properties | 46 |
| III | Calculated Thermal Radiation Properties for Photo- lyzable Film | 47 |
| IV | Satellite Depressurization System Data | 48 |
| V | Initial Pitch Tumbling Impulses, Ft-Lb-Sec | 49 |
| VI | Comparison of Three Types of Gravity Gradient Dampers | 50 |
| VII | Comparison of Yaw Control Methods | 51 |
| VIII | Tetrapod Boom Loads | 52 |
| IX | Weight-Saving Study | 53 |

LIST OF ILLUSTRATIONS

| Figure | | Page |
|--------|---|------|
| 1 | Design Summary of Preliminary Lenticular Satellite | 55 |
| 2 | Passive Communication Satellite Evolution | 56 |
| 3 | Lenticular Satellite Development Program - NAS 1-3114 . . | 57 |
| 4 | General Arrangement of Preliminary Lenticular Satellite . . | 58 |
| 5 | Collapsible Rim Functional Schematic | 60 |
| 6 | Packaging Sequence of Lenticular Satellite | 61 |
| 7 | Deployment Sequence of Lenticular Satellite | 62 |
| 8 | Deployment Sequence for Model 20-1 Vacuum Sphere Tests | 63 |
| 9 | Design Definition Alternatives | 64 |
| 10 | Base Line Asymmetrical Configuration | 65 |
| 11 | Base Line Symmetrical Configuration | 67 |
| 12 | Basic Lenticular Satellite Lens, Torus, and Rim Data . . . | 69 |
| 13 | Deployment Sequence of Base Line Asymmetrical Configuration | 70 |
| 14 | Deployment Sequence of Base Line Symmetrical Configuration | 71 |
| 15 | Sail Configuration for Lenticular Satellite | 72 |
| 16 | Effect of Temperature on Weight Loss Behavior of Clear Photolyzable Film | 73 |
| 17 | Effect of Type SP Dye on Weight Loss Behavior of Photolyzable Film | 74 |
| 18 | Boom Radar Return versus Angle of Incidence to Boom . . . | 75 |
| 19 | Proposed Configuration of Gravity Gradient Solar Sailing Communication Satellite | 76 |

| Figure | | Page |
|--------|--|------|
| 20 | Pitch Axis Phase Plane - Case A | 77 |
| 21 | Pitch Axis Phase Plane - Case B | 78 |
| 22 | Natural Frequencies versus Inertia Ratios | 79 |
| 23 | Lensat Transient Attitude Response Using Rice/Wilberforce Damper | 80 |
| 24 | Lensat Transient Attitude Response Using Ames Damper - Lens Film Photolyzed | 82 |
| 25 | Lensat Transient Attitude Response Using Amers Damper - Lens Film Not Photolyzed | 83 |
| 26 | Envelopes of Lensat Transient Attitude Response Using Hypenik 50/50 Magnetic Material Damping | 84 |
| 27 | Three-Mode Reaction Wheel and Movable Weights | 85 |
| 28 | Continuous Yaw Control | 86 |
| 29 | Geometry of Asymmetrical Configuration | 87 |
| 30 | Design Parameters for Moment of Inertia Ratio of 6 | 88 |
| 31 | Weight versus Angle of Twist of the Tetrapod | 89 |
| 32 | Geometry of Symmetrical Configuration Shown for Tumbling Calculations. | 90 |
| 33 | Tumbling - Loads on Yaw Boom versus Tumble Angle | 91 |
| 34 | Tumbling Loads at Apex | 92 |
| 35 | Stress and Strain Energy per Unit Volume versus Strain per 5.0 Mil Aluminum Wire | 93 |
| 36 | Separation-to-Return Velocity versus Stress Level in Axial Aluminum Wires of Tetrapod Booms of a Symmetric Satellite | 94 |
| 37 | Weight Trade-Off | 95 |
| 38 | Recommended Configurations | 96 |

SECTION I. INTRODUCTION

Goodyear Aerospace Corporation conducted several preliminary design and feasibility studies of a gravity gradient stabilized lenticular satellite (Figure 1) for the NASA-Langley Research Center (LRC) under Contract NAS 1-3114. Application of solar sailing to the lenticular satellite for station keeping purposes was also investigated.

The expandable satellite is packaged in a canister during payload ascent and orbital placement. During satellite deployment and inflation the canister halves and attached hardware are extended by inflatable booms and serve as fixed weights for the gravity gradient stabilization system. The torus serves as a deployment mechanism for the rim and lens caps, and also provides system stiffness while the lens caps become rigidized through controlled yielding of the photolyzable film/wire grid surfaces. The rim serves as the attachment point for the two lens caps. The damping system is attached to the space-side canister half. The earth-side canister half provides the mounting interface of the inflation system and the electronic controls. Once operational, the torus and lens film surfaces disappear through photolysis action.

The evolution of the passive communication satellite is shown schematically in Figure 2. The Echo I sphere, because of light weight and simplicity, had a distinct advantage for early tests of this type. Echo II represented an improvement over Echo I, in that the surface could be rigidized through proper pressurization and choice of proper laminate materials. Early mobility studies on spherical shapes indicated the feasibility of utilizing solar sailing for station keeping of satellites in a passive communications system. The use of the lenticular satellite shape was advantageous because a larger lens

was possible through the use of simple gravity gradient stabilization techniques within the weights realized by a similar rf reflecting sphere.

This report summarizes the over-all lenticular satellite development studies performed on this contract from July 1963 through December 1964. Figure 3 shows the various phases of the contract, their periods of performance, and the documentation. Technical data not included here can be obtained from the documents referenced in Figure 3.

Major items considered during the design studies of the satellite were stabilization and orientation systems, including damping methods; satellite deployment; satellite rf reflectivity characteristics; packaging methods; design tolerances; fabrication techniques; and the effects of perturbing forces on satellite performance. The early emphasis was placed on analysis of the Rice/Wilberforce damping system and the use of the wire mesh-photolyzable film materials in the construction of the satellite lens and related components. Incorporation of solar sailing into the lenticular configurations was investigated, based on early designs generated on this contract, to determine the best and most efficient means of solar sailing a passive lenticular satellite which had gravity gradient stabilization.

Study results have shown that the gravity gradient stabilized lenticular satellite is a feasible concept and could fulfill most of the passive satellite communication requirements.

SECTION II. TECHNICAL DISCUSSION

A. DESIGN CONSIDERATIONS

1. Preliminary Lenticular Satellite Configuration

The design summary and general arrangement of the preliminary lenticular satellite configuration are shown in Figures 1 and 4. The evolution of this configuration is described in Reference 2. The main parts of the satellite are the canister, the tripod booms, the torus, the metal rim, and the rf reflecting lens. The two spherical segments that make up the rf lens are interconnected through a metal rim of collapsible cross section as shown in Figure 5.

The lenticular lens surfaces are fabricated of 0.5-mil photolyzable film cast on a 1-mil copper wire plain weave mesh (21 wires per inch). The rim is made of 2-mil beryllium copper with two hinge joints 180 degrees apart to permit proper packaging of the system. The effective lenticular lens and rim material are encircled by a torus, which assists in unfurling the packaged lens surfaces. Two masses, one on each side of the lenticular shape, are supported at the apexes of the booms. These masses are used as gravity gradient weights. They consist of the packaging canister halves and fixed equipment such as the inflation system, damping system, and control and electronics elements.

To package the system effectively the rim cross section is flattened and then coiled around a drum. The important consideration is not to exceed the proportional limit of the material with the stresses imposed by flattening and coiling and deployment of the system, so that the structural section will be reestablished after deployment. The rim also provides the structural

attachments for the booms that support the gravity gradient masses. The metal rim makes it necessary to roll up the collapsed lens and torus surfaces as shown in Figure 6 during the initial phase of packaging rather than to use a conventional accordion fold. Model deployment tests under ambient and vacuum chamber conditions have shown that this packaging method is acceptable.

The inflatable elements of the satellite are packaged in a spherical canister which at deployment separates at its equator. A screen-type liner is spaced off the inner surface to permit passage of entrapped air to an evacuation valve. This valve is used for initial pump-down of the canister and is solenoid-controlled to be opened at orbital altitude to stabilize pressures prior to deployment. Details of the deployment sequence are discussed in Reference 7. The five key areas considered in the deployment sequence studies are as follows:

- (1) Start of canister separation
- (2) Satellite stretch
- (3) Torus and boom inflated, lens loose
- (4) Satellite completely inflated
- (5) Satellite operational

The deployment times chosen for these key positions were obtained from early studies conducted and reported in Reference 2. The torus is maintained under a relatively high pressure to support the erection loads that are imposed during pressure yielding of the lens surfaces. The torus has a series of compartments interconnected by sized orifices so that its cells will inflate in sequence to control the deployment of the over-all system as depicted in Figure 7 and to prevent buckling of the metal rim. Torus inflation to design pressures is completed in five minutes and is followed by lens inflation in another five-minute period. Rigidization of the lens starts at this time. The lens is maintained at design pressure for two minutes and the torus for four minutes during the rigidization process. Automatic pressure

relief is accomplished through evenly distributed holes that are provided in the torus and lens surfaces to minimize destabilizing moments that might result from uneven gas discharge. Sufficient helium gas is provided to allow for leakage through the depressurization holes during the inflation period and through punctures that might occur from micrometeoroids.

Structural analyses of the static and dynamic conditions indicate that no major problem areas should be encountered utilizing available materials and proven fabrication techniques for development of a lenticular satellite system. The analysis indicates that the lens radius of curvature can be held to within \pm one percent, particularly if manufacturing tolerances and lens pressures are given careful attention. The tolerance problem will be alleviated as more models are constructed and representative test data assembled for the materials under consideration.

Preliminary deployment tests (Figure 8) within the LRC vacuum sphere have shown that the method of packaging and deployment under consideration for the lenticular satellite is satisfactory.

Although initial capture can be accomplished by the gravity gradient stabilization method, several means of damping were available for consideration. These will be discussed in the "Orientation and Stabilization" (subsection B). The Rice/Wilberforce damper, depicted schematically in Figure 4, was shown to be satisfactory for this satellite under transient and steady state conditions studied in the early analyses. Damper energy is dissipated both in the spring coating during the linear action of the spring and in the viscous damper at the end of the spring through spring rotation occurring from cross coupling motions.

2. Lenticular Satellite with Solar Sailing

Studies were conducted to adapt the lenticular satellite configuration to station keeping through the use of solar sailing techniques. (Satellite mobility data is documented in Reference 8.) The general design definition

alternatives to be considered in a satellite of this type are shown in Figure 9. Weight and geometric data on the base line asymmetrical and base line symmetrical configurations are given in Figures 10 and 11 respectively. The weights of the structure and components represent state-of-the-art and best design techniques at the present time.

Major consideration was given to the areas of configuration definition, stabilization, and yaw control as concerns the station keeping aspects. The items of electronics and power supply are offered as information only at this time. Early investigations of satellites with station keeping capabilities concentrated on the asymmetrical configuration with a flat solar sail. The torus, rim, and lens configuration of the preliminary lenticular satellite studies was used as the base line for the satellite design. As shown in Figure 12, it became advisable to utilize a tetrapod boom system rather than the tripod of past configurations to enhance implementation of the solar sail. All asymmetrical and symmetrical configurations considered in this satellite study utilized the basic information shown in Figure 12, and varied only the size of the booms and fixed weights to arrive at proper moment of inertia ratios to effect gravity gradient stabilization. Corresponding structural and dynamic studies were made of each promising configuration to pinpoint major problem areas and to direct designs toward an optimum configuration. Figures 13 and 14 show the deployment sequence of a base line asymmetrical configuration and a symmetrical configuration to show moment of inertia variation against deployment for various key positions of the satellite structure. The general characteristics of these base line configurations are evaluated with respect to the preliminary lenticular satellite configuration studies in Table I. The spring mass, articulated booms, and hysteresis techniques listed in Figure 9 have the most merit for this application.

Several methods of yaw control are available for positioning of the sail, either through automatic oscillation about the yaw axis of the satellite or by

controlling the yaw angle through choice of moment of inertia ratios suitable for gravity gradient control. The advantages and disadvantages of the magnetic coil, reaction wheel, and inertia distribution methods of yaw control are discussed later in this report from the aspects of both stabilization and structural effects.

3. Solar Sail Configurations

Figure 15 summarizes the various sail configurations under consideration for the lenticular satellites during this program, based on the mobility and optical characteristic requirements established. Forces and moments encountered during the deployment and transient operational conditions of the orbit indicate that the best method for solar sailing an asymmetrical configuration is through the use of a flat sail with the lenticular lens (Figure 15, sketch A) utilizing photolyzable film-mesh materials. Several methods can readily be utilized for the symmetrical configuration, because of its more predictable deployment and capture characteristics during the early operational life of the satellite. The use of an opaque material for the lens (sketch B) for solar sailing aspects seems to have merit, except that the high yaw moment of inertia affects the over-all stabilization performance of the structure. In the event smaller sail area is required to achieve satisfactory mobility, it may be advisable to coat the booms (sketch C) to provide sufficient sail area. Additional design study must be conducted on this concept to minimize the temperature problems that might be encountered. Preliminary design studies indicate that use of the sail inside of the lens (sketches D and E) presents problems that make it impractical because of strains either at the rim or on the lens surface. These strains are not compatible with the present concept of lens rigidization for the lenticular satellite. The use of the flat sail top and bottom of the symmetrical configuration (sketch F) seems to have merit. The effects of this sail configuration on the rf performance of the satellite certainly must be considered. A new concept which has just been investigated is the possibility of coating the actual wires in the mesh

(sketch G) so that proper optical characteristics can be obtained for both the wire in the booms and in the lens surface. This coated wire concept should be considered new and not state-of-the-art because it is in the advanced research stage at the present time and much more test data and fabrication data must be obtained prior to use in any detail design.

Methods of attaching a solar sail to the structure are within the state-of-the-art of fabrication techniques for packageable and inflatable structures. Attachment of concentrated and distributed loads to supposedly flimsy and foldable structures is amenable to structural analysis and the techniques have been utilized for many years in areas of airship and balloon fabrication.

4. Materials Considerations

- a. General. Several types of structural and coating materials are used in the lenticular satellite. The following paragraphs briefly discuss the materials selected for each of the main components of the satellite.

- b. Lens.

- (1) Film-Wire Composite. The lens material consists of a plastic film to which a system of interwoven wires has been added. The general requirements are that the film have sufficient mechanical strength to serve as an inflation bladder and that the wire mesh have sufficient buckling strength after yielding to maintain shape. Wire diameter and spacing must also be selected on the basis of microwave reflectance requirements.

In most of the lenticular satellite designs it has been found desirable to have the film "disappear" after deployment and inflation. To provide this characteristic, The Goodyear Tire and Rubber Company Research Division has developed a photolyzable film which has the desirable property of undergoing photodegradation and evaporation when exposed to outer space sunlight and vacuum.

Detailed studies have been made in the areas of mesh weaving,

film-wire composite fabrication, film-wire seaming techniques, and photolyzable film weight loss behavior. This work is reported in References 1, 9, 10, 11, and 12.

Many types of wire and film-wire combinations were examined as part of the lens material development effort (Reference 1). The combination that has been investigated to a greater degree than others is 0.7-mil photolyzable film cast on 24 x 24 mesh, 1.6-mil phosphor bronze wire cloth. A summary of tensile properties of this and other film-wire combinations appears in Table II.

Improvements in the present lens material should be possible with continued development. Reductions in composite weight are desirable and may be accomplished with improvements in weaving and woven mesh handling techniques. Reductions in film thickness may be possible. Development of a 0.5-mil photolyzable film cast on a 1-mil copper wire plain weave mesh (21 wires per inch) has presently not been undertaken.

- (2) Photolyzable Film Weight Loss Behavior. Film removal characteristics are best determined by simulated space testing. Considerable work has been done to establish suitable experimental techniques and to obtain quantitative behavior information. Data obtained from these tests has demonstrated the feasibility of the photolyzable film concept. At present, studies have been limited to only one type of photodegradable polymer system. The work conducted thus far has been directed toward supplying much-needed behavior data for satellite design purposes. A more basic materials development program is desirable and would lead to broader understanding of the phenomenon involved.

Details of the experimental techniques used and results obtained are found in References 9, 10, and 13. Typical weight loss behavior characteristics of the film are shown in Figure 16.

- (3) Modification of Film Solar Absorptance (α_s) Properties. As can be seen from Figure 16, film temperatures of approximately 225°F are required for reasonable film photolyzation. Since the basic photolyzable polymer is highly transparent, skin temperatures of a satellite made from this clear film material would not approach the desired temperature. Thus, to achieve the correct skin temperature, the film must be colored to provide the proper solar absorptance (α_s) and infrared emittance (ϵ) characteristics.

Various experimental investigations have shown that the material α_s/ϵ properties can be modified over a broad range. This has been accomplished by incorporating small quantities of dye.

Studies have shown that two to three parts of dye per 100 parts of photolyzable polymer by weight will provide the required change in solar absorptance (α_s). Dye additions do not greatly affect infrared emittance (ϵ). Typical thermal radiation properties of clear and dyed photolyzable film are listed in Table III.

Incorporating dyes tends to reduce photolyzation rate. This behavior is demonstrated in Figure 17. The reduction in rate, however, is not considered to have a significant effect on the basic deployment-film removal concept.

- (4) Seams. A substantial development effort has been conducted on seams applicable to the lenticular satellite lens material. Details of this work are reported in References 1, 11 and 12.

In general, two types of seaming methods have been studied: adhesive and metal-joined. Adhesive type seams make use of various commercial tapes of the heated-activated and pressure-

sensitive types. These seams are the easiest to construct and have been studied in greater detail than the metal-joined seams.

Metal-joined seams are in the exploratory stage. Basically, resistance welding and soldering of foil to the wire have been examined. Although some success has been obtained, additional work will be required to fully evaluate these methods.

At present, adhesive-backed tapes appear to be the best choice, since they are easily applied without elaborate equipment and are commercially available.

- c. Torus. It is desirable that the torus of the lenticular satellite "disappear" after deployment has been completed. Ideally the torus would be constructed of a high strength photolyzable film so that it would evaporate much like the lens material.

Development of a suitable high strength photolyzable film has not been undertaken to date. Development of a new high strength film may be possible, or it may be possible to meet strength requirements by incorporating a non-microwave reflective Dacron or fiberglass scrim into the available low strength photolyzable film.

- d. Beryllium Copper Rim. The optical characteristics of the rim will be adjusted to ensure that temperature of the rim does not exceed proper limits. Conventional pigmented coating systems are considered satisfactory for this application.
- e. Booms. Booms on the lenticular satellite will be constructed of fine wire bonded to photolyzable film. The photolyzable film will act as an inflation bladder during deployment. After the booms are rigidized, the film will photolyze in the same manner as the lens material. Aside from special tooling for fabrication, the basic materials problems are the same as for the lens.

- f. Solar Sail. The lenticular satellite solar sail material is envisioned as a thin lightweight plastic film, such as 0.25-mil Mylar, coated on each side to provide the desired optical properties. It has been established (Reference 7) that to obtain efficient momentum transfer from solar electromagnetic energy, the sail must have the following minimum optical properties:

Side No. 1

Solar Reflectance (r_1) = 0.8 (Diffuse)

Infrared Emittance (ϵ_1) = 0.8

Side No. 2

Solar Reflectance (r_2) = 0.1

Infrared Emittance (ϵ_2) = 0.2

Most pigment-binder type thermal control coatings must be applied in thicknesses of one mil or more and may have questionable long-life stability of their optical properties (Reference 14). Vapor deposited inorganic materials appear to have the most promising physical characteristics for this application. The Echo I satellite utilized this approach with a nominal 2200 Å vapor deposit of aluminum on 1/2-mil Mylar. Based on results in Reference 4, this surface is proving very stable in a space environment. The solar absorptance and emittance of such metal surfaces can be altered by coatings of thin nonabsorptive homogeneous dielectric materials (References 15, 16, and 17).

The reflectivity of these vapor deposits is basically specular. The reflectance of these metals can be reduced (absorptance increased) to approximately 0.1 by alternate coatings of aluminum with SiO₂ to produce what is basically a graded dielectric absorber or interference filter. The emissivity of these materials can also be increased by coating with SiO₂. Flexible coatings in the micron thickness range

can be applied which, depending on thickness, can increase the emissivity up to about 0.7. Tests related to solar concentrator applications indicate that this material should be quite stable in a space environment. Other flexible coatings, such as metal phosphates, can be utilized if the specular reflective characteristics are not required.

While the infrared emissivity cannot be varied completely independent of the solar reflectivity, careful selection of materials should allow independent selection of emissivities from less than 0.1 up to 0.7 and solar absorptance from 0.1 to about 0.9. The vapor deposit process coats only one side of the material so a selection of absorptivity and emissivity on either side of the sail is available.

A limited number of samples of sail material have been fabricated and the actual weight and optical properties of these samples have been determined. Vacuum deposited multilayer coatings were applied to each side of a 0.25-mil Mylar substrate. Low solar reflectance and low infrared emittance properties were obtained through the application of a "dark mirror" coating of Al-SiO-Al-SiO to one side. On the other side high reflectance was obtained by the deposition of aluminum. An attempt was made to increase the emittance without loss of reflectance by overcoating the aluminum with SiO. However, samples prepared did not have sufficient thickness of SiO to bring about the desired emittance increase. Additional development is needed in this area. Properties of samples prepared are as follows:

| <u>Side No. 1</u> | <u>Side No. 2</u> |
|-------------------|-------------------|
| $\alpha_S = 0.72$ | $\alpha_S = 0.24$ |
| $\epsilon = 0.05$ | $\epsilon = 0.06$ |

5. Satellite Depressurization System

It is generally agreed that perforations are required in the lens and torus surfaces to permit evacuation of all entrapped air prior to initiation of the deployment sequence. Assuming that the surfaces are perforated, the inflation system must be designed so that the gas flow rate "in" (stored gas source) is greater than the gas flow rate "out" (gas exhausting through surface perforations) in order that the pressure differential required to yield the structure can be effected. After attainment of the correct pressures in the proper time and sequence, the pressure is permitted to decay (depressurization) by exhaust through the surface perforations. Since the perforations are uniform over the entire surface area (see Table IV), the disturbing forces relative to the cg of the satellite are theoretically zero. If unbalancing forces on the satellite are developed during exhausting of the inflation gas, they will also be developed during the erection cycle, because the gases are continually exhausted through the perforations during this phase. Therefore, suggestions that some system of plumbing be provided to reroute the inflation gas to a small number of exhaust ports after full erection has been effected do not appear attractive. Only the magnitude of the assumed problem would be affected, and absolute values would still be indeterminate. If consideration is given to the number of perforations, it should be a simple matter to show statistically that a large number of small perforations is more effective than a small number of large perforations.

In view of the foregoing, the basic question becomes whether unplanned openings in the film surfaces will develop, thus permitting non-symmetrical exhausting of the inflation gas, which will apply upsetting torques to the satellite. Only engineering judgments can be applied, but it must be assumed that a proper testing program will verify that proper packaging and deployment techniques will preclude the possibility of rips and tears developing after final packaging of the satellite for launch. Further, adequate quality control and inspection procedures will have to be established to ensure a homogeneous wire-film structure.

The photolysis rates will be sufficiently slow so that holes will not appear in the surfaces before the inflation gas has been dissipated through the perforations.

In conclusion it is judged that perforation of the film surfaces is an effective and satisfactory means of depressurization, and that a more complex system of depressurization is not warranted.

6. RF Performance Review

- a. General. A microwave analysis and test program was undertaken to prove the feasibility of the lenticular configuration as a passive relay satellite. A preliminary investigation of the lenticular shape indicated that a significant radar return was to be expected because of the edge diffraction phenomenon. Theoretical calculations of the edge diffraction were made, and a computer program was set up to calculate the expected radar returns as a function of frequency.

Reflectivity measurements were made on a 20-inch diameter scale model of the lenticular shape to determine the magnitude of the edge diffraction return and to predict the over-all rf return that might be expected from the full-scale and flight test satellites.

Theoretical consideration was given to the effect of the boom and canister on radar return, effects of the yaw and damper booms on rf return, the reflectivity of the wire-grid material used for lens caps, the effect of model scaling, and the effect of the lens surface tolerance.

The following discussion is a general analysis of the theoretical and experimental results of the program. A more detailed analysis and summary of these results are included in GER 11502 (Reference 2).

- b. Lens Reflection. A theoretical analysis was undertaken to determine if the radar return due to the edge diffraction and the radar return from the front convex surface of the satellite are comparable in

magnitude. The results of the analysis on the 267-foot diameter, 200-foot radius of curvature lenticular shape were determined by equation, computing radar cross section of convex surface and radar cross section of edge diffraction. The results indicated that the return from the proposed configuration could suffer from large amplitude variations. The variation was computed to be approximately 21.5 db for the nose-on monostatic conditions. A complete cycle of constructive and destructive interference occurs with a 10-mc frequency change for the 267-foot diameter lenticular satellite.

A 20-inch diameter scale model of the lenticular satellite was fabricated and monostatic reflectivity patterns were taken on a 150-foot test range at X-band. The reflectivity tests were conducted to determine:

- (1) The peak magnitude of the edge scattering or diffraction return for correlation with the return predicted by theory.
- (2) The over-all rf return that might be obtained from the complete satellite.

Reflectivity patterns indicate that large variations ($\cong 4$ db) in monostatic return as the satellite is rotated over its included angle very closely approximate (± 2 db) the radar return magnitude of a complete sphere of the same radius of curvature (200 feet) as the lenticular satellite.

- c. Boom and Canister Interference Effects. Boom and canister effects on the rf return from the lenticular satellite were first analyzed by considering the radar return of the booms and canister at various aspect angles. The effects were analyzed for low dielectric material and conducting booms, one of which contained a 1/8-inch conducting wire to simulate the pressure and temperature sensor leads. The equations for the radar cross section of the booms are given in

Appendix G of GER 11502 (Reference 2). Figure 18 shows the plot of radar return versus angle of incident energy to boom for polarization parallel to the boom. The return is referenced to a 200-foot radius sphere to show the effect of the boom on the over-all lenticular return. The effect of the wire is seen to be negligible except in the $90 (\pm 1)$ degree region. Outside this region, the return from the wire is at least 43 db down from the spherical portion of the lenticular satellite.

It is concluded that the return from the boom in the angular regions of interest is quite small and will have a negligible effect on the lenticular return, even under the extreme conditions where the booms are totally conducting material.

When analyzing canister effects on rf return, the canister was considered to be a sphere 56 inches in diameter. Analysis revealed that radar return of the canister is down 40 db from that of the spherical portion of the satellite and would have a negligible effect on the lenticular satellite rf return.

- d. Effects of Yaw and Damper Booms. The yaw and damper booms (Figure 28) that have been considered have been investigated briefly to determine their possible effect on the rf return. The 400 foot metal booms could have a diameter of from 0.5 inch to 1.125 inches. They are mounted parallel to the lenticular disc at a height above the disc of from 250 to 400 feet. The two booms will cross each other at an included angle of 60 degrees.

The maximum radar return that could be expected from a single boom was calculated as 9.63×10^3 meters² for a 1.125-inch diameter boom. This return can only be expected when the illumination direction is normal to a completely straight boom and the incident polarization is parallel to the axis of the boom. The

maximum return that could be expected from both tubes having a 1.125-inch diameter and a 60-degree intersection angle is 2.17×10^4 meters². Both of these values compare in magnitude to the 1.17×10^4 meter² radar cross section of a lenticular disc having a 200-foot radius of curvature.

The fact that the return from a long straight wire falls off as the cosine⁴ ϕ , where ϕ is the angle between the wire axis and the polarization direction, limits the range of angles over which the boom return will be large. Since the booms will no doubt bend and flex, the actual peak returns should be much less than the above values. In this case the return would be equivalent to that from a large wire ring segment. Since the beamwidth of the boom return will be very narrow, the booms should not have an appreciable effect on the lenticular rf performance.

- e. Model Scaling Effects. Microwave tests were performed on a 20-inch diameter scaled model of the lenticular satellite to determine the effects of the edge diffraction phenomenon. Five-foot scaled model tests are proposed to determine the effects of boom and canister on the rf return and to more closely approximate the return from the full-scale model.

The test results indicate that the 20-inch model tests closely approximate the results expected from a full-scale model. The five-foot model would provide additional verification.

7. Summary

Utilizing the lenticular satellite configuration and design philosophy along with the materials data discussed previously, it becomes necessary to analyze the basic design guidelines for lenticular satellites with station keeping capabilities. Original sailing studies were concentrated on the use of an asymmetrical satellite in an effort to minimize weight and complexity.

Intensive study of deployment and dynamic characteristics of the lenticular satellite indicated the desirability of considering only symmetrical designs to enhance the reliability and simplicity throughout the complete operational spectrum. The use of the flat sail or the opaque lens as the sail is still open to question, although minimization of the area-to-mass ratio of the satellite may be required to control orbit eccentricity. The preliminary investigation of the effect of orbit inclination indicated the desirability of investigating only the inclinations of 60 to 65 degrees, because of resonant conditions occurring throughout the other inclination angles. This inclination range will be satisfactory for the communications systems presently contemplated. Cognizant NASA and GAC personnel are in agreement on these decisions as the starting point for any future design considerations, either from the system aspect or in the detailed satellite structure design. The reasons for some of these design decisions are explained in discussions of the structural analysis and dynamic considerations.

B. ORIENTATION AND STABILIZATION

1. General Requirements

Two of the primary requirements for a system of passive communication satellites are orbital position keeping and attitude stabilization. To provide uninterrupted communication service with a minimum number of satellites requires a means of maintaining the desired separation of the various satellites in their respective orbits. Likewise, the attitude of the satellite must be so stabilized that the rf reflecting surfaces provide satisfactory communication service over the earth. High system reliability and long system lifetime requires that orbital position keeping and attitude stabilization be provided by as nearly passive methods as possible. These requirements are difficult to meet because of the high area-to-mass ratio of these type satellites. Solar pressure exerted on the large reflecting surfaces is the

source of strong perturbing forces and torques that disturb both the orbital position and the attitude of the satellite.

Figure 19 is a sketch of a proposed form of the communication satellite that meets the requirements of gravity gradient stabilization and orbital position keeping by solar sailing.

To provide orbital position keeping it has been proposed that the satellite be equipped with a solar sail (or that the rf reflecting surfaces be used as a solar sail), which must be so oriented in relation to the sun line that solar pressure forces on the sail either offset undesired orbital perturbing effects, or else slowly change the orbital attitude and mean anomaly rate to effect a position correction. Orienting the solar sail relative to the sun line must not disturb verticality of the satellite and the rf reflecting surfaces.

Gravity gradient stabilization has been proposed as a means of ensuring the proper attitude of the satellite relative to the earth. Gravity gradient stabilization also constrains the over-all mass distribution of the satellite. In general, the large rf reflecting surface of the lenticular satellite creates a large mass moment of inertia about the optical axis of the lens. This axis must be continually aligned with the local vertical by the gravity gradient stabilization system. To achieve this alignment by gravity gradient forces, large canisters with their instrumentation and equipment are attached to the lens at a considerable distance both above and below the lens along the optical axis.

Likewise, to establish a preferred yaw orientation so that the sail may be controlled relative to the sun line, weights have to be added at least at two points around the periphery of the lens or to the ends of booms extended perpendicular to the optical axis of the lens. Also, a librational energy damping device must be provided which may consist of additional weights on a pivoted boom with a dashpot at the pivot axis or lossy magnetic wire in the lens. The lengths of booms and tip weights must be selected to

provide certain desirable ratios between the moments of inertia about the principal axes of the satellite.

A further requirement of the gravity gradient stabilization system is the initial capture of the satellite attitude by gravity gradient torques in the presence of attitude and attitude rate errors at the time of satellite deployment. Especially contributing to the initial capture requirement is the fact that the direction of local vertical relative to an inertial reference frame is continuously varying at orbital rate about the pitch axis of the satellite, and no provision is made to give the satellite this angular rate initially. This initial pitch rate error in conjunction with initial perturbation torques is likely to induce tumbling of the satellite about the pitch axis. Therefore, the damping device of the gravity gradient system must be capable of dissipating tumbling energy, in addition to being capable of suppressing attitude librations. Moreover, because of the likelihood of initial tumbling, the satellite configuration must either be such that a "right side up" capture is not required, or some method of inverting the satellite attitude must be provided.

It is difficult to define precisely the transient damping time constants and steady state accuracy requirements of the gravity gradient stabilization system. The best estimate of the requirements seems to be as follows:

- (1) The transient settling time constant of the least damped mode of satellite librations should be less than 10 orbital periods.
- (2) The root-sum-square vertical pointing error caused by all steady state attitude perturbing sources should be less than five degrees.
- (3) The yaw axis orientation error due to steady state yaw perturbations should be less than 30 degrees in order not to excessively degrade the orbital mobility available from the solar sail.

From the preceding discussion it is evident that the requirements for solar sailing and gravity gradient stabilization are somewhat difficult to meet. However, the results of this study indicate that it is feasible to meet these requirements without an excessive penalty in satellite weight or complexity. Methods are presented for achieving the required accuracy in attitude stabilization and for maneuvering the solar sail into the proper relation to the sun.

2. Initial Gravity Gradient Capture

The deployment sequence by which the satellite changes from a densely packaged canister into a large inflated lenticular communication satellite is not expected to ensure an initial "right side up" capture by the gravity gradient stabilization system. A high probability exists that the deployment sequence will result in the satellite tumbling about the nominal pitch axis of the satellite. After sufficient time has elapsed for the damping of this initial tumble by the gravity gradient damper and incidental structural and eddy current damping in the lens portion of the satellite, there is a 50 percent probability that the ensuing capture by gravity gradient torques will be "upside down" rather than "right side up."

The first aspect of the capture problem studied was the likelihood of initial tumbling. Several perturbing torques and initial conditions contribute to the likelihood of such tumbling. These may be summarized as follows:

- (1) Local vertical rotates at orbital rate relative to inertial space about the nominal pitch axis of the satellite. No simple passive means are available to impart this required initial rate of rotation about the pitch axis of the satellite. The rate error by itself is almost sufficient to cause an initial tumbling of the satellite.
- (2) Pitch and roll attitude errors of the canister spin axis prior to deployment and satellite inflation.

- (3) Uncertainties in reducing the canister spin vector to zero by the yo-yo despin device, and uncertainties in growth of satellite inertia during inflation.
- (4) Escape of the inflation gas through the holes in the lens and torus. The holes are necessary to avoid entrapping air during the folding of the satellite for packaging.
- (5) Solar pressure torques due to offset between the center of solar pressure and the satellite center of mass. These torques are especially severe in an unsymmetrical satellite configuration, in which a large shift in the effective center of solar pressure occurs when the film is photolyzed.
- (6) Photolization of the film material of the lens and torus.
- (7) Orbital eccentricity.

The problem of initial tumbling prior to gravity gradient capture was considerably simplified by confining consideration to the pitch axis of the gravity gradient stabilization system and ignoring damping. Such a simplification of the dynamics is justifiable on the following basis:

- (1) The gravity gradient restoring torques about the pitch axis are significantly less stiff than the restoring torques about the roll axis.
- (2) The pitch axis has more perturbing sources than does the roll axis. For instance, orbital rate appears as an initial condition error in the pitch axis and does not appear in the roll axis. As shown later, this source alone is equivalent to an integrated torque impulse sufficient to cause a 45-degree libration amplitude in the pitch axis. This amounts to a librational momentum condition equal to 72 percent of that possessed by the satellite when librating with an amplitude of 90 degrees; i. e., just on the borderline of tumbling.

- (3) The nature of the body axis cross coupling is such that large amplitude librations may exist in the pitch axis without transferring into either the roll or yaw axis. This, of course, is a consequence of the gyroscopic coupling due to the rotation rate of local vertical about the pitch axis.
- (4) The assumption is conservative, in that any gravity gradient damping and any coupling from the pitch axis into the roll or yaw axis gives a higher apparent stiffness in the pitch axis, and therefore gives the pitch axis a reduced sensitivity to perturbations. Thus the ability to absorb disturbing impulses and withstand adverse initial condition errors without tumbling is somewhat greater than indicated by this analysis. The simplification of pitch axis dynamics without damping or cross coupling therefore amounts to the assumption of a small factor of safety in assessing the likelihood of initial tumbling.

The pitch axis tumbling equation is

$$I_y \ddot{\phi} + \frac{3}{2} \omega_0^2 (I_x - I_z) \sin 2\phi = T_y,$$

where

I_y = pitch axis inertia of the satellite

ω_0 = orbital angular rate

ϕ = pitch attitude error

I_x = roll axis inertia of the satellite

I_z = yaw axis inertia of the satellite

T_y = perturbing torque acting in the pitch axis.

The transient response portion of this equation was solved by elliptical integral methods, and phase plane curves of $\dot{\phi}$ vs ϕ were plotted for various

amplitudes of pitch axis libration up to and including 90 degrees. Curves are shown for two different sets of satellite inertia distribution. Case A (Figure 20) is representative of the performance expected of a configuration where the pitch and roll moments of inertia are close to 1,000,000 slug-ft² and the yaw axis inertia is approximately 300,000 slug-ft², the lens and torus film material not yet having been photolyzed. Case B (Figure 21) is representative of a taller satellite with the tetrapod boom lengths essentially 40 percent longer than for Case A, corresponding to pitch and roll axis moments of inertia of 2,000,000 slug-feet². Case B gives approximately twice as much gravity gradient stiffness in resistance to tumbling, but requires considerably stronger tetrapod booms with associated weight penalty. Most design study has been concentrated around the inertia distribution values of Case A.

Inspection of the curves of Case A reveals the following. An initial pitch rate error of $1 \omega_0$ triggers a libration amplitude of essentially 45 degrees amplitude. The $1 \omega_0$ initial pitch rate is shown to be the equivalent of a short term integrated torque impulse of 620 ft-lb-sec. The total impulse absorbing capability is 861 ft-lb-sec. Thus the initial pitch rate error of $1 \omega_0$ corresponds to a perturbing impulse equal to 72 percent of the total impulse absorbing capability of the pitch axis on the threshold of tumbling. For the higher inertia satellite of Case B, an initial pitch rate of $1 \omega_0$ corresponds to only a slightly better condition, a $1 \omega_0$ pitch rate error being a torque impulse equivalent to 65 percent of the impulse absorbing capability of the satellite. Thus the higher pitch and roll inertias of Case B provide little benefit in preventing an initial tumble of the satellite.

Table V shows a breakdown of all the contributing perturbing torque impulses to the satellite and the resultant tumble rates. Maximum tumbling rates are determined by direct algebraic addition of the individual perturbing impulses. Probable tumbling rates are calculated by root-sum-square addition. Case 1 is for a configuration having upper and lower symmetry

such that the center of solar pressure and center of mass of the satellite are always at the center of the lens, regardless of the degree of film photolyzation. Case 2 is for a configuration where upper and lower symmetry is not preserved, the lower set of tetrapod booms having been eliminated and a solar pressure balancing sphere having been added at the top so that solar pressure forces on the lens after completion of film photolyzation are balanced by solar pressure forces on the sphere. After photolyzation the center of pressure is coincident with the center of mass of the satellite. Before photolyzation the center of solar pressure is very close to the center of mass. Case 3 is essentially a large size version of Case 2 with additional gravity gradient stiffness in pitch and roll.

The dynamic response characteristics of the pitch axis of Cases 1 and 2 are in accord with the phase plane plots of Case A. Case 3 pitch axis dynamics correspond to the phase plane plot of Case B. Because of the lack of upper and lower symmetry, Cases 2 and 3 are very easily upset by solar pressure unbalance during the film photolyzation interval.

Torque impulses due to inflation gas escape were calculated assuming escape of the entire 17 pounds of inflation gas with a specific impulse of 85 seconds and a balancing out of reaction forces to within $1/2$ of 1 percent. For Case 1 the effective radius arm of the escaping gas to the cg was taken to be 150 feet. Cases 2 and 3 assumed 200 feet and 300 feet respectively for the radius arm. Yo-yo despin uncertainties were calculated assuming a 1500-pound canister, a radius of gyration of $1-1/2$ feet, a spin rate of 150 rpm known to within 3 percent, and the yo-yo despin device accurate to 1 percent. Orbital eccentricity effects assumed a sensitivity of one-degree pitch error per 1 percent eccentricity for Cases 1 and 2 and a sensitivity of 0.7-degree pitch error per 1 percent eccentricity. Initial eccentricity was assumed to be 2 percent.

Two solutions to this uncertainty of "right side up" capture exist:

- (1) Configure the satellite symmetrically as far as rf reflectivity is concerned, so that "right side up" is indistinguishable from "upside down." This implies identical upper and lower lenticular reflecting surfaces and no significant rf blockage or extraneous rf reflecting surfaces to interfere with the communications function of the satellite. The satellite is thus usable for communication regardless of the sense of the gravity gradient capture.
- (2) Provide a method for inverting the satellite to the "right side up" condition. This may be done by the simple expedient of repeatedly "tumbling" the satellite until a "right side up" capture is accomplished. No complex attitude sensing or accurate metering of tumbling impulses is required for this approach. This approach is, of course, analogous to randomly flipping a coin until a "heads up" flip is realized. A simple beacon or corner reflector on the lower canister and ground based interrogation could determine whether "upside down" or "right side up" capture had been realized. If "upside down" has resulted, then a crudely programmed tumbling impulse by gas jets in the canister could be called for by ground command. On a fifty-fifty probability basis, four such tumbling cycles result in 97 percent probability of achieving "right side up" capture.

3. Gravity Gradient Damping

The accuracy and dynamic response of the gravity gradient stabilization system is largely determined by the presence of attitude perturbing torques in the space environment, the inertia distribution of the satellite about its principal axes, and the effectiveness of the gravity gradient damper in suppressing transient attitude librations. A satellite experiences both constant and cyclical perturbing torques which are periodic at the fundamental orbital frequency and its harmonics. These torques are caused by such factors as orbital eccentricity, solar pressure on the satellite, and the interaction of

the earth's magnetic field with any residual dipole moment in the satellite. To minimize attitude errors due to these torques it is essential to use a satellite inertia distribution that provides strong gravity gradient restoring torques. The restoring torques that provide stiffness about the roll and pitch axes of the satellite and preserve the verticality may be increased by making the satellite as nearly in the form of a long dumbbell as possible. To increase the stiffness about the yaw axis, it is necessary to increase the pitch axis inertia relative to the roll axis inertia. Thus an ideal gravity gradient configuration with three-axis stability is shaped like a cross, the arm of the cross tending to align with the orbital velocity vector and the mast of the cross tending to align with the local vertical. This ideal configuration from a gravity gradient viewpoint can, of course, be only crudely approximated in the solar sailing lenticular communication satellite.

The inertia distribution must also provide a set of natural frequencies of satellite libration which must be remote from the frequencies present in the perturbing torques to avoid resonant rises in the satellite attitude response. The natural frequencies of the satellite as a function of the inertia ratios of the satellite principal axis inertia are shown in Figure 22.

Because even the best types of gravity gradient dampers provide only very light damping, it is not possible to depend on the damper to suppress the resonant rises. Because of these factors the satellite inertia ratios are constrained within the following bounds:

$$0.93 < \frac{I_{\text{roll}}}{I_{\text{pitch}}} < 0.97$$

$$0.15 < \frac{I_{\text{yaw}}}{I_{\text{pitch}}} < 0.20$$

The moment of inertia of the yaw axis is fixed by the inertia contribution of the large rf reflecting lenticule. Prior to film photolyzation the yaw axis

inertia is about 300,000 slug-ft², and after photolyzation is reduced to about 120,000 slug-feet². The pitch and roll moments of inertia thus should be in the region of 1,000,000 slug-ft², which is realized by the hemispherical canisters being attached through the tetrapod booms to the lenticule.

Three types of gravity gradient dampers were compared regarding damping performance and general suitability to the lenticular satellite. These dampers were (1) the Ames damper, (2) the Rice/Wilberforce damper, and (3) the use of Hypernik 50/50 lossy magnetic wire in fabricating the wire mesh lenticule. The results of the comparison study are summarized in Table VI. The criteria taken for comparison purposes were:

- (1) Damper weight
- (2) Convenience and suitability of the tie-in between the damper and the lenticular satellite
- (3) Damper simplicity
- (4) Damping capability in suppressing transient natural librations
- (5) Effect of damper on satellite response to perturbing torques
- (6) Capability of providing damping during satellite tumble

The transient attitude damping capability of three types of libration dampers were investigated. Figure 23 shows the transient response of satellite attitude in response to initial attitude errors when the lenticular satellite is equipped with a Rice/Wiberforce gravity gradient damper. This transient response was determined by both digital and analog computer simulation of the eight-degree-of-freedom dynamic system equations of the satellite attitude.

The curves in Figures 24 and 25 show the transient attitude response when an Ames type damper is employed. The curves in Figure 24 apply for the case where the satellite inertia about the yaw axis is minimum because the lens film is assumed to have photolyzed away. The curves shown in Figure 25 show the response under the assumed condition that the lens film has not photolyzed. These curves show that the use of unphotolyzed film slightly

increases the weight of the damper to achieve a given transient time constant.

Figure 26 shows the envelopes of the pitch and roll transient attitude response of the Lensat when Hypernik 50/50 magnetic material is used for damping. In this case damping is achieved by the magnetic hysteresis losses in the material as a result of the earth magnetic field. Note that only 40 pounds of magnetic material were employed. If the total weight of 200 pounds of the copper wire mesh is replaced by Hypernik 50/50, then the damping time constant will be bettered by a factor of five.

It is quite evident that the Hypernik 50/50 magnetic material damper is not as efficient as either the Ames or Rice/Wilberforce damper. However, because of its simplicity and the fact that the weight of the damper material replaces an essentially equivalent weight of copper wire mesh, the magnetic approach should continue to be considered. It is also evident that both the Ames damper and Rice/Wilberforce damper give satisfactory transient damping characteristics.

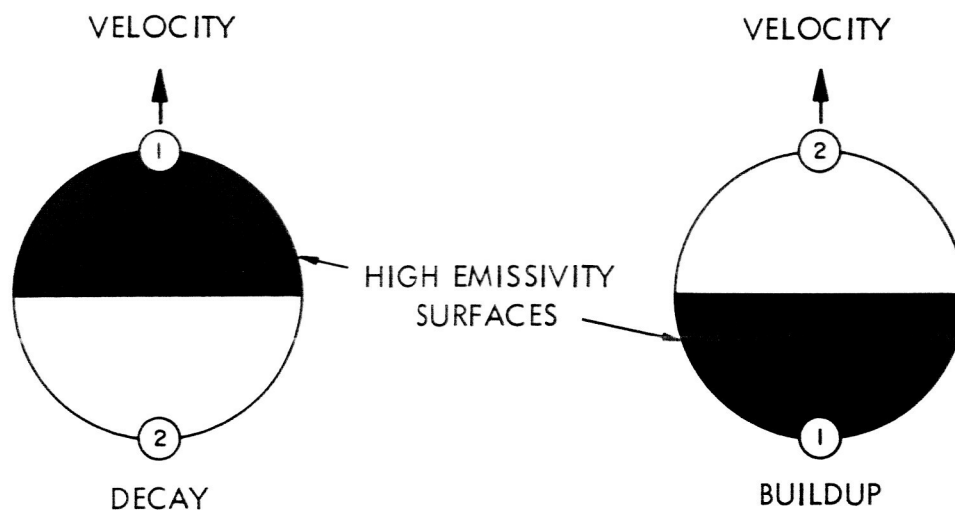
The transient response curves using the Ames damper were calculated by NASA, Ames Research Center, Moffet Field, California. The damping curves shown for the Hypernik 50/50 magnetic damper were calculated by the Applied Physics Laboratory, Johns Hopkins University, Silver Spring, Maryland.

4. Yaw Control Methods

Yaw axis attitude control may be used to fix the orientation of the solar sailing forces relative to the orbital velocity vector. Yaw control of the satellite attitude has a minimum effect on the verticality of the satellite. It provides a means for orienting the sail for orbital position keeping purposes without upsetting the desired horizontal attitude of the reflecting surfaces of the lenticule. Two operating modes of sailing are necessary: (1) orbital period buildup and (2) orbital period decay. A third mode of

operation, which is desirable but not absolutely necessary, is standby. The standby mode can be dispensed with at the expense of increased usage of the other two modes.

Two-mode yaw axis control is easily accomplished. The pitch axis moment of inertia of the satellite is made larger than the roll axis moment of inertia to provide sufficient yaw axis gravity gradient restoring torques. This may be accomplished by placing two equal weights at diametrically opposite positions on the rim of the lenticule whose inertia contribution to the pitch axis is from 2 to 5 percent of the total pitch axis inertia. Gravity gradient forces and centrifugal forces combine to drive the weights into the orbital plane and into alignment with the orbital velocity vector. Two stable equilibrium yaw attitudes exist, so that either of the two weights may lie forward in the satellite. The plan view of the lenticule and weights for the modes of orbital buildup and decay are as follows:



Switch-over from one mode to the other is accomplished by applying a yaw axis torque from an inertia reaction wheel which overrides the gravity gradient restoring torque about the existing stable null.

As the other stable null at the 180-degree point in the yaw maneuver is approached, the reaction wheel is brought to a stop, which minimizes any yaw

transient overshoot about the other stable null. Any transients associated with the maneuver are damped out by the gravity gradient damper. It is desirable that the transient disturbance of this maneuver be minimized by nominally programming the two successive reaction wheel torques to optimum values. In the plan view on the preceding page, the lenticule is being made to function as a sail by coating one-half of the outer surface of the lens with a high emissivity material and the other half with a low emissivity material, the sailing forces being generated nominally by reradiation forces.

A three-mode yaw control system may be achieved at the expense of increased complexity by using a variable inertia distribution which effectively rotates the position of the pitch and roll body axes about the yaw axis of the satellite. Such rotation may be accomplished on either a discrete or continuous basis. The discrete method will be discussed first. As shown in Figure 27, various chambers are distributed around the rim of the lens. Any desired diametrically opposite pair of chambers may be filled with a dense fluid with all other chambers empty. The line between the two filled chambers thus constitutes the roll axis of the satellite. The position of the stable null about the yaw axis may be selected at will by redistributing the dense fluid to that pair of chambers giving the preferred yaw reference orientation. Since the sail is fixed rigidly to the satellite body, changing the preferred yaw reference changes the sail orientation relative to the velocity vector and the sun. Because of the bistable nature of the gravity gradient restoring torques, there are actually six stable yaw reference positions. For the arrangement shown in Figure 27, there are two buildup modes with the possibility of either a positive or negative 30-degree offset between the velocity vector and the reradiation forces. Similarly, there are two positions for orbital decay and two for orbital standby. This particular arrangement, which provides for the selection of either positive or negative 30-degree biasing, materially increases the mobility capability of solar sailing over a wide range of orbital inclinations.

At the expense of increased complexity, the yaw reference axis may be varied continuously by using a motor to rotate a yaw reference boom with attached weights relative to the satellite body. The null position of the gravity gradient torques acting on the boom may thus be continuously varied relative to the solar sail and lenticule. Any desired bias or attitude setting about the yaw axis may be called for by the yaw control system. Figure 28 shows two versions of this yaw control method, a method employing a single yaw boom and the second method showing the integration of yaw control with an Ames gravity gradient damper boom.

Various other methods of achieving yaw control were considered. A magnetic coil torquing method was briefly studied, but it became evident that this approach required extensive in-flight attitude sensing in order that the instantaneous currents required for the torquing coils could be correctly calculated.

The Phillip's concept of setting up a natural oscillation of satellite attitude about the yaw axis so that the desired relative orientation between the solar sail and the sun line could be maintained continuously in orbit was considered. However, study disclosed that this concept required precise synchronism of yaw motion and orbital motion. Such synchronism would be very difficult to accomplish, because of the necessity to control simultaneously the yaw axis natural frequency of satellite librations, the amplitude of the librations, and the required reference phase angle. Achieving such a synchronous relationship would require airborne attitude sensing and computation, taking into account instantaneous phase and amplitude measurements of the libration angle. The system would also have to take into consideration the non-linear relationship existing between yaw axis natural frequency and amplitude of the yaw axis libration. It became evident that such a system would be too complex for a long-life orbital vehicle. Similar considerations prevented the use of a constant synchronized spin method. Table VII represents a summary of the features of the various types of yaw control methods considered.

C. STRUCTURAL ANALYSIS

1. General

The structural analyses performed during this program are summarized in this section. This effort consisted primarily of feasibility and parametric studies relative to the incorporation of solar sailing in the lenticular satellite. In order to concentrate the effort on the solar sailing aspects of the design, the lens, rim, torus, and inflation system shown in Reference 2 for the original design were retained in the advanced design studies. Figure 10 presents the lens, torus, and rim data.

2. Asymmetrical Configuration Study

The general arrangement for the asymmetrical configuration is shown in Figure 29. There are a number of parameters that must be considered in the arrangement that are not independent of one another. These parameters are:

- (1) Total weight
- (2) Moment of inertia ratio
- (3) Center of gravity
- (4) Available sail area
- (5) Sail centroid
- (6) Sail area-to-weight ratio
- (7) Boom length

The relationship between these parameters are derived in Appendix C of Reference 5. The weights and inertias for the lens, torus, and rim of the full-scale design shown in Reference 2 were used, with the variations of the parameters determined as a function of the upper mass and the moment of inertia ratio.

Figure 30 is a plot of the parameters versus the upper mass weight, W_1 , for a moment of inertia ratio of 6. Additional plots for moment of inertia ratios of 4, 8, and 10 may be found in Reference 5.

3. Preliminary Loads

The asymmetrical configuration, when fully deployed in orbit, is subject to load distributions arising from various causes. These are discussed below.

- a. Orbital. The satellite in orbit, but having an angular displacement from its stable vertical position, was considered. The gravity gradient and the centrifugal forces from the orbital angular velocity, plus the inertia forces required for equilibrium of the satellite, were studied. The resultant force at any point on the satellite was expressed in terms of the satellite position coordinates, the orbital angular velocity, the displacement angle from the vertical, and the moment of inertia ratio of the satellite. These were then collected to define the loading condition on the tetrapod booms, in-plane loads on the rim, and out-of-plane loads on the rim. The derivation and results are shown in Reference 18.
- b. Torque Coil. A concept utilizing three mutually perpendicular coils interacting with the earth's magnetic field to orient the satellite for solar sailing was considered. The load distribution due to these torque coils was determined and combined with inertia forces required to satisfy equilibrium of the satellite. Nine unit solutions were obtained that can be superimposed to obtain a general solution. The derivation and a summary of the results are shown in Reference 19.
- c. Damper. The loads and their directions induced by the Rice/Wilberforce damper were investigated by examining the digital computer runs made for the lenticular satellite. The maximum load was 0.0041 pounds and the maximum angle was 28.48 degrees (Appendix E, Reference 6).
- d. Sail. The maximum sail load was estimated to be 1.5×10^{-6} times the satellite weight.

- e. Photolysis of Film. In Appendix P of Reference 6 it was found that the forces due to photolysis of the film are less than one percent of that due to direct solar pressure. These forces can, therefore, be neglected insofar as the structural analysis is concerned.

Boom loads were computed for three asymmetrical configurations and the results tabulated in Appendix G of Reference 6. Table VIII is a typical set of boom loads. It was found that the maximum compression load was 0.00145 pounds and the maximum transverse load was 0.0012 pounds. These two maximums do not occur at the same time.

Using wire-film material for the tetrapod booms, it was estimated that a tetrapod weight of 12.5 pounds was required to support the critical loads.

4. Yaw Control

Because the torque coil system weight is high, several other concepts were considered. In most of these concepts it was necessary to introduce moments at the apex of the tetrapod and in some it was necessary to limit the twist of the apex with respect to the lens. A parametric study of tetrapod weight was made in Appendix J of Reference 6. The principal results are shown in Figure 31, a plot of weight versus angle of twist for several values of torque, M_z . It was found that the other two components of moment, M_x and M_y , would generally not be critical.

Another concept, described previously in paragraph B4 "Yaw Control Methods" involved the use of concentrated masses mounted on the satellite rim. The in-plane rim deflections for this arrangement were determined in Appendix W of Reference 6. Three sources of loads are considered:

- (1) In-plane components of tetrapod loads.
- (2) Gravity gradient forces associated with the two 50-pound masses.
- (3) Gravity gradient forces associated with the rim mass.

The maximum rim deflection was found to be approximately 0.30 inch, which is nearly the same as for the configuration described in Reference 2. It is anticipated that the out-of-plane deflections would also be comparable.

5. Tumbling

It is shown in paragraph B2 "Initial Gravity Gradient Capture" that tumbling of the satellite is likely to occur. In Reference 7 the effect of tumbling on the structure is investigated. Two cases are considered, tumbling in the direction of the orbital angular velocity and tumbling normal to the orbital angular velocity. General expressions are found for the forces as a function of position coordinates in the satellite, the orbital angular velocity, the tumbling velocity, the angular position of the satellite, and the moment of inertia ratio of the satellite.

These equations were then used to investigate the symmetrical configuration shown in Figure 32. The axial and transverse loads on the yaw rod are plotted in Figure 33 as a function of the tumble angle β for a tumbling rate four times the orbital angular velocity about the roll axis. The critical condition occurs at $\beta = 80$ degrees. The deflection of the yaw rod at the tip due to these loads is 35.1 inches for a tube diameter of 1-1/8 inches. The total deflection including thermal deflection is approximately 75 inches.

The six components of load at the apex are shown in Figure 34. The critical angle is 70 degrees, and for this set of loads a tetrapod weight of 75 pounds is required.

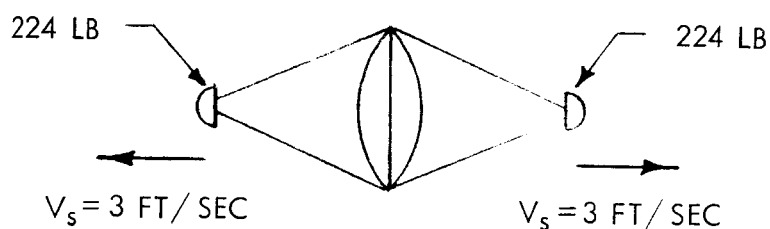
6. Structural Damping

The damping capacity of wire-film tubes used for the tetrapod was investigated theoretically in Appendix V of Reference 6. It was found that these would contribute very little damping because the axial loads develop only small stresses in the wire. It was shown that a wire-film boom could be added to the satellite to act in bending, which could contribute damping of the order of magnitude required for the satellite.

7. Deployment

The effect of 3 foot/second separation velocity (V_s) of the canisters on the structure was investigated in Reference 7. The other problems associated with the deployment sequence have been treated in Reference 2 and the results are applicable to the advanced configurations since the lens, torus, and rim are the same.

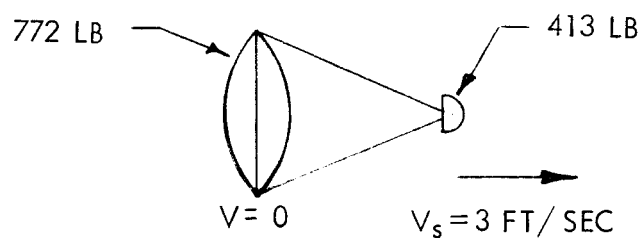
Both the symmetrical and asymmetrical configurations are considered. The masses and initial velocities used for the symmetric case are shown below:



In the symmetrical case the energy to be dissipated per tetrapod is

$$\Delta E = 12 \times 224 \times 3^2 / 2 \times 32.2 = 376 \text{ in-lb.}$$

The masses and initial velocities used for the asymmetric case are as follows:



The energy to be dissipated per tetrapod is

$$\Delta E = 12 \times 32 \times 413 \times 772 / [2 \times 32.2 (772 + 413)] = 451 \text{ in-lb.}$$

It can be concluded that there is no substantial difference between the symmetric and asymmetric configurations insofar as this problem is concerned.

The energy is dissipated by unfolding of the structure and by stretching of the longitudinal wires of the tetrapod booms. The amount of energy dissipated by

the first source is unknown and will be neglected. This is conservative as a determination of the maximum stress attained in the longitudinal wires.

The stress and the strain energy density of the wire is shown as a function of strain in Figure 35. In one boom the volume of the longitudinal wires is 26.4 cubic inches and the strain energy density required is $376/264 = 14.23$ in.-lb/cu in. From Figure 35 the corresponding stress is 5,500 psi, which is satisfactory, since the ultimate stress of the wire is 12,000 psi.

After stopping, the canister energy will be stored in the wire which will impart a return velocity to the canister. The return velocity, which is a function of the stress level attained in stopping the canister, is shown in Figure 36. Up to a maximum stress of 3,000 psi the behavior is elastic and the return velocity is equal to the separation velocity. Above this value the return velocity decreases with increasing maximum stress. Therefore, the maximum return velocity possible would occur if three booms were effective in stopping the canister. Under this assumption the strain energy density to be dissipated is $14.23/3$ or 4.75 in.-lb/cu in. This corresponds to a maximum stress of 5,000 psi and a return velocity of $0.52 \times 3 = 1.56$ ft/sec.

The distance from the lens to the fully deployed canister is approximately 300 feet. It would take about 100 seconds to reach this position with a separation velocity 3 ft/sec and approximately 200 seconds to make the return trip, or a total of about 300 seconds. The inflation system is initiated 15 seconds after separation, so the tetrapod booms should be inflated before the return is completed. The inflated booms, even though they may be buckled, will provide sufficient force to arrest the canister on its return trip before it can reach the lens.

8. Weight Study

The present studies have been limited to a particular set of design parameters for the purpose of determining the feasibility of incorporating solar sailing in a lenticular satellite. The effect of the various design parameters on the

launch weight of the satellite must now be examined so that data on satellite weight can be presented in a manner suitable for a system study, and areas of potential weight reduction can be evaluated. The assumptions used and the development of the equations for the weight of the satellite are given in Reference 7. The general form of the equation is:

$$W = \rho^2 F(\theta)$$

where

W = launch weight (pounds)

ρ = radius of curvature of the lens (inches)

θ = half angle of the lens

F = a function depending upon several design parameters

The quantities ρ and θ are the principal microwave parameters that would be used in a system study. The remaining parameters consist primarily of material properties, factors of safety, and weighting factors that must be specified in order to determine $F(\theta)$. A parametric curve of satellite weight using the design parameters for the full-scale lenticular satellite of Reference 2 is shown in Figure 37.

Potential weight savings that may be possible are shown in Table IX. Listed in this table are the design parameters of Reference 2, a projected value which may be attainable, and the weight saving resulting in the improvement of this particular parameter. If all of the projected values were achieved, the launch weight of the lenticular satellite of Reference 2 would reduce from 1250 pounds to 360 pounds.

9. Summary

It is concluded that:

- (1) Solar sailing can be incorporated in the lenticular satellite for a modest increase in structural weight.
- (2) Potential areas of weight reduction do exist and should be explored.

SECTION III. CONCLUSIONS AND RECOMMENDATIONS

Studies to date indicate that the gravity gradient stabilized lenticular satellite concept is feasible, and that the incorporation of solar sailing is also feasible. It is clear that passive communication satellites are useful and promising for many applications. It is also clear that the lenticular satellite is the most flexible and the most promising of the satellite family.

Figure 38 shows the lenticular satellite configurations recommended as a result of the technical studies to date. For low altitude it appears that a symmetrical satellite with a hysteresis-type damper and flywheel fixed weight yaw control offers both simplicity and reliability. For high altitude applications the symmetrical lenticular satellite would use an Ames-type damper and a boom drive yaw control for improved performance. A flat sail is indicated for both configurations, but further studies to investigate compatibility with rf characteristics of the satellite will be required before design finalization. Both configurations have merit and could be considered a starting point for follow-on detail design study of a lenticular satellite system. As more technical information becomes available, slight changes to these configurations may be necessary, but it is expected that they will remain close to these concepts.

It is strongly recommended that more extensive systems studies be made to explore these applications in depth and to conduct trade-off studies important to potential users, treating areas such as cost effectiveness, multiple access and terminal sharing, advanced satellites, operational modes, and ground environment, to mention a few.

Equally important in keeping the practical engineering and design effort in focus is the initiation of a program to define a realistic and meaningful flight

test program. A simple flight test program would be valuable in pinpointing major problems, showing in what specific areas additional work should be accomplished.

Research and development, of course, should be continued to investigate such areas as rf performance when the lens is partially shadowed by gravity gradient booms, canister, and solar sail; structural tolerance limitations; station keeping via solar sailing as compared to propulsion techniques; and fabrication and testing of additional ground models.

Methods other than solar sailing should be investigated to provide the orbital position keeping capability. Especially promising is the use of small jets in the micropound and millipound region of force level to provide both the propulsive forces required for mobility and the attitude control torques to augment the gravity gradient stabilization system. Such a small jet system looks particularly rewarding at synchronous altitude, having no eccentricity build-up penalty, as does solar sailing, and considerably better gravity gradient damping characteristics.

REFERENCES

1. GER 11452, Materials Development Report - Phase II for Feasibility Study and Preliminary Design of a Gravity Gradient Stabilized Lenticular Test Satellite. Akron, Ohio, Goodyear Aerospace Corporation, 1 February 1964.
2. GER 11502, Feasibility Study and Preliminary Design of Gravity Gradient Stabilized Lenticular Test Satellite. Akron, Ohio, Goodyear Aerospace Corporation, 1 June 1964.
3. GER 11790, Application of Rice/Wilberforce Gravity-Gradient Damper to NASA Lenticular Communication Satellite. Akron, Ohio, Goodyear Aerospace Corporation, 3 November 1964.
4. GER 11648, Photometric Measurements of Surface Characteristics of Echo I Satellite. Akron, Ohio, Goodyear Aerospace Corporation, 19 June 1964.
5. GER 11789, Advanced Passive Communications Lenticular Satellite Studies - Summary Report - Phase I. Akron, Ohio, Goodyear Aerospace Corporation, October 1964.
6. GER 11816, Advanced Passive Communication Lenticular Satellite Studies - Summary Report - Phase II. Akron, Ohio, Goodyear Aerospace Corporation, November 1964.
7. GER 11891, Advanced Passive Communication Lenticular Satellite Studies - Summary Report - Phase III. Akron, Ohio, Goodyear Aerospace Corporation, December 1964.
8. GER 11926, Orbital Mobility Program for Artificial Earth Satellites, Akron, Ohio, Goodyear Aerospace Corporation, January 1965.
9. GER 11251, Weight Loss Behavior of Type I Photolyzable Film Under Simulated Space Conditions. Akron, Ohio, Goodyear Aerospace Corporation, 10 September 1963.
10. GER 11362, Report on Photolyzable Film Development Studies for 1963. Akron, Ohio, Goodyear Aerospace Corporation, 1 January 1964.

11. GER 11386, Photolyzable Film-Metal Cloth Composite Material Seam Development. Akron, Ohio, Goodyear Aerospace Corporation, December 1963.
12. GER 11605, Photolyzable Film-Metal Cloth Composite Material Seam Development. Akron, Ohio, Goodyear Aerospace Corporation, June 1964.
13. GER 11892, Photolyzable Film Development Studies for 1964. Akron, Ohio, Goodyear Aerospace Corporation, December 1964.
14. GER 10906, Progress in Developing Thermal Control Coating for Space Applications. Akron, Ohio, Goodyear Aerospace Corporation, June 1963.
15. Edwards, D. K. , et al, "Spectral and Directional Thermal Radiation Characteristics of Selective Surfaces for Solar Collectors", Solar Energy, Vol. VI, No. 1, January 1962.
16. Hass, George, "Filmed Surfaces for Reflecting Optics", Journal of the Optical Society of America, Vol. 45, No. 11, November 1955.
17. Harmann, H. H. , et al, Improved Coatings for Temperature Control in a Space Environment, Aeronautical Systems Division, AF Systems Command, USAF, May 1962.
18. GER 11716, Study of Orbital Design Conditions for the Advanced Gravity Gradient Stabilized Lenticular Satellite Configuration. Akron, Ohio, Goodyear Aerospace Corporation, 31 August 1964.
19. GER 11704, Load Distributions Due to Torque Coils for the Advanced Gravity Gradient Stabilized Lenticular Satellite. Akron, Ohio, Goodyear Aerospace Corporation, August 1964.

Table I. Satellite Evaluation Summary

| No. | Configuration | Damper System | Yaw Control Method | Solar Sail Technique | Weight (Lb) | | Moment of Inertia Data (Slug-Ft ²) | | | | | |
|--|--|---------------|-------------------------------------|---|-------------|-------------|--|----------------|----------------|--------------------------------|--------------------------------|--------------------------------|
| | | | | | Launch | Operational | I _x | I _y | I _z | I _x /I _z | I _y /I _z | I _x /I _y |
| 1 | Base Line Symmetrical | R/W | Flywheel - two 20-lb weights on rim | Two Triangular Sails - 4000 ft ² each | 1484 | 987 | 985,000 | 1,007,000 | 164,000 | 6 | | 1.022 |
| 2 | Base Line Asymmetrical | Ames X | Canister Drive | Flat Sail - lens photolyzed, sphere counter-balance | 1408 | 871 | 1,144,942 | 1,167,021 | 190,807 | 6 | | 1.019 |
| 3 | Preliminary Lenticular Satellite (Reference 2) Photolyzable film included | R/W | N/A | N/A | 1250 | 758 | 528,000 | 528,000 | 114,000 | 4.6 | | 1.0 |
| R/W - Rice/Wilberforce N/A - Not applicable | | | | | | | | | | | | |

Table II. Summary of Film-Wire Mesh Properties

| Item | Material | Wire Dia (Inches) | Count (Wires /Inch) | Film t (Inches) | Yield (Lb/ In.) | Yield* (psi) | Ultimate (Lb/In.) | Ultimate* (psi) | E* (psi x 10 ⁻⁶) | Percent Elongation |
|------|--------------------------|----------------------|---------------------------|-----------------------|------------------------|-----------------|-----------------------|--------------------|---------------------------------|-----------------------|
| 1W | Phosphor Bronze | 0.0016 | 24 x 24 | 0.0007 | 2.33 | 50,800 | 3.38 | 73,700 | 13.0 | 24.5 |
| 1F | Phosphor Bronze | 0.0016 | 24 x 24 | 0.0007 | 2.16 | 47,100 | 3.23 | 70,400 | 11.7 | 22.0 |
| 1W | Phosphor Bronze at 200°F | 0.0016 | 24 x 24 | 0.0007 | 2.28 | 49,700 | 2.82 | 61,600 | 9.3 | 11.9 |
| 1F | Phosphor Bronze at 200°F | 0.0016 | 24 x 24 | 0.0007 | 1.76 | 38,400 | 2.72 | 59,400 | 7.7 | 26.2 |
| 2W | Copper | 0.0012 | 21 x 21 | 0.0006 | 0.91 | 35,300 | 1.16 | 45,000 | 6.12 | 2.55 |
| 2F | Copper | 0.0012 | 21 x 21 | 0.0006 | 0.94 | 36,450 | 1.40 | 54,300 | 5.54 | 7.39 |
| 2W | Copper at 200°F | 0.0012 | 21 x 21 | 0.0006 | -- | -- | 0.39 | 15,130 | 3.38 | 4.58 |
| 2F | Copper at 200°F | 0.0012 | 21 x 21 | 0.0006 | 0.56 | 21,700 | 0.72 | 27,950 | 3.77 | 8.49 |

*Based on wire cross section

Table III. Calculated Thermal Radiation Properties for Photolyzable Film

| No. | Sample Description | | Grid | $\alpha_s^{(2)}$ (80°F) | $\epsilon_{tn} (^{\circ}\text{F})^{(3)}$ | | | | | a_s | |
|-----|---------------------|--------------------------|------|----------------------------|--|------|------|------|------|-------|-----------------|
| | Thickness (mils) | Dye (1) Concentration | | | -64 | 8 | 80 | 152 | 224 | 296 | ϵ_{tn} |
| 1 | 1.0 | 0 | No | 0.08 | 0.17 | 0.23 | 0.29 | 0.32 | 0.35 | 0.35 | 0.28 |
| 2 | 0.7 | 2 | No | 0.61 | 0.20 | 0.25 | 0.28 | 0.30 | 0.32 | 0.32 | 2.18 |
| 3 | 0.7 | 3 | No | 0.70 | 0.21 | 0.25 | 0.29 | 0.32 | 0.34 | 0.35 | 2.42 |
| 4 | 0.7 | 5 | No | 0.80 | 0.22 | 0.27 | 0.32 | 0.34 | 0.37 | 0.37 | 2.50 |

NOTES: (1) Dye concentration, parts Nigrosine dye/100 parts resin by weight

(2) α_s = Solar absorptance(3) ϵ_{tn} = Total normal emittance

Table IV. Satellite Depressurization System Data

| LENS SURFACE | |
|-----------------------|-------------------|
| Hole Diameter | 0.020 inches |
| Hole Density | 20 holes/sq ft |
| Number of Holes | 2.6×10^6 |
| Lens Design Pressure | 0.0003 psi |
| Surface Area | 129,000 sq ft |
| Enclosed Volume | 3,070,000 cu ft |
| TORUS SURFACE | |
| Hole Diameter | 0.020 inches |
| Hole Density | 1 hole/sq ft |
| Number of Holes | 4.2×10^4 |
| Torus Design Pressure | 0.17 psi |
| Surface Area | 21,300 sq ft |
| Enclosed Volume | 41,700 cu ft |

Table V. Initial Pitch Tumbling Impulses, Ft-Lb-Sec




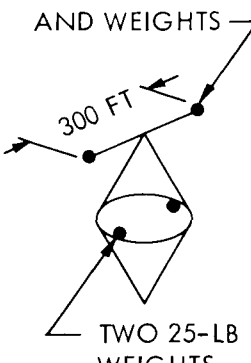
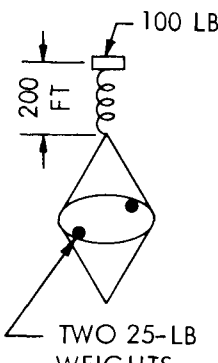
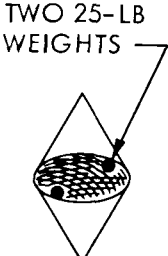
| PERTURBING SOURCE | CASE 1 | CASE 2 | CASE 3 |
|---|---|---|--|
| |  $I_x = 960,000$ $I_y = 1,000,000$ $I_z = 122,000$ Tumbling Impulse = 861 Ft-Lb-Sec |  $I_x = 960,000$ $I_y = 1,000,000$ $I_z = 122,000$ Tumbling Impulse = 861 Ft-Lb-Sec |  $I_x = 1,920,000$ $I_y = 2,000,000$ $I_z = 122,000$ Tumbling Impulse = 1928 Ft-Lb-Sec |
| Initial Pitch Error Rate = $1\omega_0$ | 620 | 620 | 1240 |
| Initial Pitch Error = 30 degrees | 430 | 430 | 960 |
| Yo-Yo Despin Uncertainty | 66 | 66 | 66 |
| Inflation Gas Escape | 1080 | 1400 | 2160 |
| Solar Pressure During Photolyzation | 15 | 1100 | 1500 |
| Photolyzation Particle Ejection | Negligible | Negligible | Negligible |
| Orbital Eccentricity = 0.02 | 30 | 30 | 20 |
| Algebraic Sum of Impulses | 2241 | 3686 | 5946 |
| Maximum Tumbling Rate - rad sec | $3.55\omega_0$ | $5.9\omega_0$ | $4.7\omega_0$ |
| RSS of Impulses | 1320 | 1960 | 3060 |
| Probable Tumbling Rate - rad sec | $2.15\omega_0$ | $3.16\omega_0$ | $2.47\omega_0$ |

Table VI. Comparison of Three Types of Gravity Gradient Dampers

| PERFORMANCE | | Ames 65-LB BOOM AND WEIGHTS  | Rice/Wilberforce  | Magnetic Wire (Hypemik 50/50)  |
|---------------------------------|-------|--|--|---|
| Damping Time Constants (Orbits) | Vert. | 5 | 4 | 30** |
| | Yaw | 8 | 25 | 100*** |
| Steady State Errors (Degrees) | Vert. | 5 | 3 | 10 |
| | Yaw | 8 | 15 | 30 |
| Upright Capture | | Desirable | Desirable | Not needed |
| Tumble Capability | | Limited | None | Unlimited |
| High Altitude Capability | | Synch | Synch | Limited |
| Complexity | | High | Medium | Low |
| Weight* (pounds) | | 115 | 150 | 50 |

*Includes 50 pounds of weight to establish yaw stiffness.

**Assumes 200-lb Hypemik 50/50 magnetic material in wire mesh.

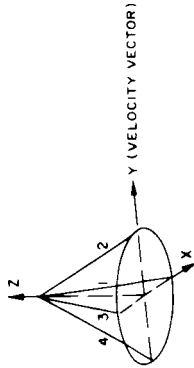
***Estimated.

Table VII. Comparison of Yaw Control Methods

| Characteristics | Two Mode - Buildup - Decay | | Three-Mode - Buildup - Decay - Standby | Continuously Variable Yaw Reference | Phillip's Yaw Oscillation | Constant Yaw Spin Method |
|--|---|---|---|--|---|---|
| | Two fixed weights | | | | | |
| System Components | Reaction Wheel | Fluid Drive (Ref 6) | Two movable weights to selectable position | Motor-driven yaw boom(s) | Amplitude, frequency, and phase controller of yaw oscillations | Constant speed and phase controller of yaw spin |
| | 50-lb rim weights plus 25-lb reaction wheel | 50-lb rim weights plus 63 lb fluid drive | 50-lb Hg plus 25-lb chambers and actu- ators | 50-lb booms and tip weights plus 4-lb motor drive | 50-lb rim weights plus 25-lb electronic com- puter and 50-lb torque coils | 25-lb electronic computer plus 50-lb magnetic coil system |
| Power (watts) | 10 watts | 10 watts | 5 watts | 2 watts | Excess of 25 watts | Excess of 25 watts |
| Complexity | Simple | Moderate complexity | Complex | Complex | Very high - in-flight attitude sensing and computation required | Very high - in-flight spin rate and angle sensing required |
| Severity of Induced Yaw Disturbance | Moderate yaw axis disturbance | Moderate yaw axis disturbance | Moderate yaw axis disturbance | Minimum yaw axis disturbance | | |
| Influence on Mobility Capability | Reduces capability by 25% | Reduces capability by 25% | Maximum mobility capability | Maximum mobility capability | | |
| Influence on Eccen- tricity Growth | Acceptable eccen- tricity buildup | Acceptable eccen- tricity buildup | Minimum buildup of eccentricity | Minimum buildup of eccentricity | | |
| Remarks | Simplest of yaw con- trol methods. | Scaling problem and micrometeroid pen- etration problem prevent usage of this method. | Acceptable method if increased complexity and fluid leak prob- lem can be tolerated. | Very good method if increased complexity can be tolerated. | Too complex an airborne controller would be re- quired to fix amplitude, phase, and frequency of yaw oscillation. | Too complex an airborne controller would be re- quired to fix the yaw spin rate and reference angle. |

Table VIII. Tetrapod Boom Loads

$W_1 = 600 \text{ lb}, \ell = 345, h = 318$
 $KBI = 1.2 \times 10^{-6} \text{ for ring; } KBI = 1.46 \times 10^{-6} \text{ for triangular coil}$
 $M_u H_u = M_r H_r = 300 \times 212.1 = 63,630 \text{ ft-lb}$
 $h, R = 318/133.8 = 2.385; \sqrt{1 + (h/R)^2} = 2.58$
 $R h = 133.8 \cdot 318 = 0.418; \sqrt{1 + (R/h)^2} = 1.085$



| Condition | Axial* and Transverse** Loads in Booms of Tetrapod† | | | | | | | |
|------------------|---|---------------------|---------------------|---------------------|---------------------|---------------------|---------------------|---------------------|
| | ① | | ② | | ③ | | ④ | |
| | L x 10 ³ | P x 10 ³ | L x 10 ³ | P x 10 ³ | L x 10 ³ | P x 10 ³ | L x 10 ³ | P x 10 ³ |
| COIL | +0.250 | -- | -- | -- | -0.250 | -- | -- | -- |
| | -- | -- | +0.250 | -- | -- | -- | -0.250 | -- |
| | -- | -- | -- | -- | -- | -- | -- | -- |
| | -- | -0.465 y | -- | -- | -- | +0.465 y | -- | -- |
| | +0.045 | +0.504 n | +0.045 | -- | +0.045 | +0.504 n | +0.045 | -- |
| | -- | -0.196 y | +0.000169 | -- | -- | -0.196 y | -0.000169 | -- |
| | +0.045 | -- | +0.045 | +0.504 n | +0.045 | -- | +0.045 | +0.504 n |
| | -- | -0.465 x | -- | -- | -- | -- | -- | +0.465 x |
| | +0.000169 | -- | -- | -0.196 x | -0.000169 | -- | -- | -0.196 x |
| SAIL | ±0.872 | -- | -- | +0.675 x | ±0.872 | -- | -- | +0.675 x |
| GRAVITY GRADIENT | ±0.325 | Very small | 0 | Very small | ±0.325 | Very small | 0 | Very small |
| | 0 | Very small | ±0.325 | Very small | 0 | Very small | ±0.325 | Very small |

* L - Axial load

** P - Transverse load in the boom. This represents the resultant of the uniformly distributed load in all conditions except "Sail," for which P is a concentrated load at the midpoint of the boom.

† Boom axial loads caused by damper spring are tensions and therefore will not be considered here. (Provided that the angle between spring and satellite z-axis does not exceed ±67°).

Table IX. Weight-Saving Study

| Item | Parameter | G^2S^2 Value (Ref 2) | Projected Value | Potential Weight Saving |
|----------------------|----------------|---------------------------------|---|-------------------------------|
| Lens Material | W | 29.7×10^{-6} | $12.97 \times 10^{-6} \text{ lb/in.}^2$ | 321 lb |
| Lens Material | N | 0.3792 lb/in. | 0.0471 lb/in. | 294 lb |
| Torus Material | F_T/γ_T | $0.263 \times 10^6 \text{ in.}$ | Same | None |
| Bottle Material | F_B/γ_B | 10^6 in. | $1.8 \times 10^6 \text{ in.}$ | 93 lb |
| Inflation Gas | m | 4 | Same | None |
| Geometry | r/R | 0.02927 | Same | None |
| *FS Torus Pressure | a_1 | 1.25 | 1.10 | 37 lb |
| *FS Torus Strength | a_2 | 1.25 | Same | None |
| Inflation System | a_3 | 1.12 | Same | None |
| *FS Bottle | a_4 | 3.00 | 1.50 | 103 lb |
| Gas Leak and Reserve | a_5 | 3.04 | 2.00 | 77 lb |

*FS - Factor of Safety

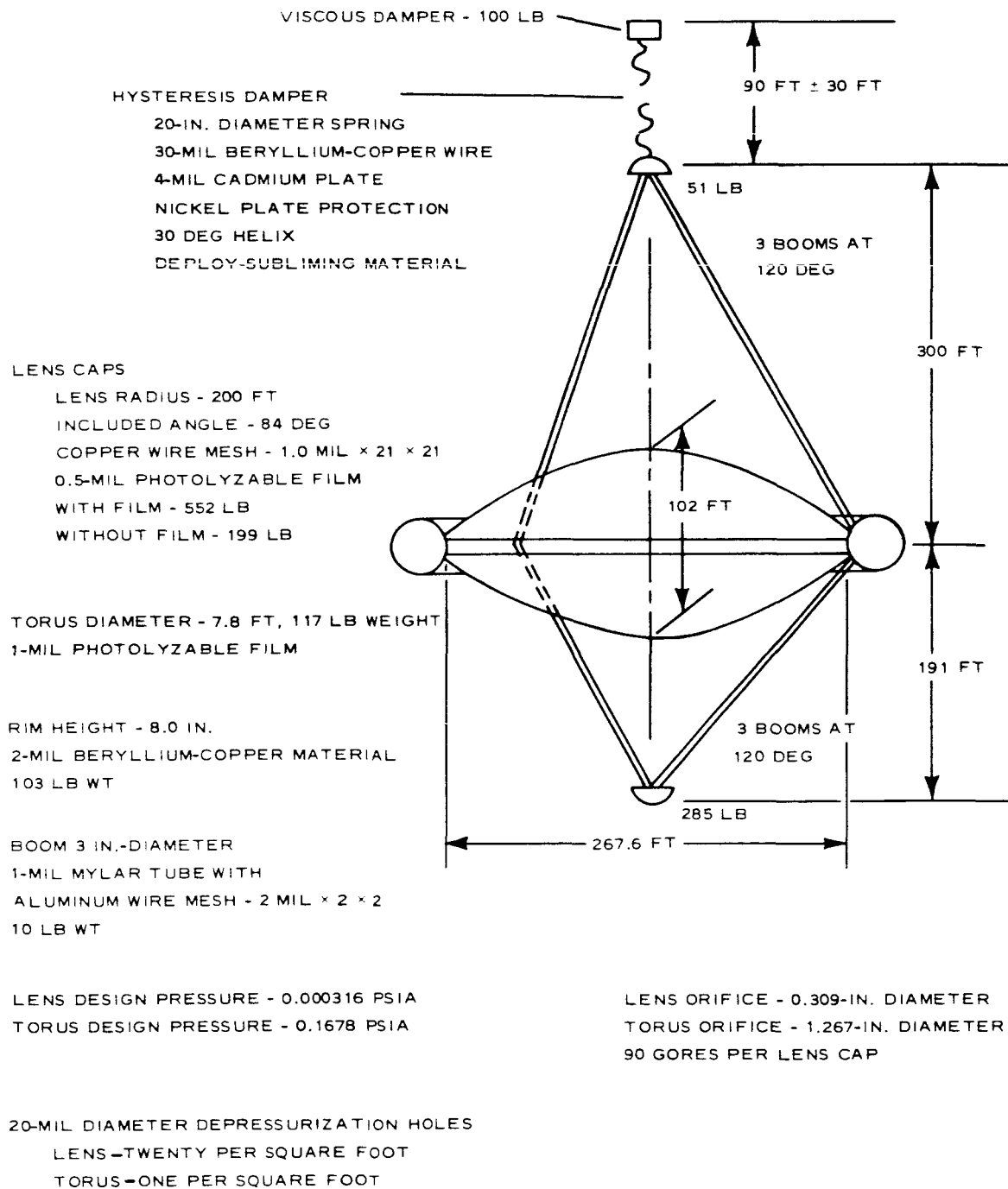


Figure 1. Design Summary of Preliminary Lenticular Satellite

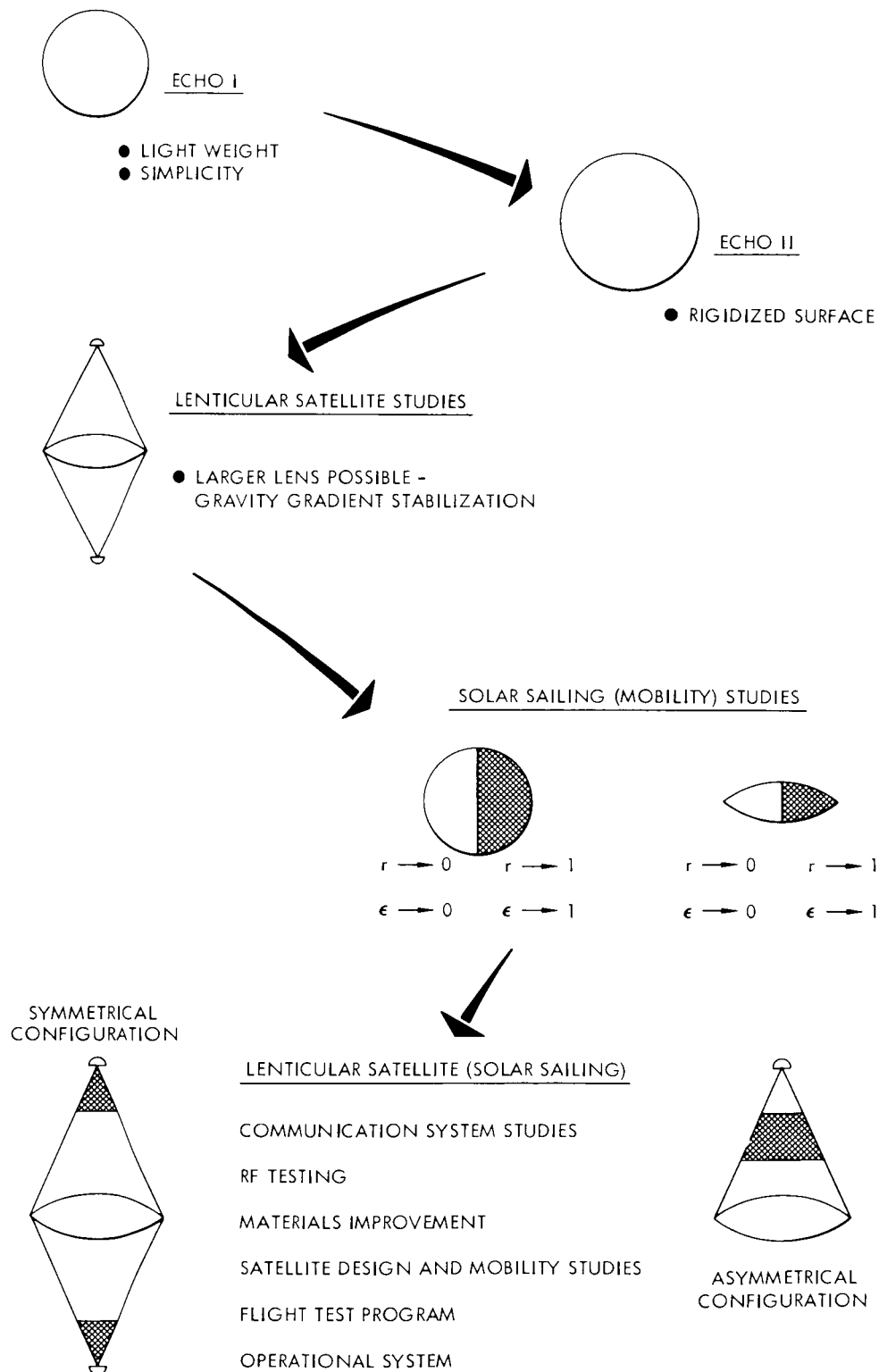


Figure 2. Passive Communication Satellite Evolution

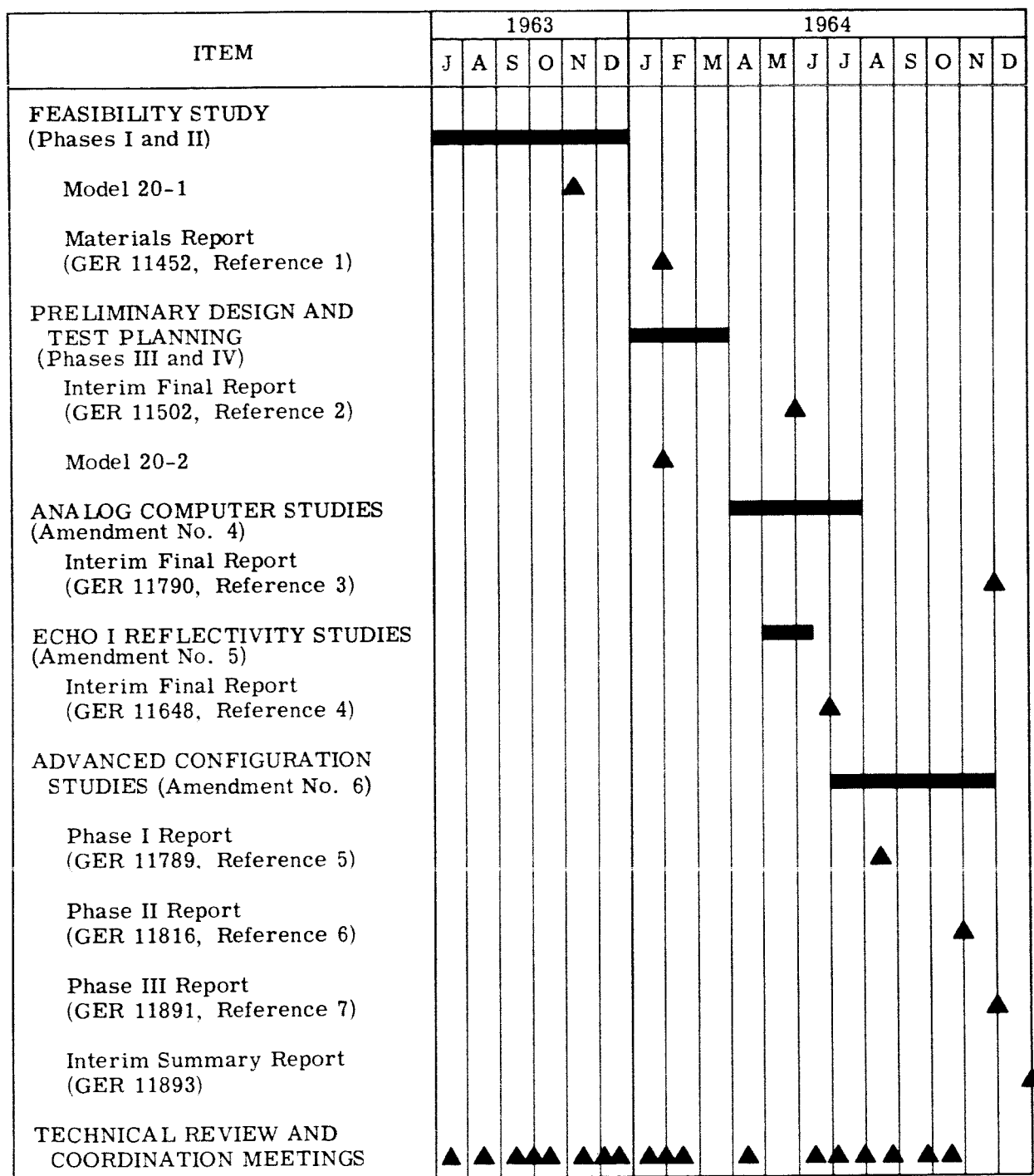


Figure 3. Lenticular Satellite Development Program - NAS 1-3114

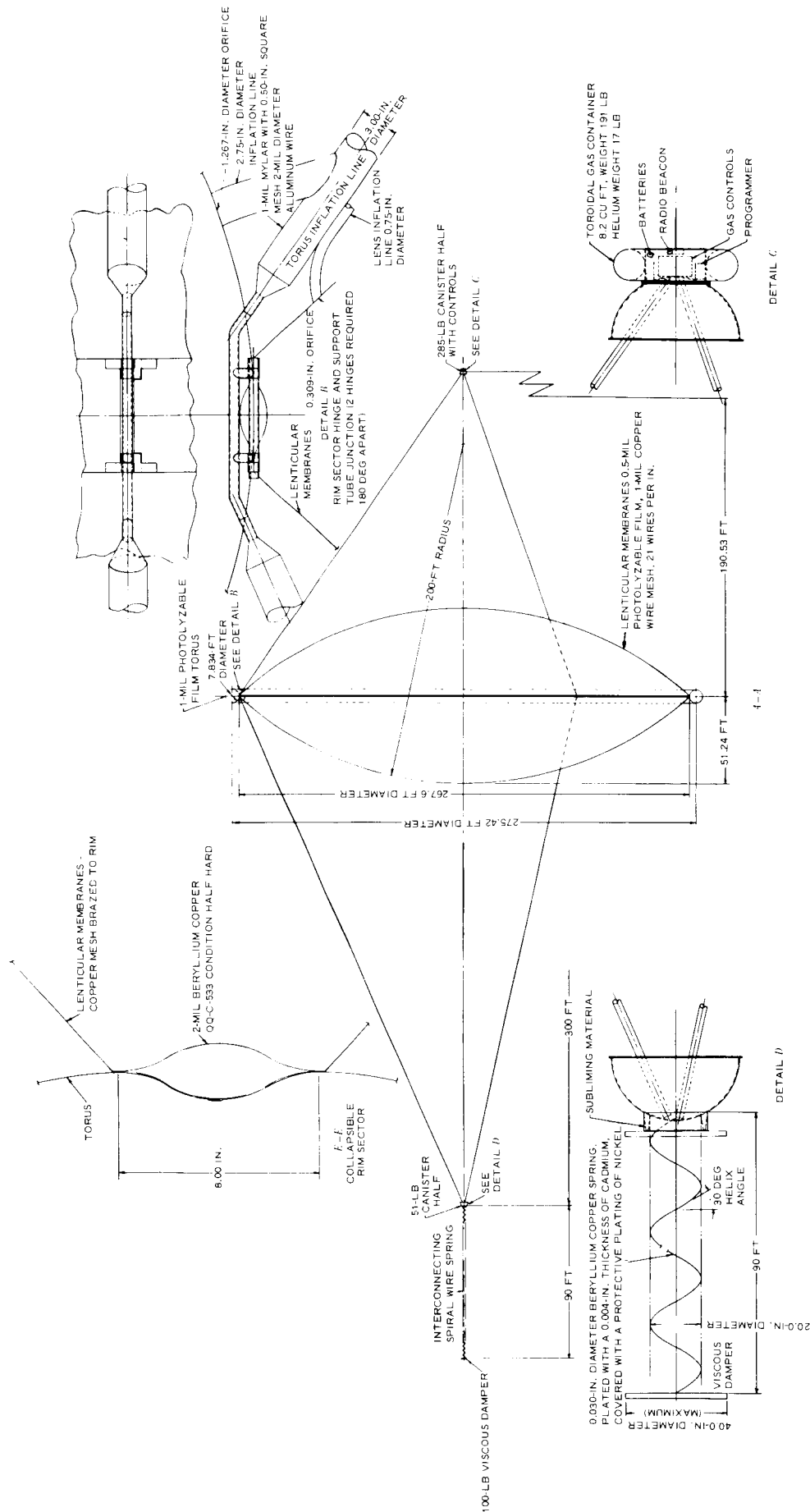


Figure 4. General Arrangement of Preliminary Lenticular Satellite (Sheet 1)

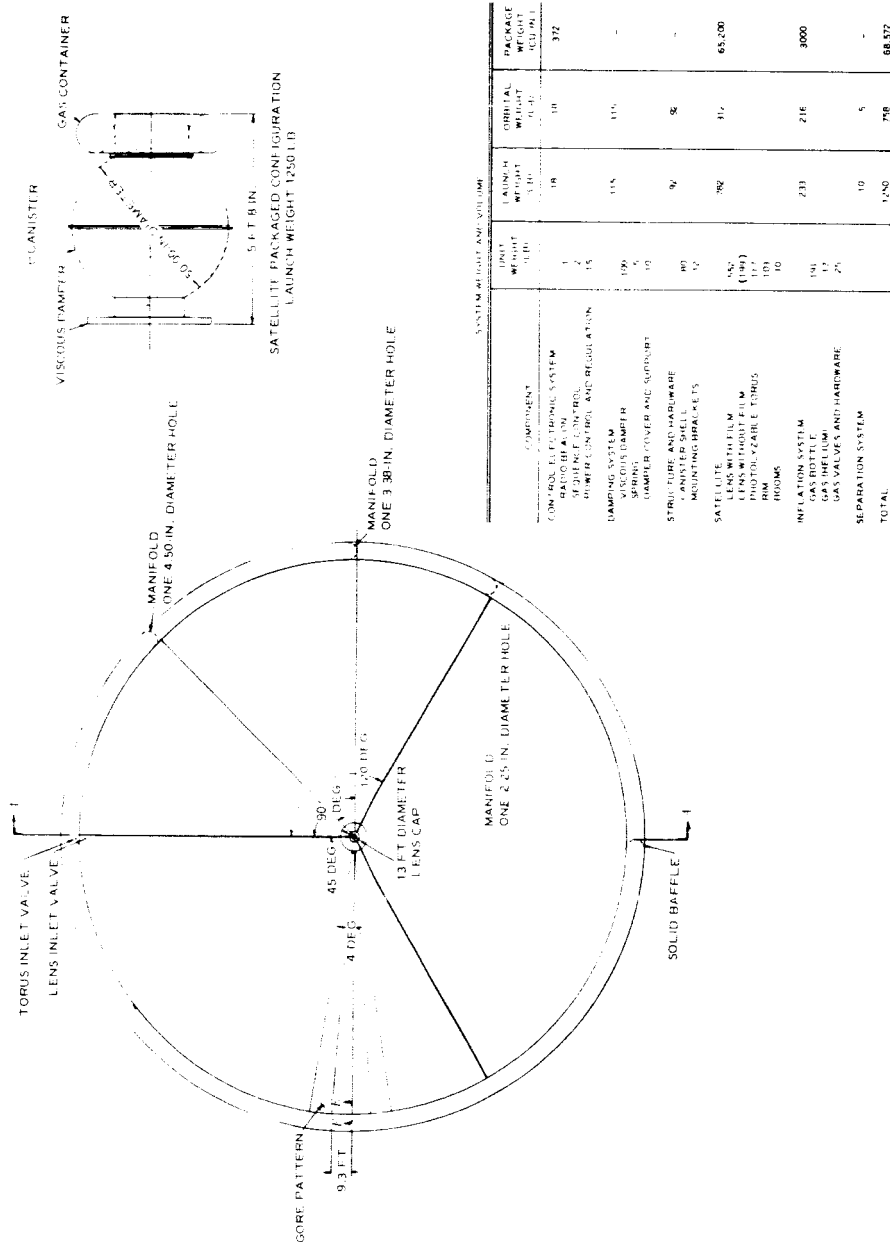


Figure 4. General Arrangement of Preliminary Lenticular Satellite (Sheet 2)

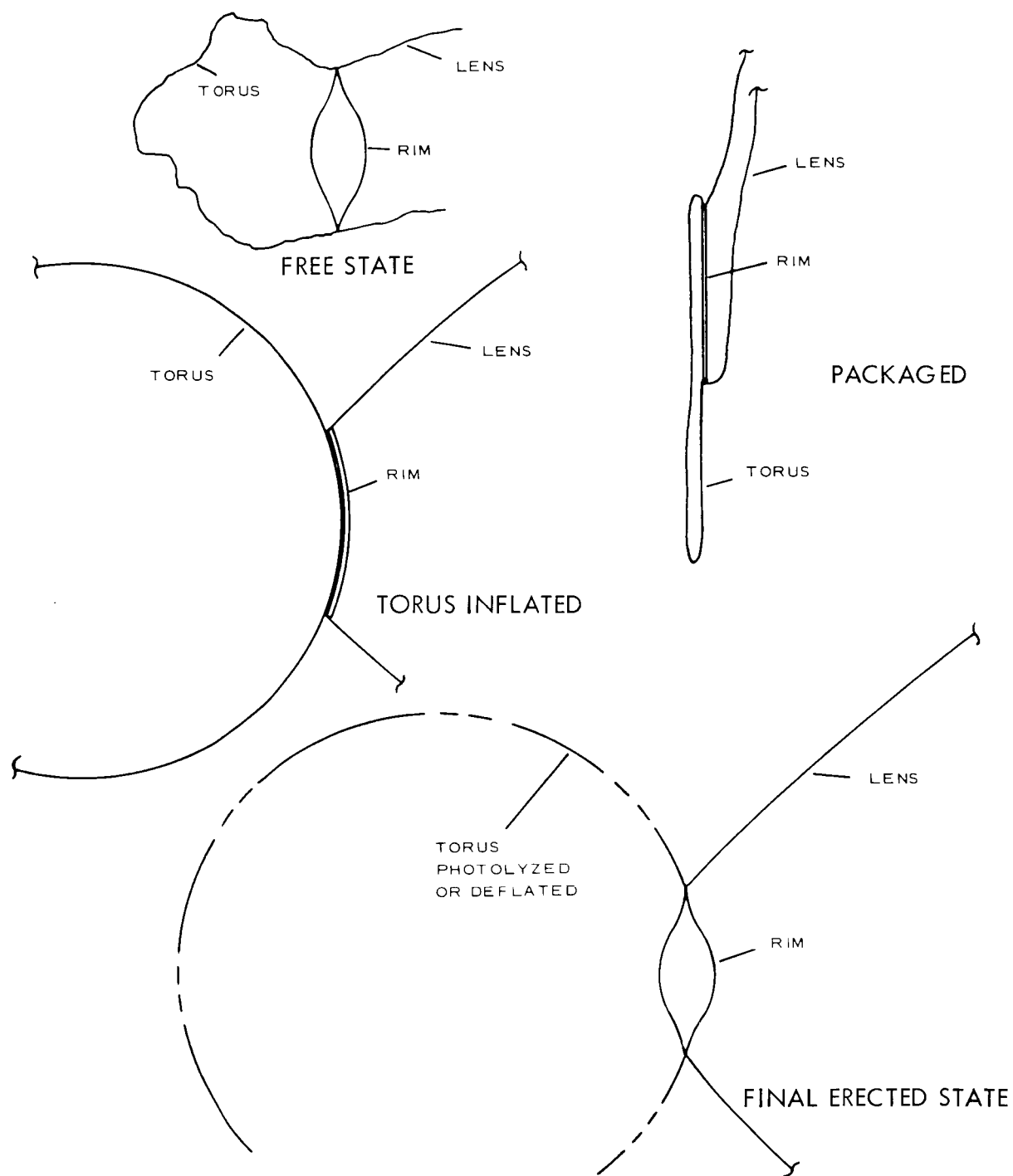


Figure 5. Collapsible Rim Functional Schematic

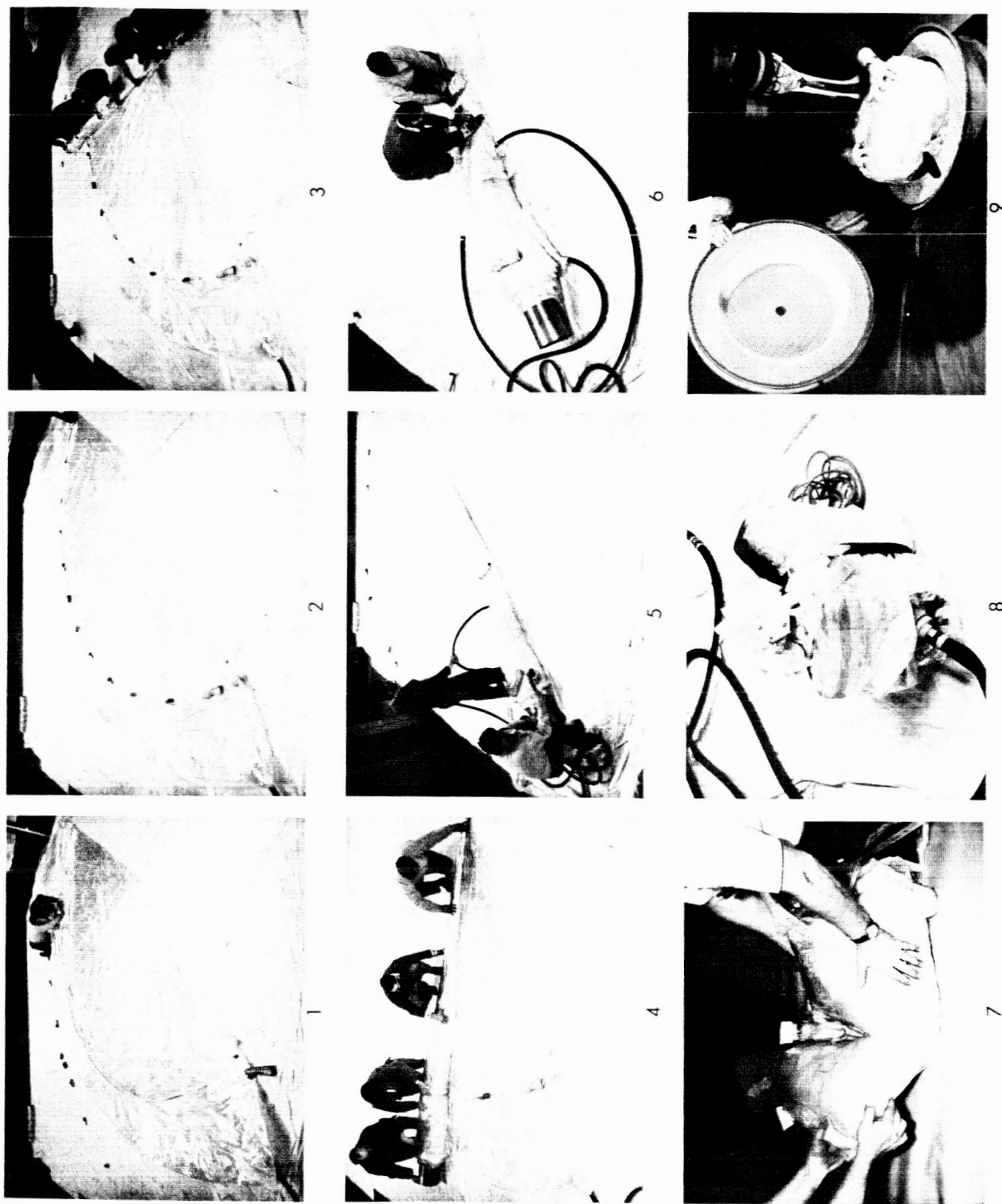


Figure 6. Packaging Sequence of Lenticular Satellite

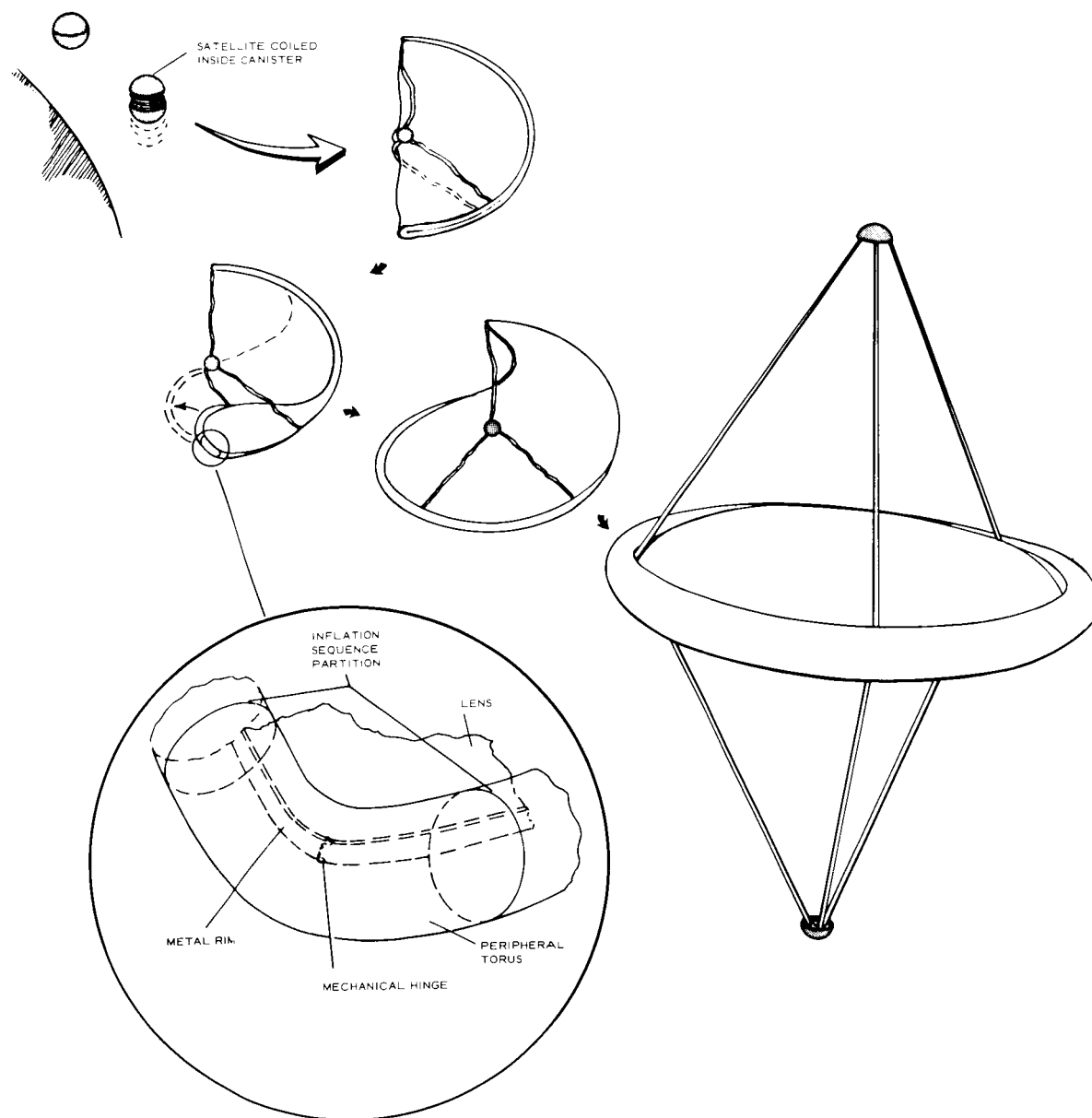


Figure 7. Deployment Sequence of Lenticular Satellite

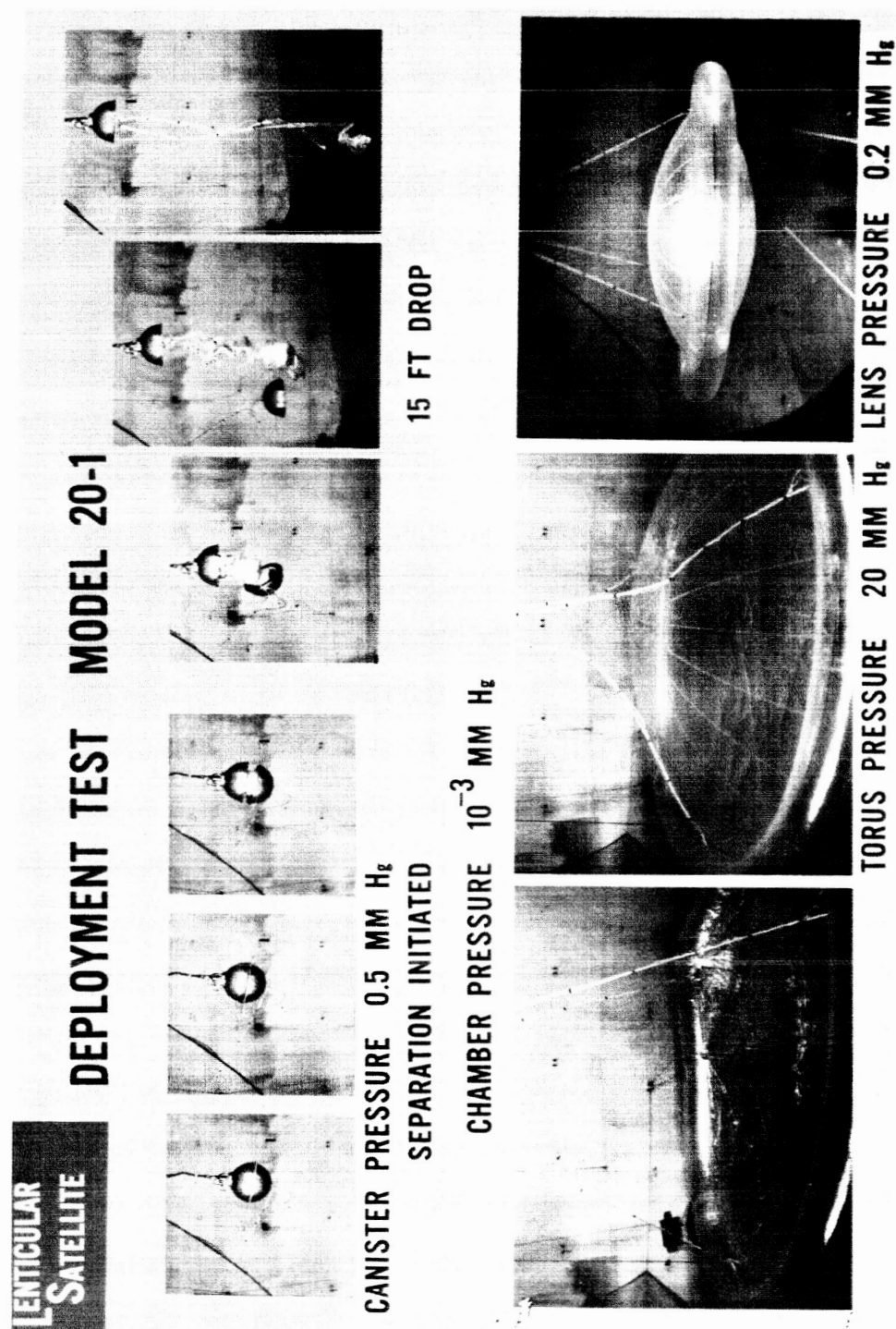


Figure 8. Deployment Sequence for Model 20-1 Vacuum Sphere Tests

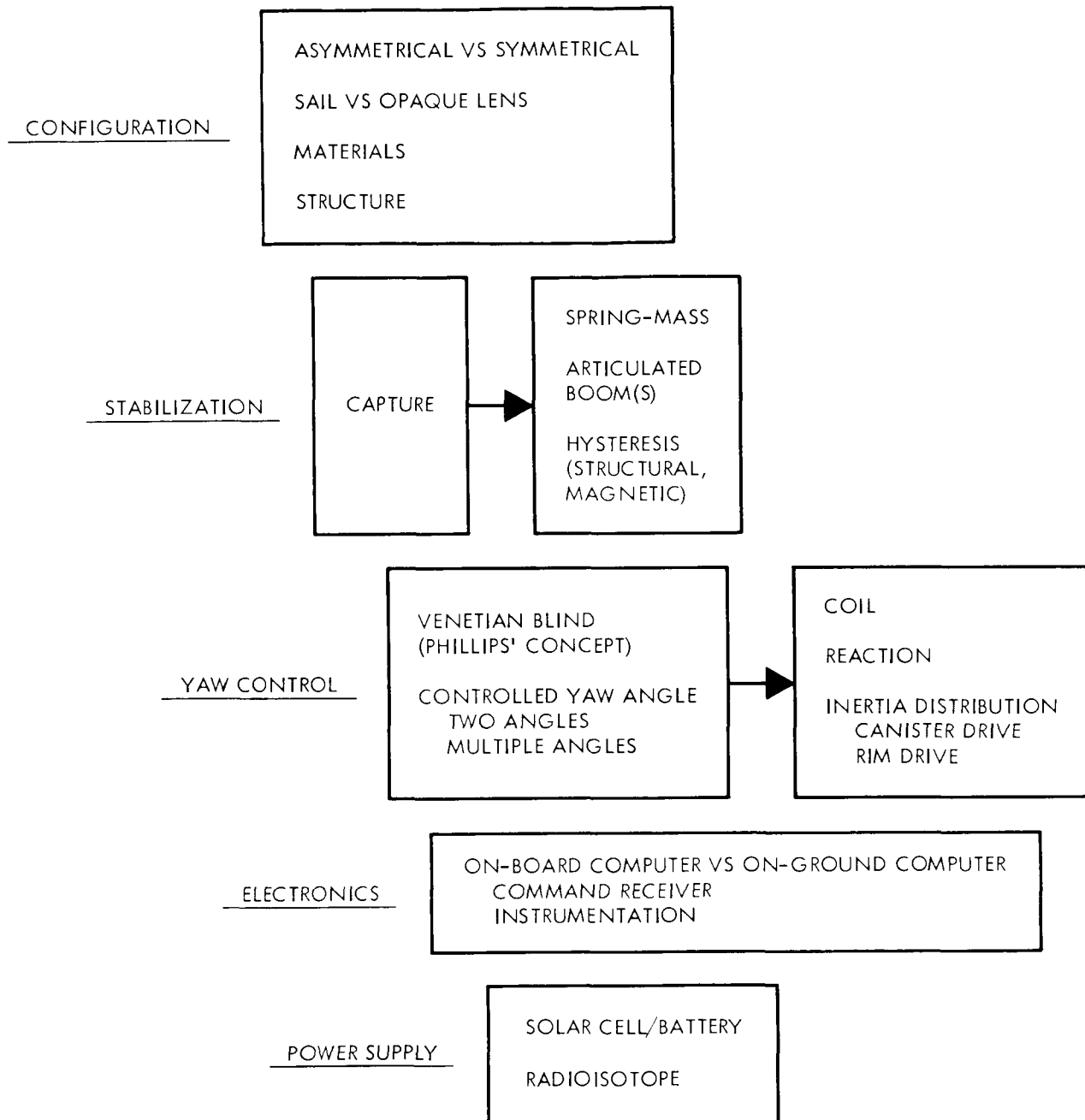


Figure 9. Design Definition Alternatives

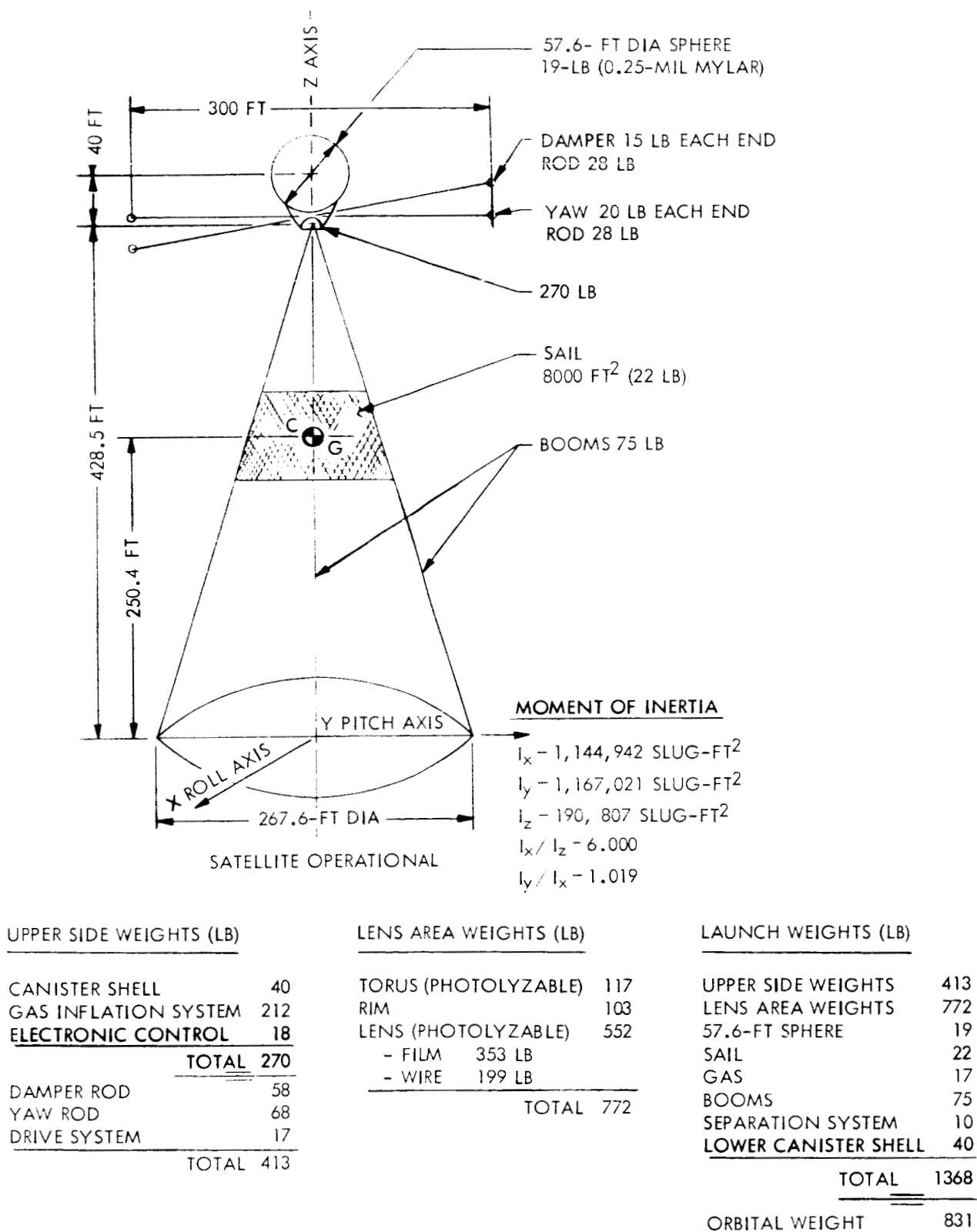


Figure 10. Base Line Asymmetrical Configuration (Sheet 1)

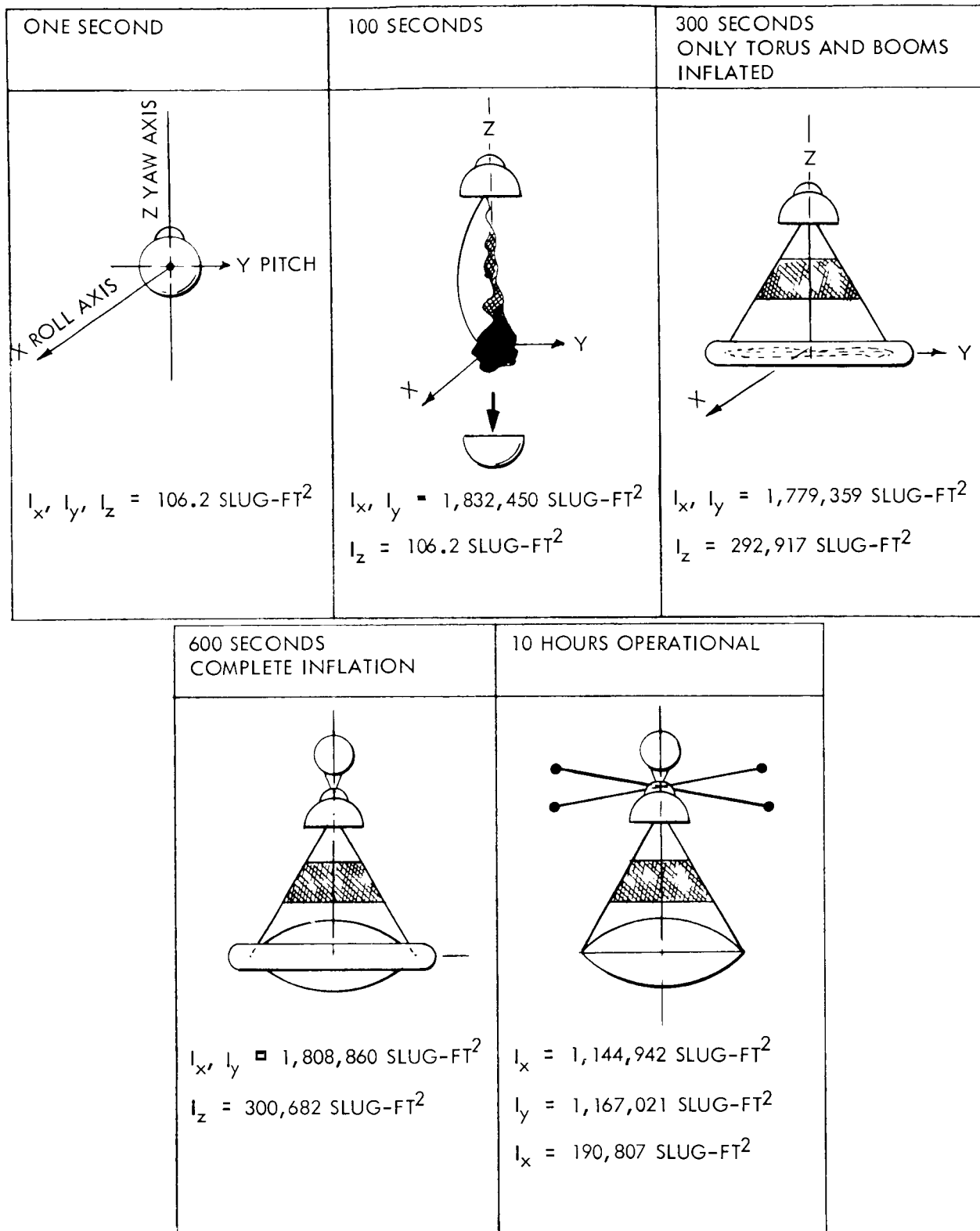
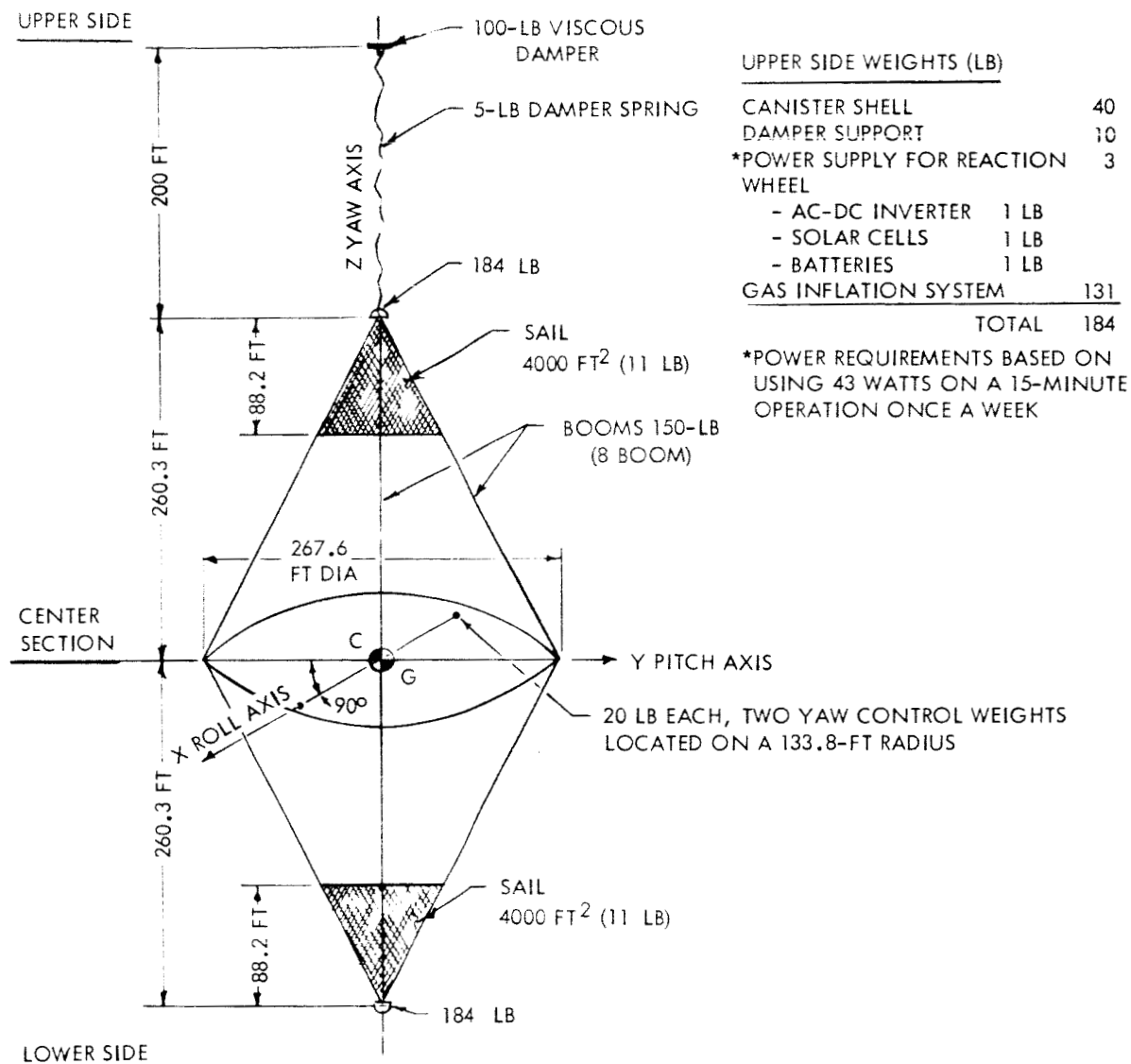


Figure 10. Base Line Asymmetrical Configuration (Sheet 2)



SATELLITE OPERATIONAL

CENTER SECTION WEIGHTS (LB)

| | |
|----------------------|------------|
| TORUS (PHOTOLYZABLE) | 117 |
| RIM | 103 |
| LENS (PHOTOLYZABLE) | 552 |
| - FILM | 353 LB |
| - WIRE | 199 LB |
| YAW CONTROL WEIGHT | 40 |
| TOTAL | 812 |

LOWER SIDE WEIGHTS (LB)

| | |
|--------------------------|------------|
| CANISTER SHELL | 40 |
| REACTION WHEEL | 25 |
| SUPPORT BR'KT & HARDWARE | 4 |
| ELECTRONIC CONTROLS | 18 |
| BR'KTS & HARDWARE | 2 |
| GAS INFLATION SYSTEM | 95 |
| TOTAL | 184 |

LAUNCH WEIGHT (LB)

| | |
|-------------------|-------------|
| VISCOUS DAMPER | 105 |
| UPPER SIDE | 184 |
| CENTER SECTION | 812 |
| LOWER SIDE | 184 |
| SAIL | 22 |
| GAS | 17 |
| BOOMS | 150 |
| SEPARATION SYSTEM | 10 |
| TOTAL | 1484 |
| ORBITAL WEIGHT | 987 |

Figure 11. Base Line Symmetrical Configuration (Sheet 1)

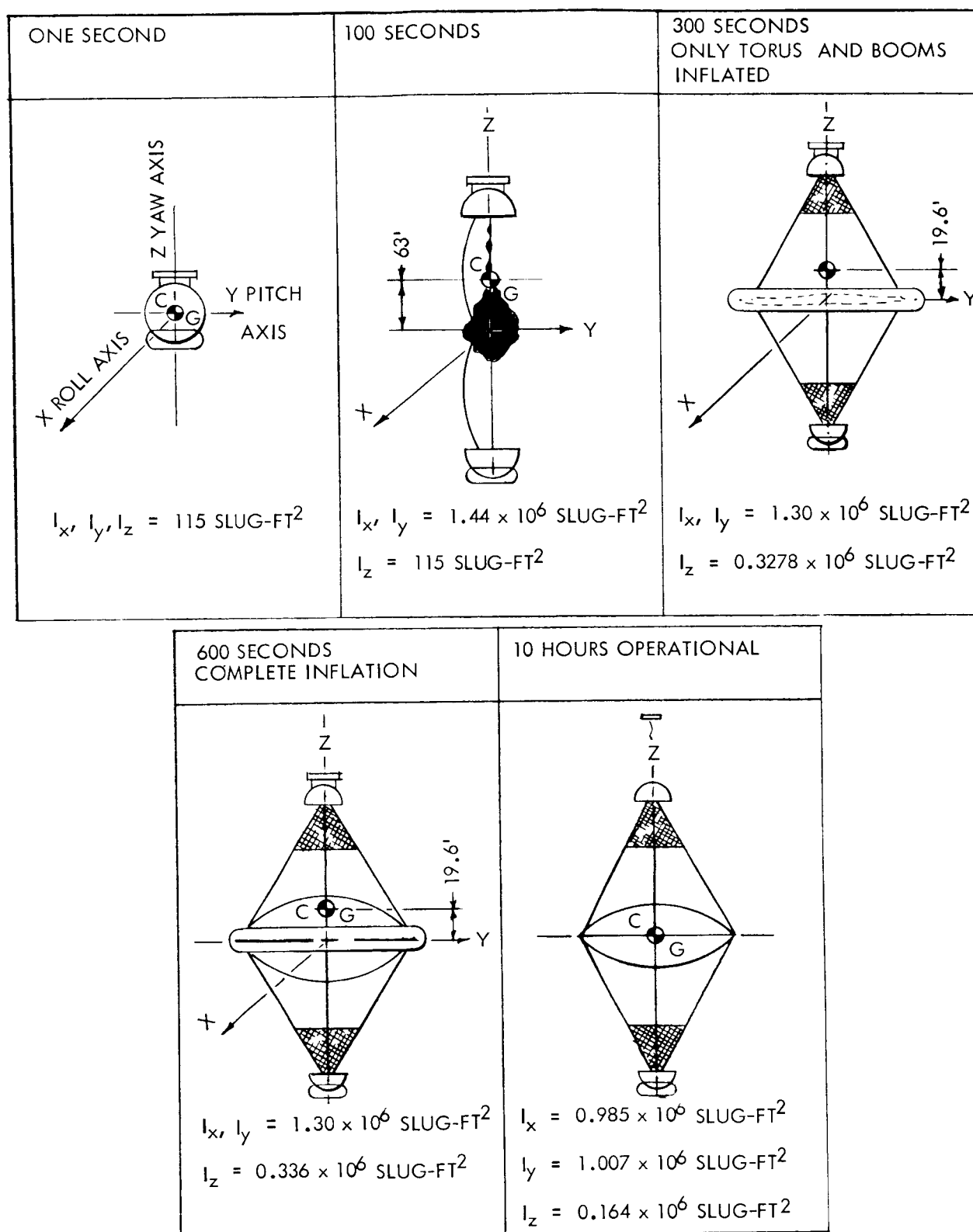
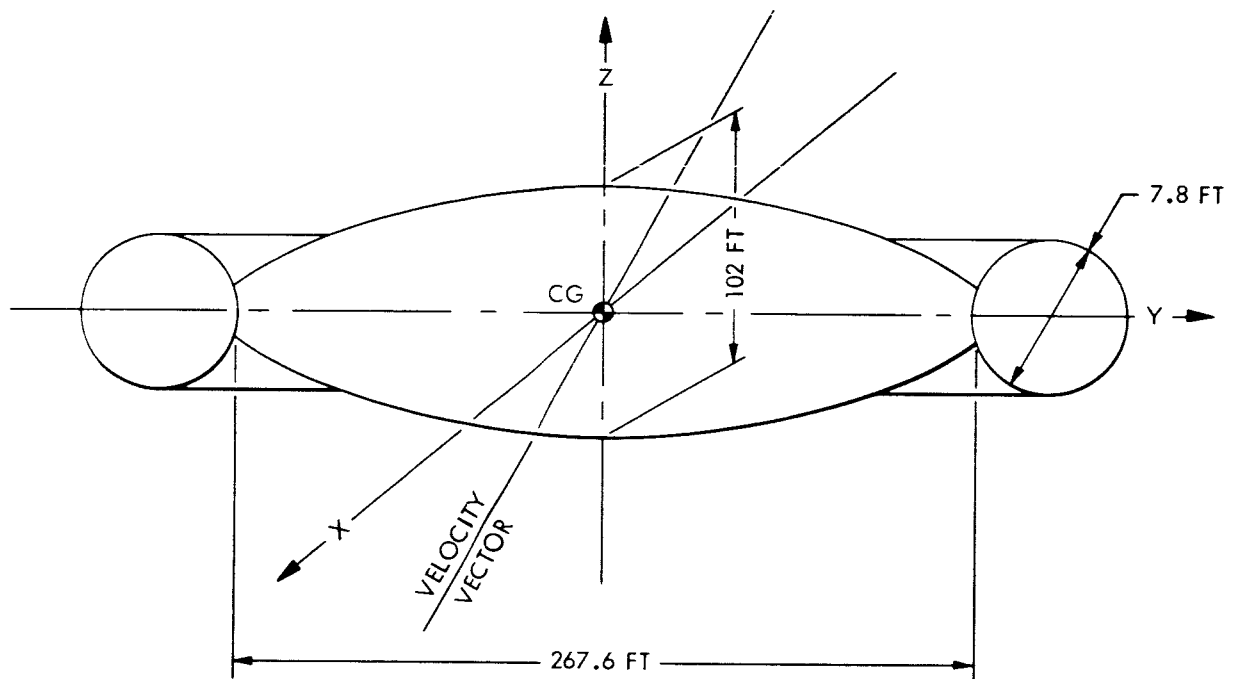


Figure 11. Base Line Symmetrical Configuration (Sheet 2)



| | WITHOUT FILM | WITH FILM |
|-----------------------------|-----------------|----------------|
| I_x (LB-FT ²) | 2.20 (10^6) | 5.1 (10^6) |
| I_y (LB-FT ²) | 2.20 (10^6) | 5.1 (10^6) |
| I_z (LB-FT ²) | 3.7 (10^6) | 9.2 (10^6) |
| W (LB) | 300 | 770 |

Figure 12. Basic Lenticular Satellite Lens, Torus, and Rim Data

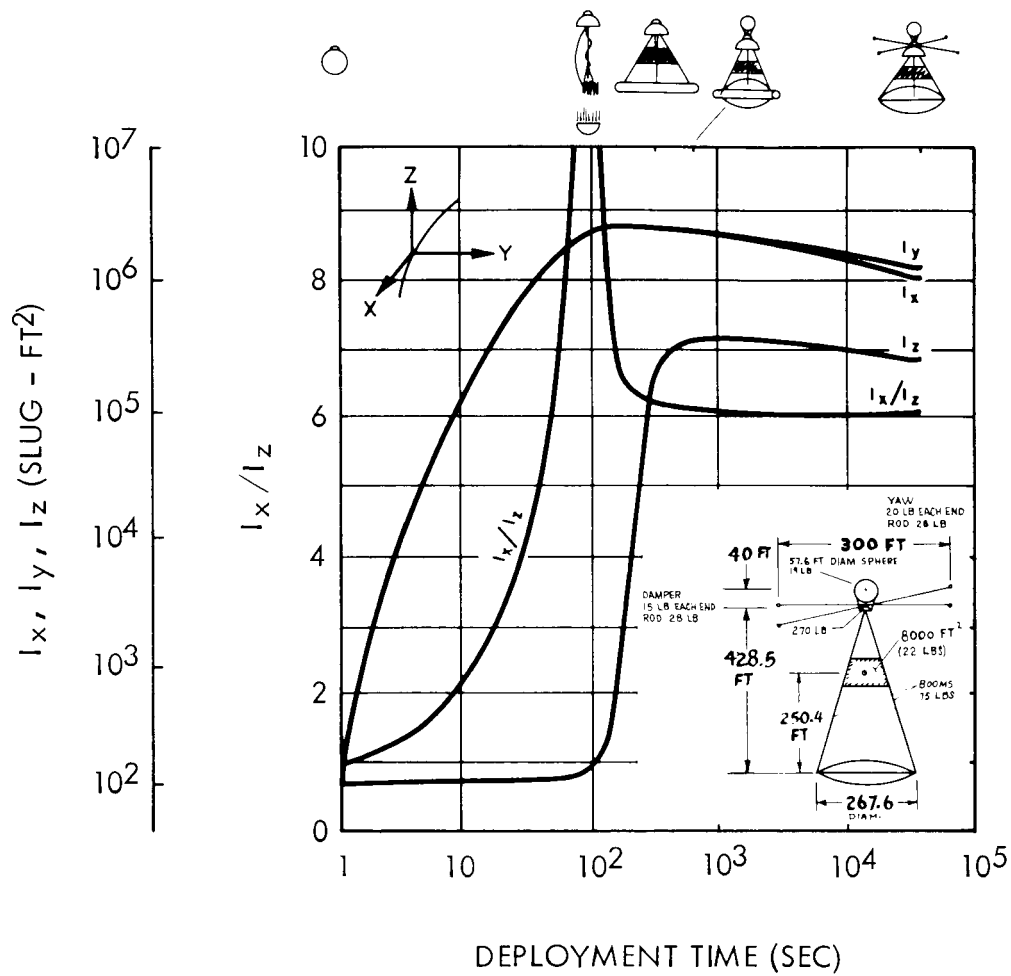


Figure 13. Deployment Sequence of Base Line Asymmetrical Configuration

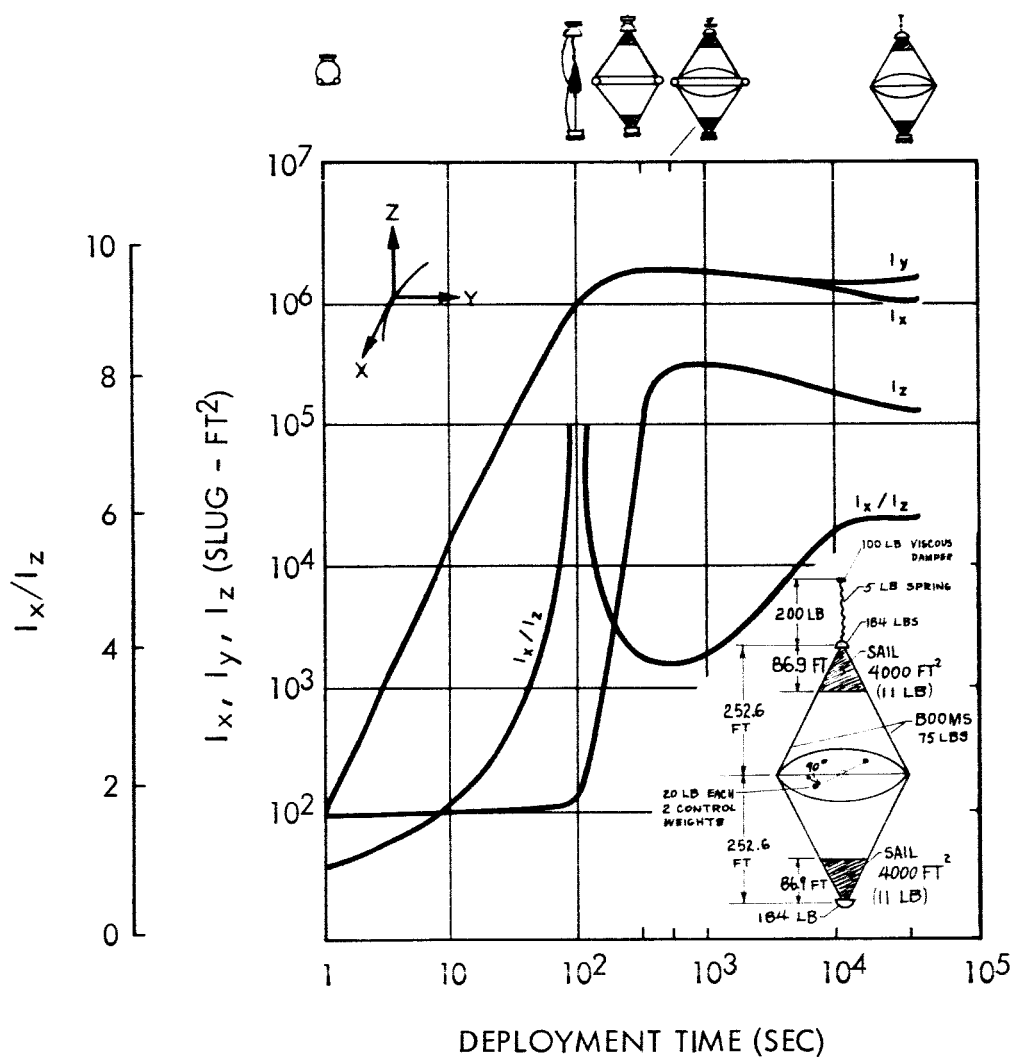
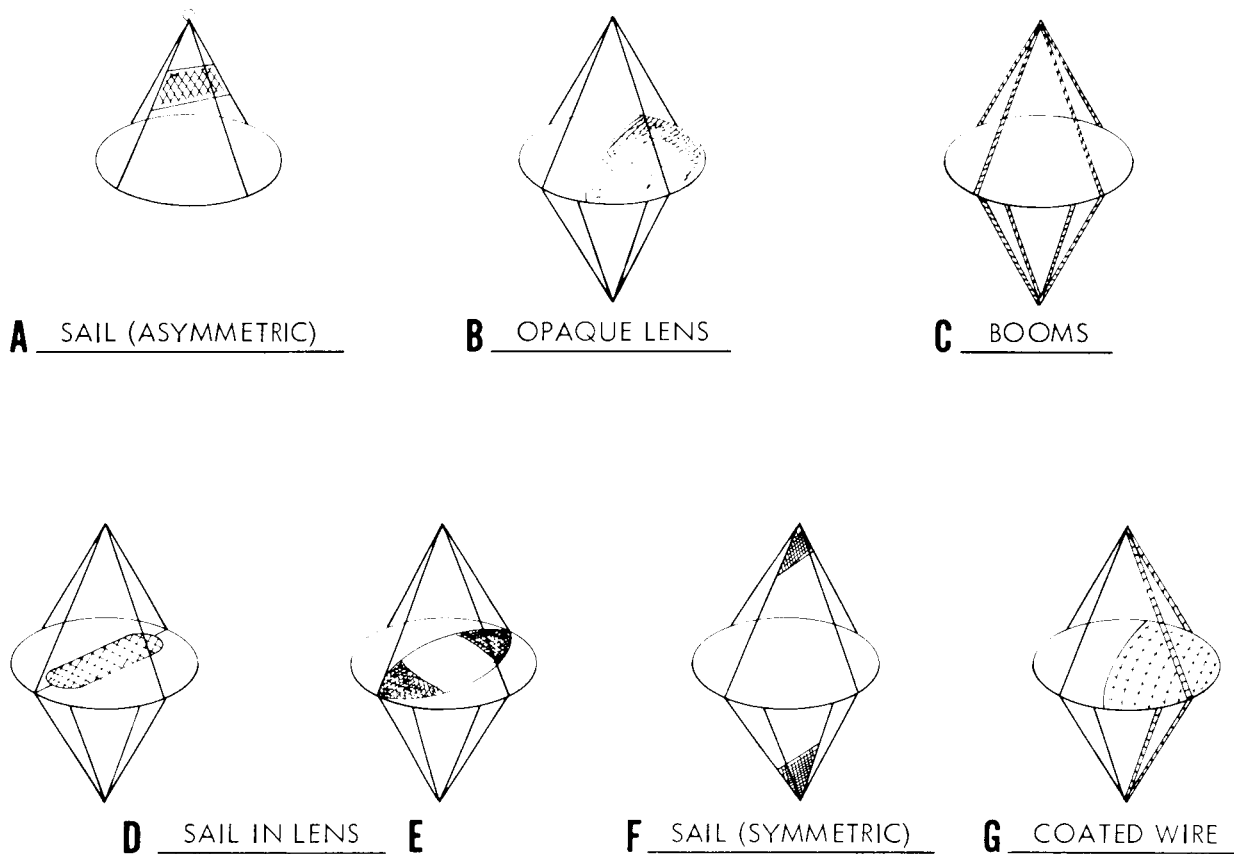


Figure 14. Deployment Sequence of Base Line Symmetrical Configuration



MOBILITY - 100 DEG/MONTH

OPTICAL CHARACTERISTICS - DIFFUSE REFLECTANCE

ENERGY INPUTS - SOLAR RADIATION, ALBEDO, RERADIATION

UPSETTING TORQUES - MINIMUM OR BALANCED

Figure 15. Sail Configuration for Lenticular Satellite

CONDITIONS

- 1. UV INTENSITY* - APPROXIMATELY 0.012 W/CM²
- 2. VACUUM PRESSURE - APPROXIMATELY 5 x 10⁻⁵ mm Hg

*UV SUPPLIED BY GE TYPE UA-2 LAMP

**SAMPLE AGED AT 400°F IN VACUUM FOR 3 HOURS, THEN PHOTOLYZED AT 350°F

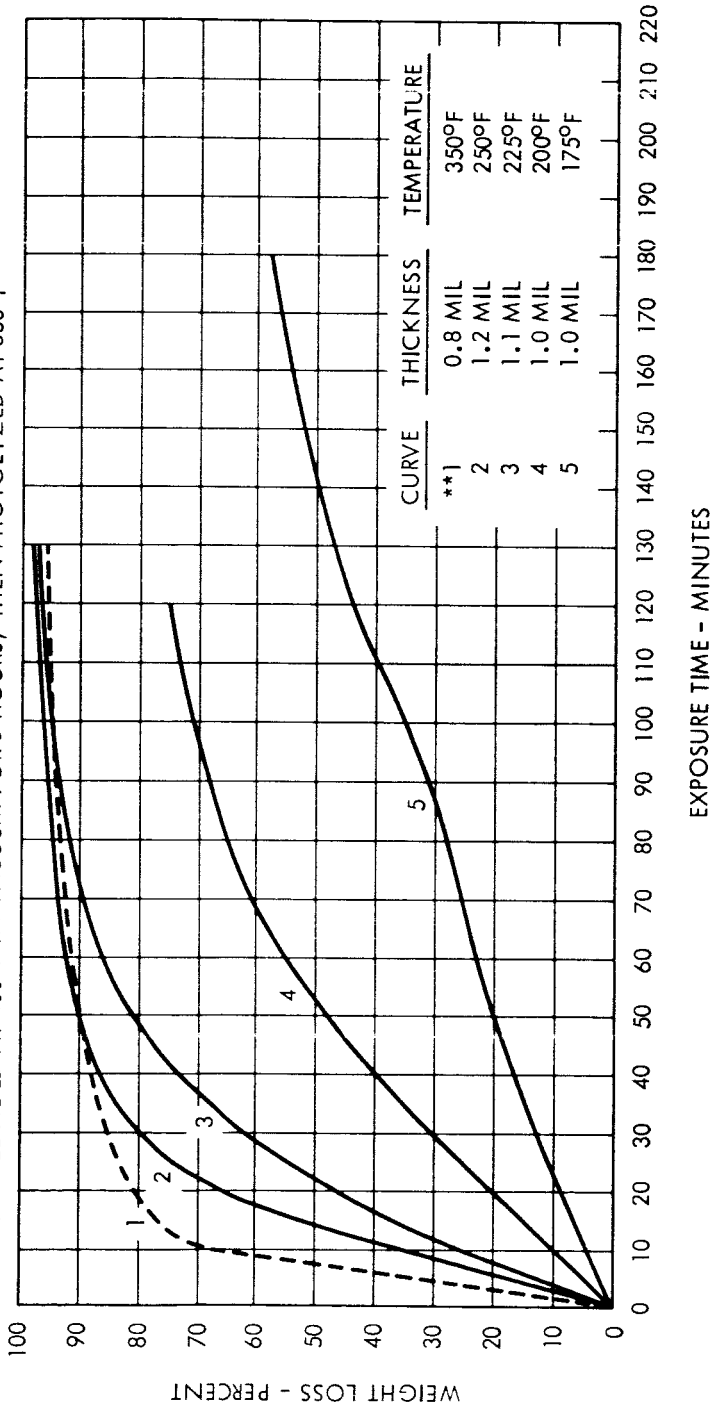


Figure 16. Effect of Temperature on Weight Loss Behavior of Clear Photolyzable Film

CONDITIONS

1. SAMPLE TEMPERATURE - 225°F
2. UV INTENSITY* - APPROXIMATELY 0.012 W/CM²
3. VACUUM PRESSURE - 5×10^{-5} mm Hg

*UV SUPPLIED BY GE TYPE UA-2 LAMP

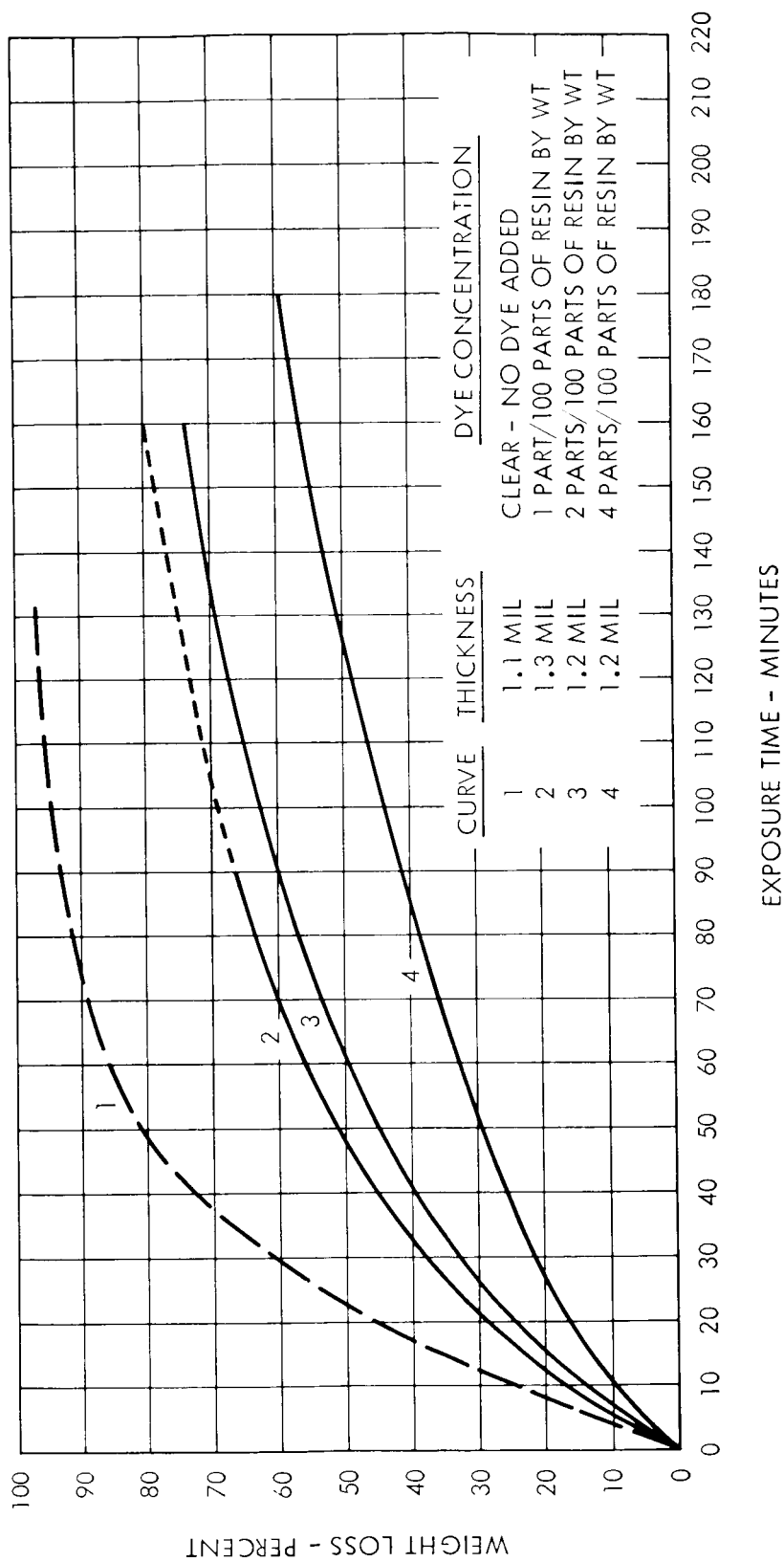


Figure 17. Effect of Type SP Dye on Weight Loss Behavior of Photolizable Film

NOTES: WIRE - 210 FT LONG, 1/8-IN. DIA ($\lambda = 1.18$)
WIRE GRID - 210 FT LONG, 4.1-IN. DIA ($\lambda = 5.59$)

FUNCTION OF θ

σ REFERENCED TO 200-FT RADIUS SPHERE

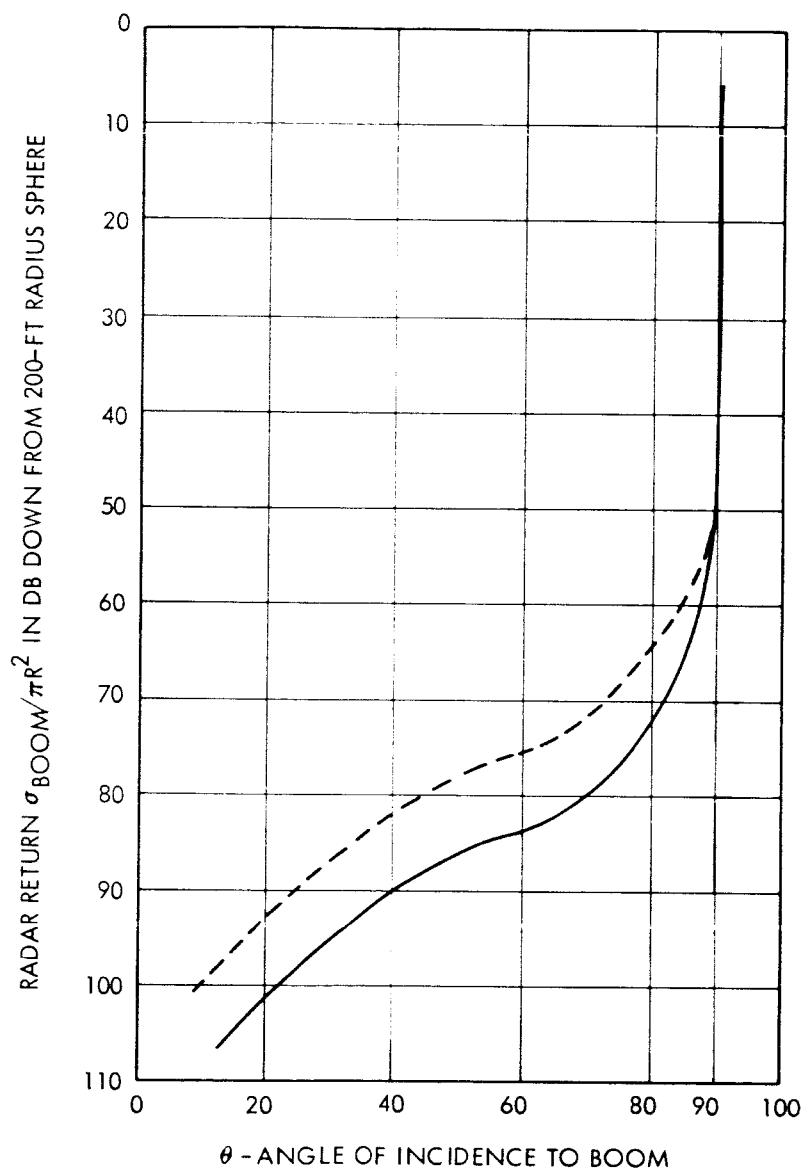


Figure 18. Boom Radar Return versus Angle of Incidence to Boom

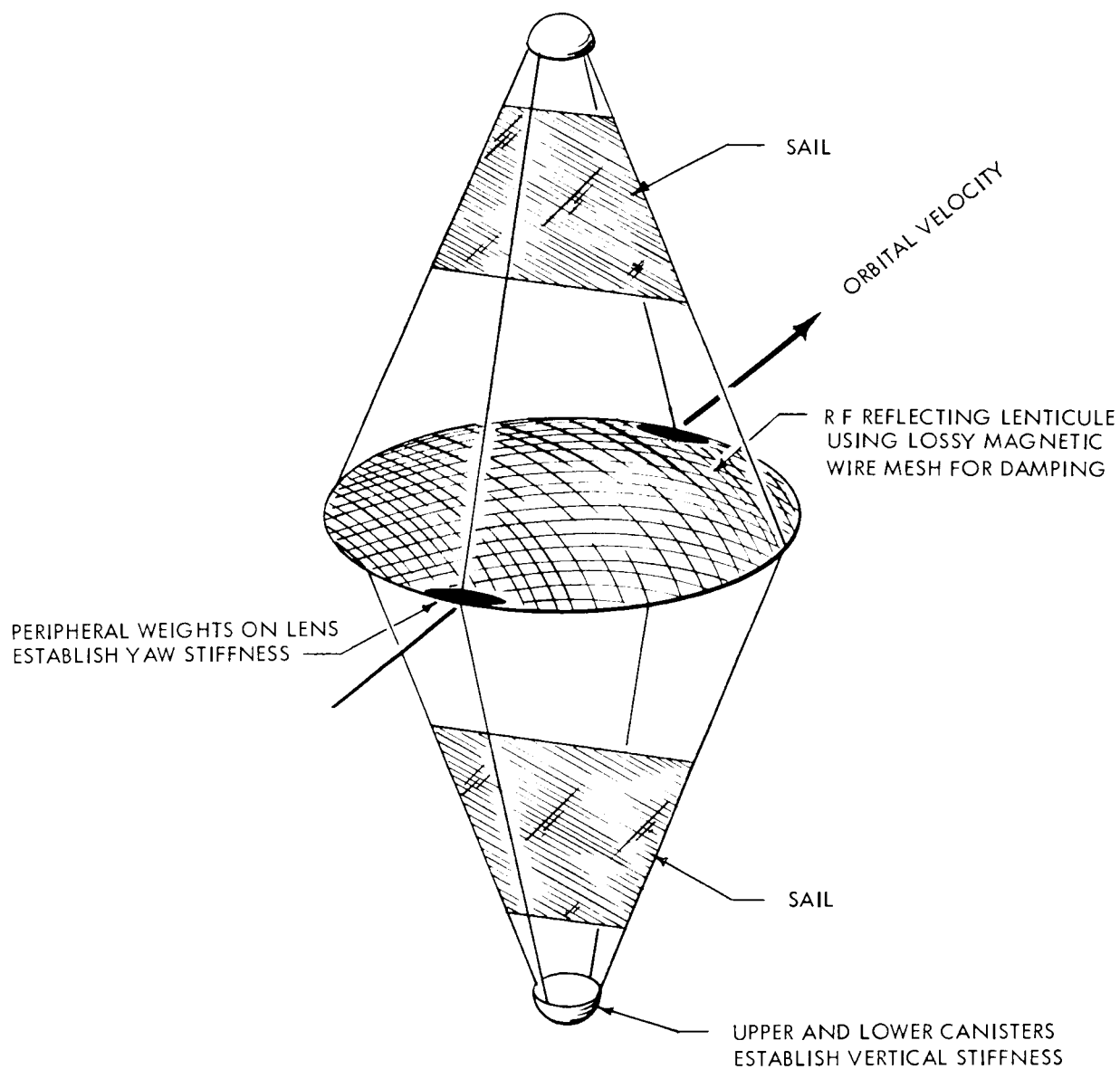


Figure 19. Proposed Configuration of Gravity Gradient Solar Sailing Communication Satellite

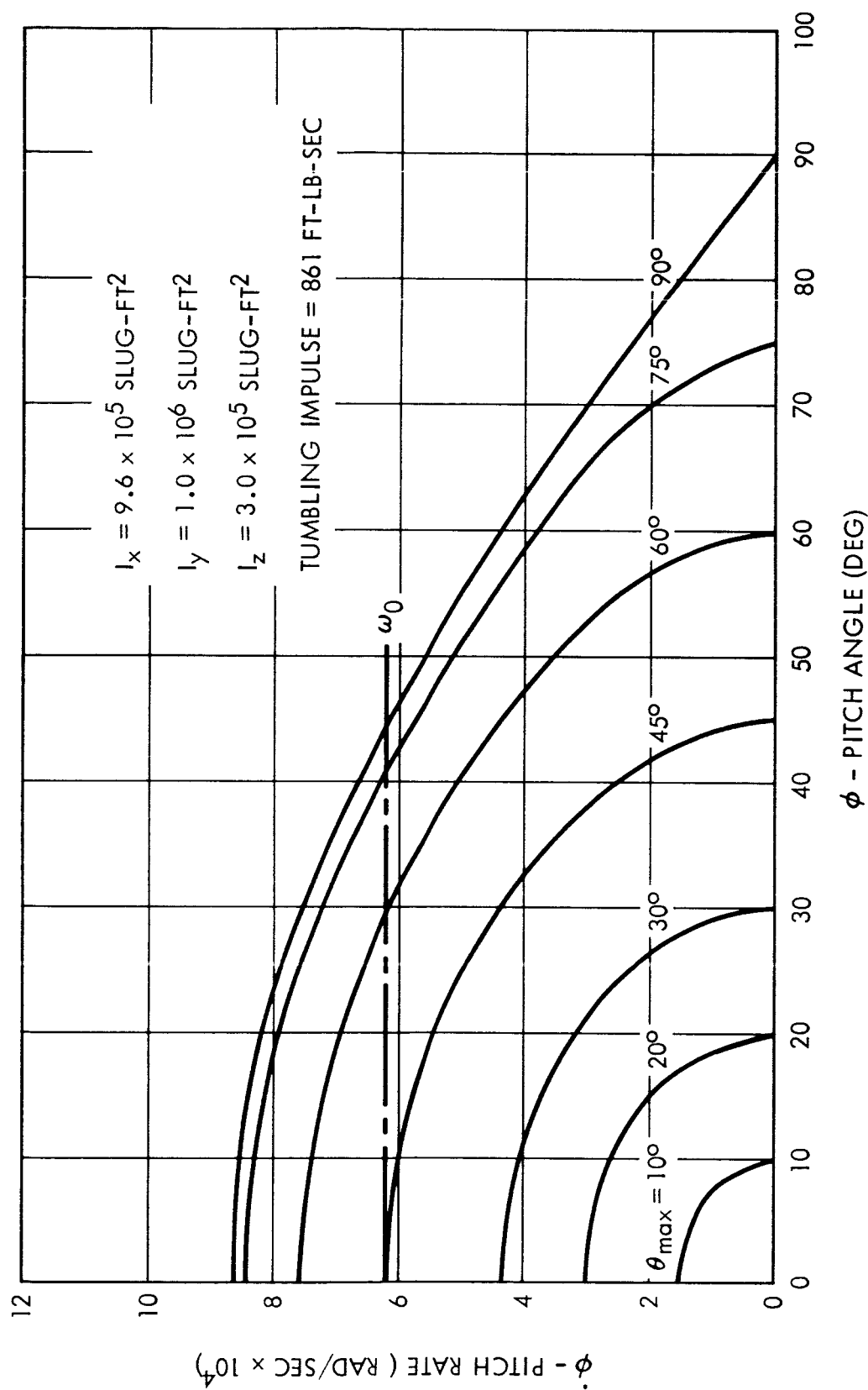


Figure 20. Pitch Axis Phase Plane - Case A

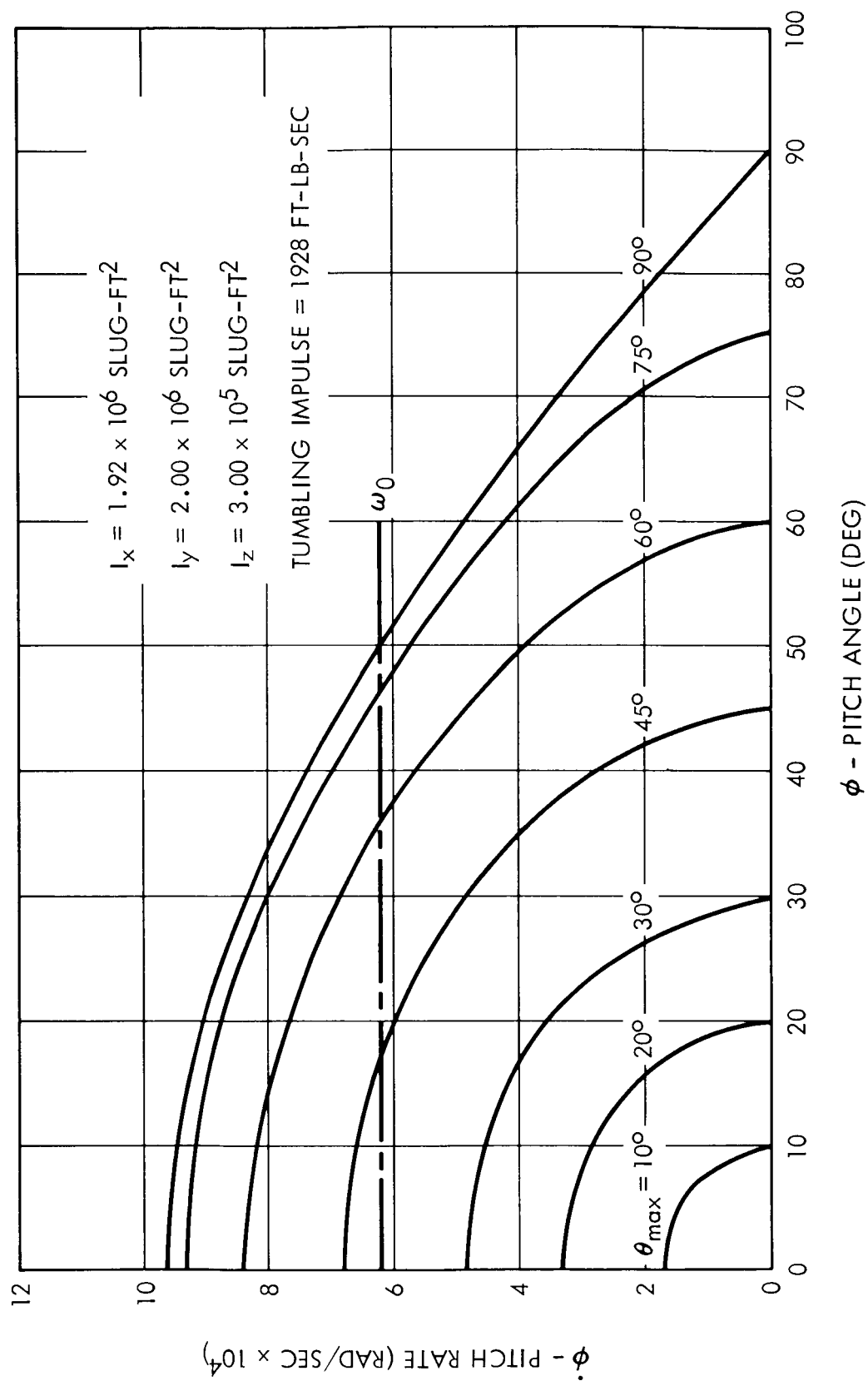


Figure 21. Pitch Axis Phase Plane - Case B

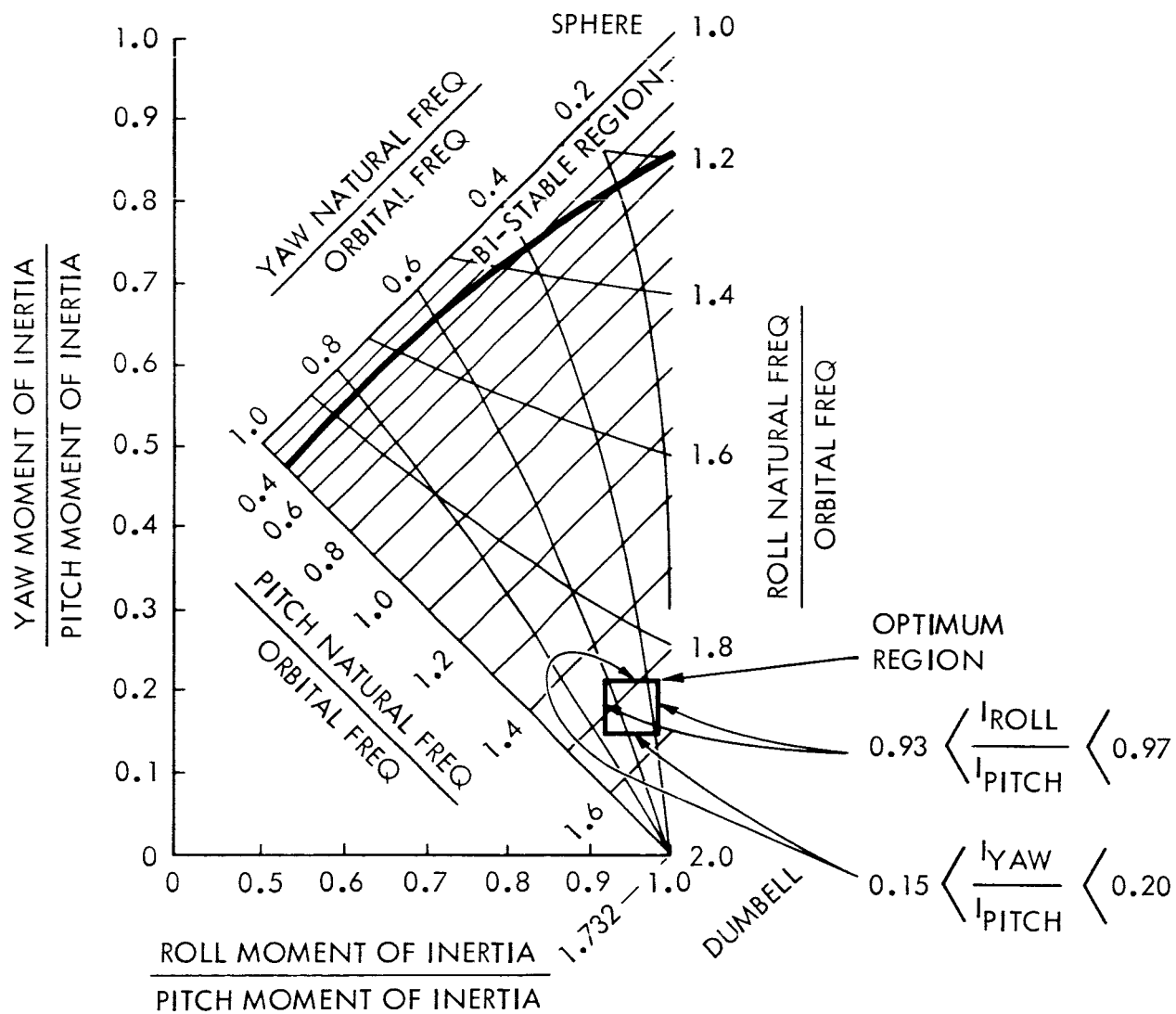


Figure 22. Natural Frequencies versus Inertia Ratios

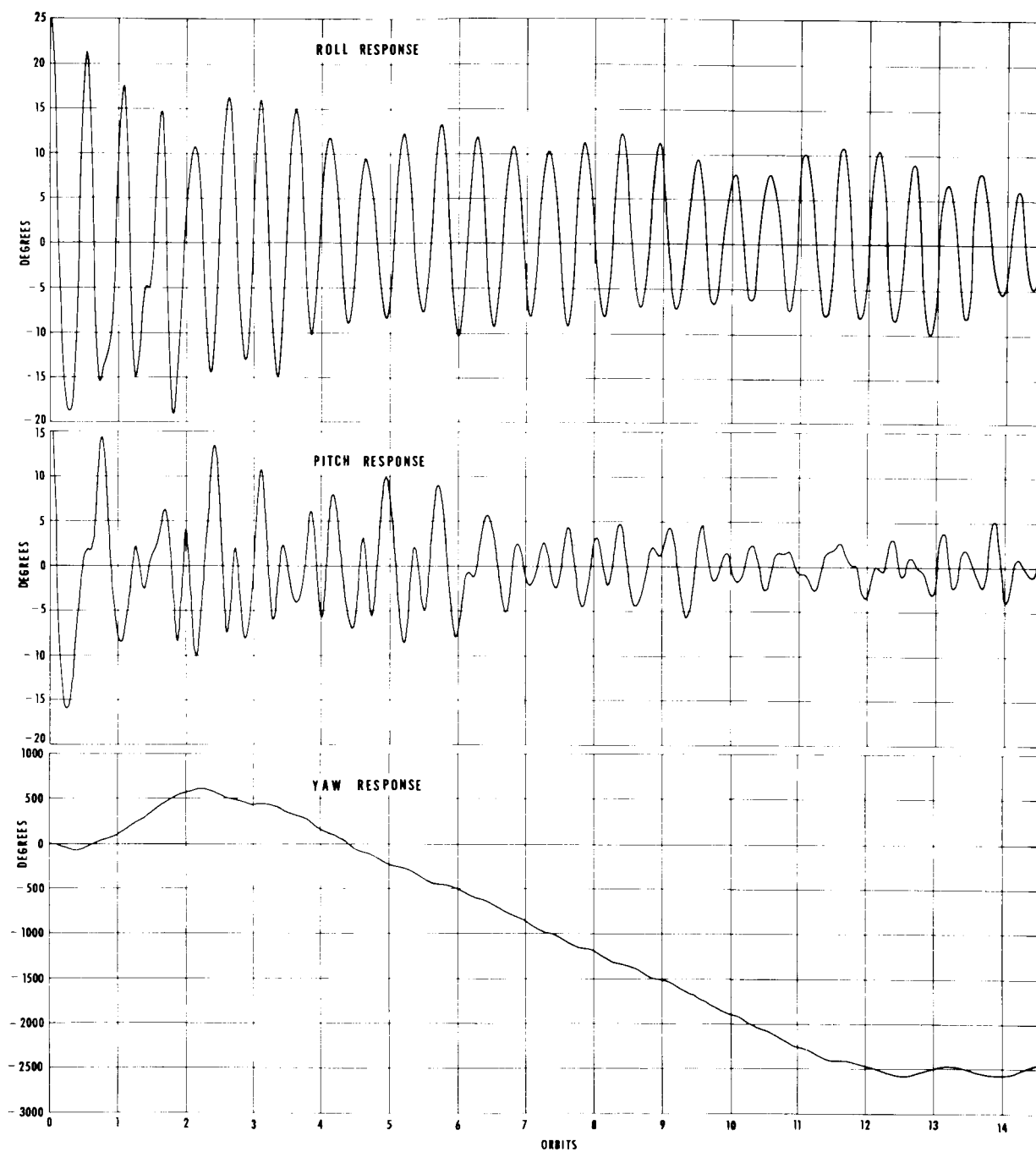


Figure 23. Lensat Transient Attitude Response Using Rice/Wilberforce Damper (Sheet 1)

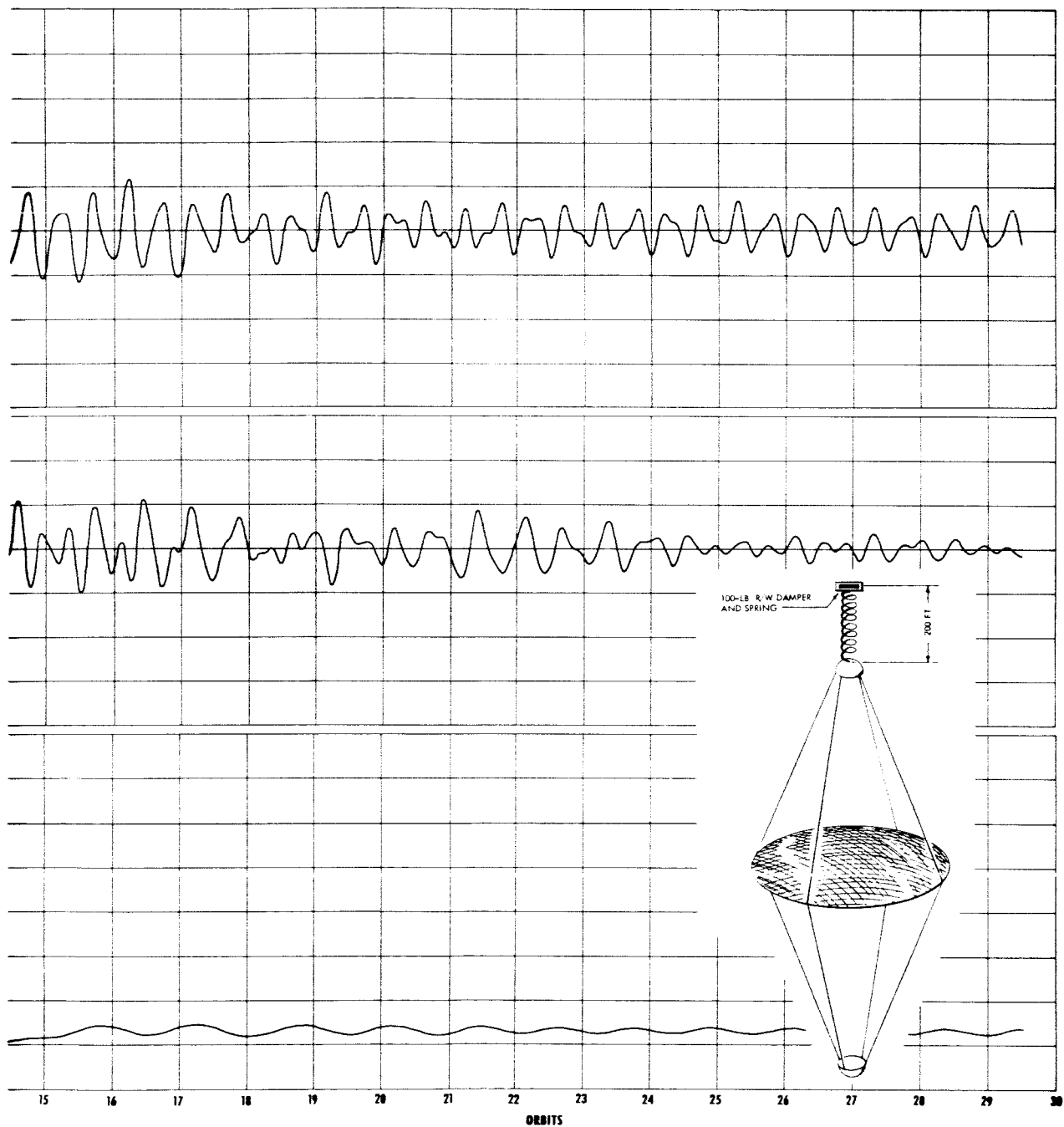


Figure 23. Lensat Transient Attitude Response Using
Rice/Wilberforce Damper (Sheet 2)

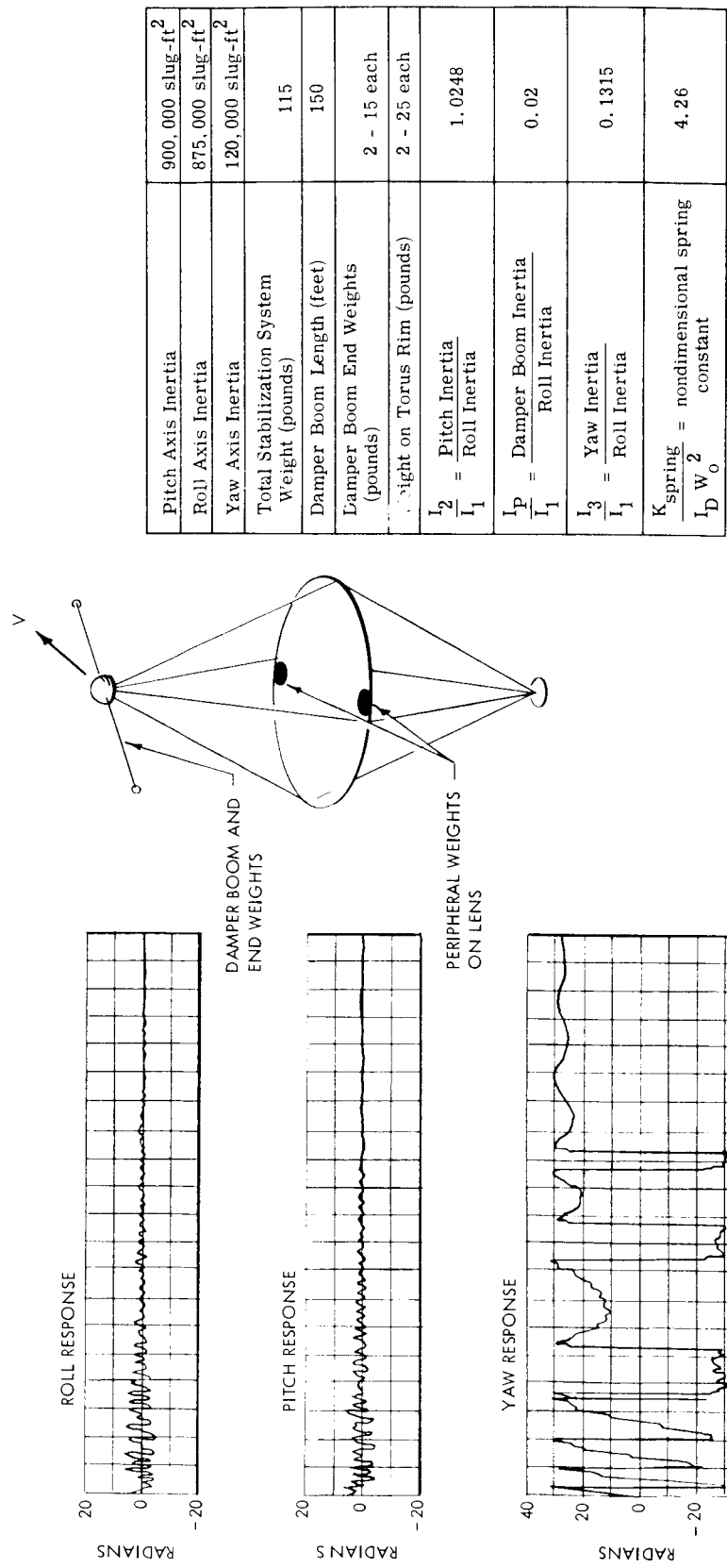


Figure 24. Lensat Transient Attitude Response Using Ames Damper - Lens Film Photolyzed

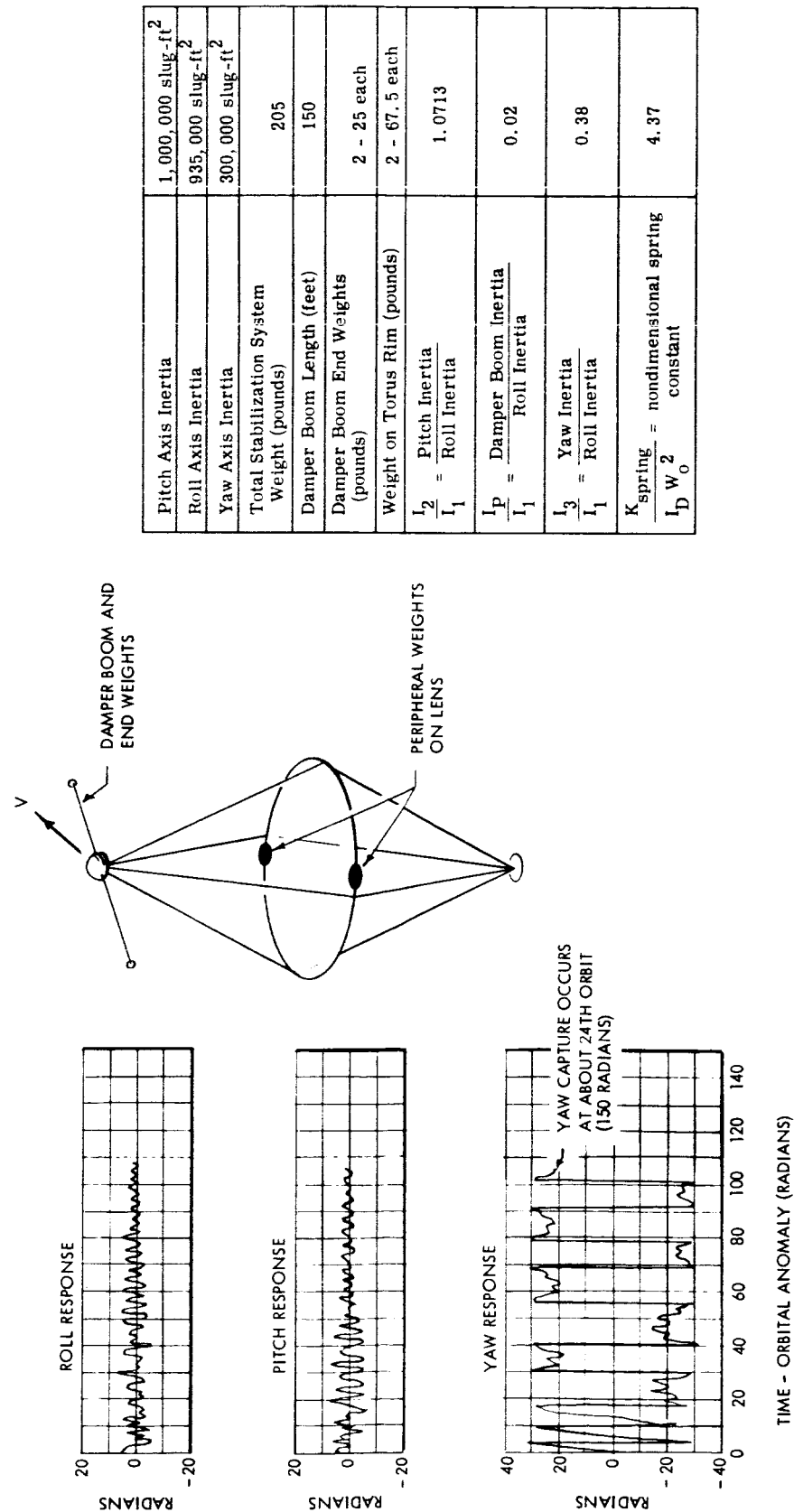


Figure 25. Lensat Transient Attitude Response Using Ames Damper - Lens Film Not Photolyzed

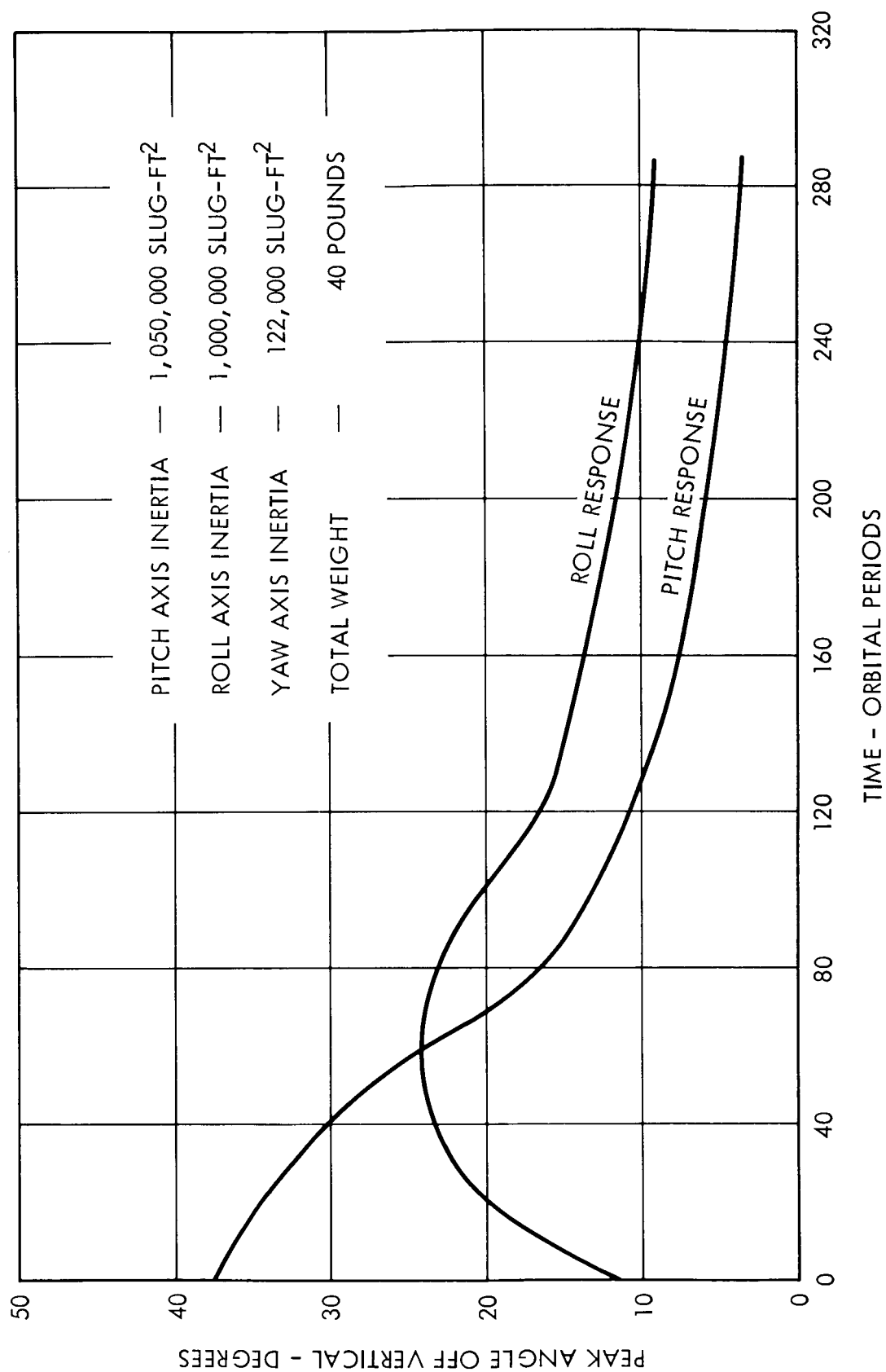


Figure 26. Envelopes of Lensat Transient Attitude Response Using Hypernik 50/50 Magnetic Material Damping

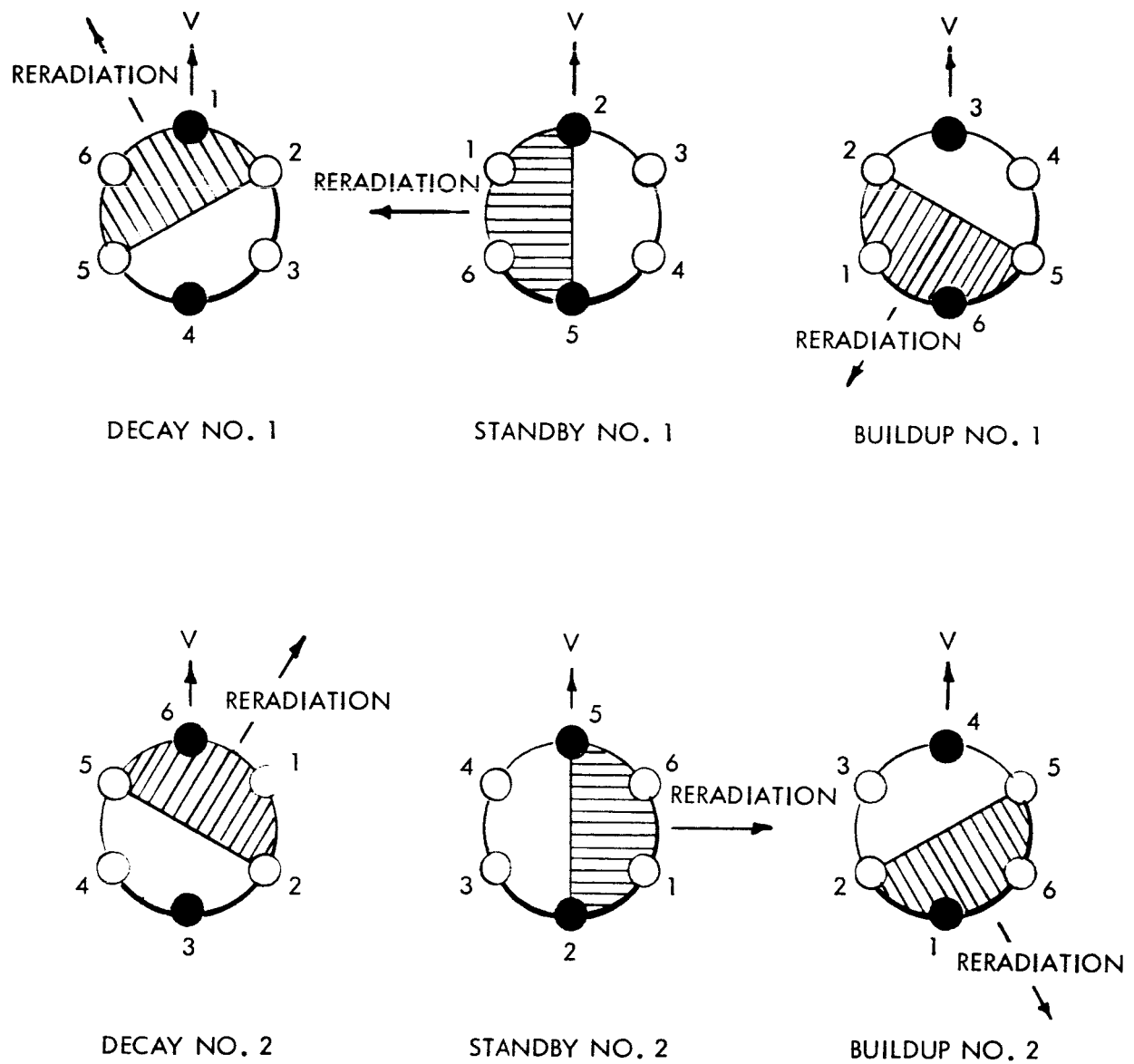


Figure 27. Three-Mode Reaction Wheel and Movable Weights

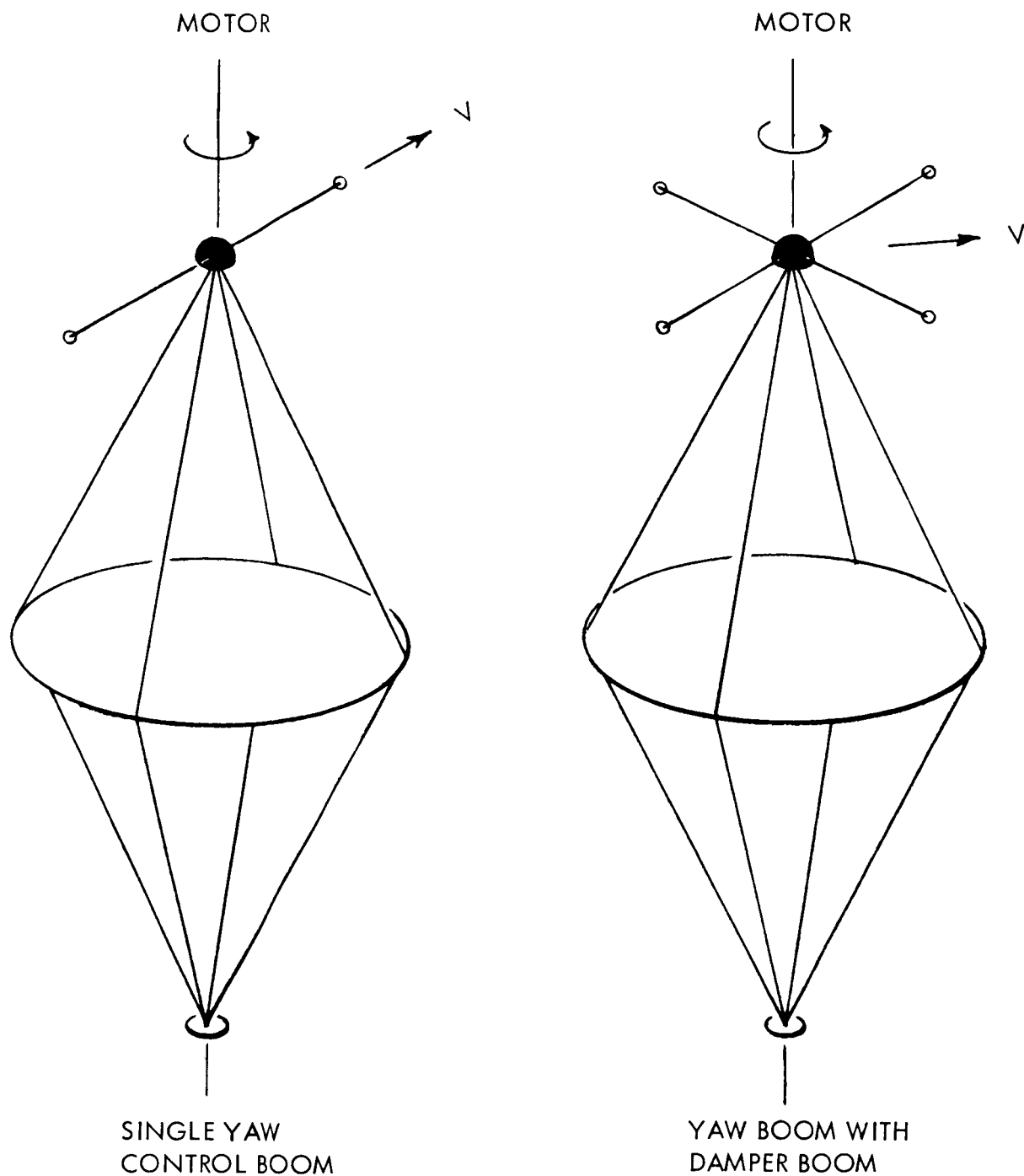


Figure 28. Continuous Yaw Control

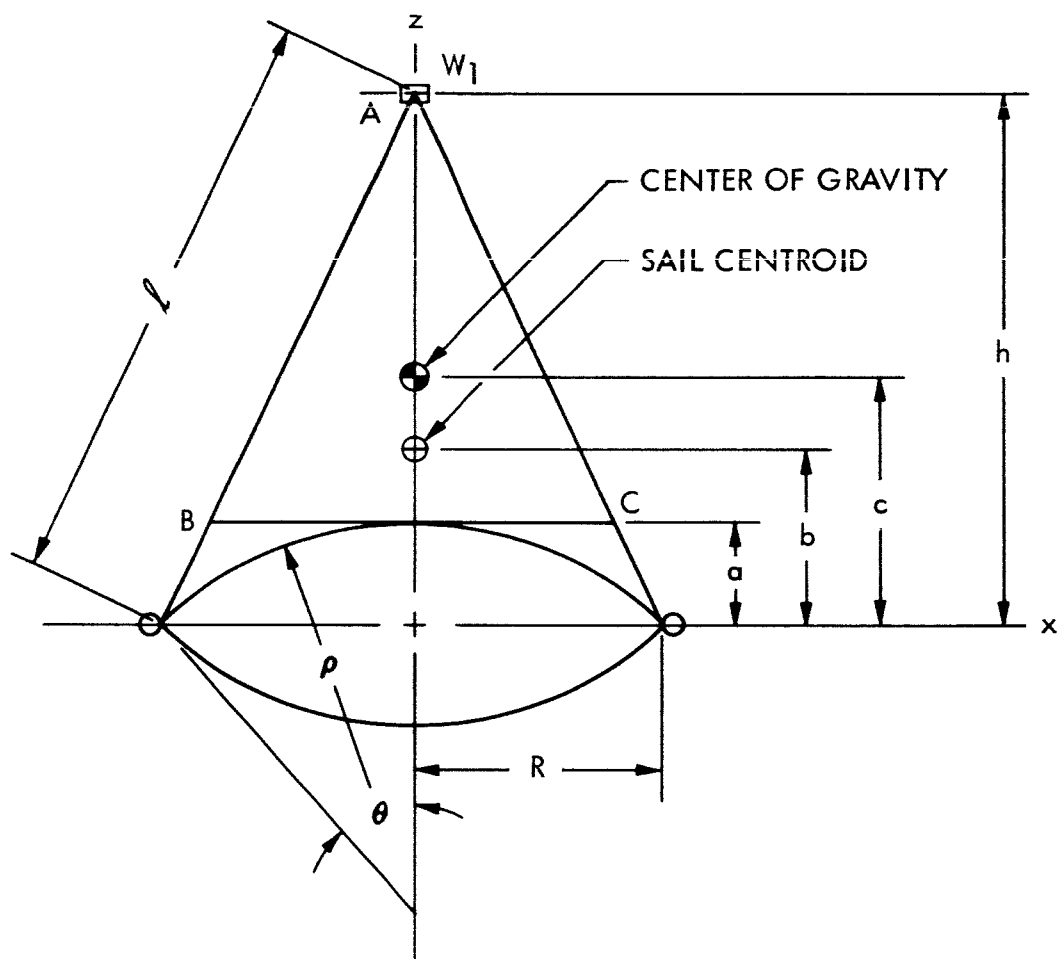


Figure 29. Geometry of Asymmetrical Configuration

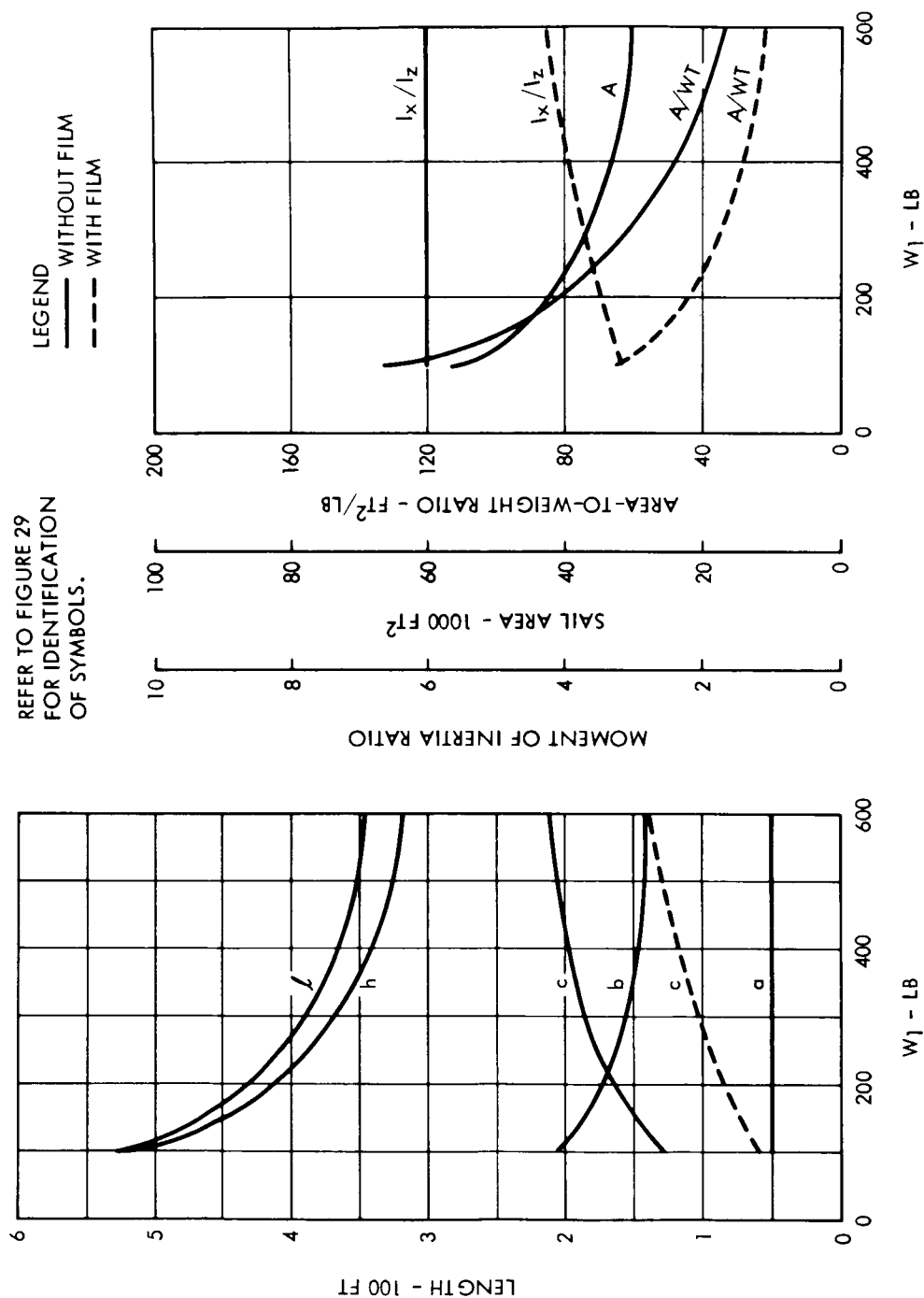
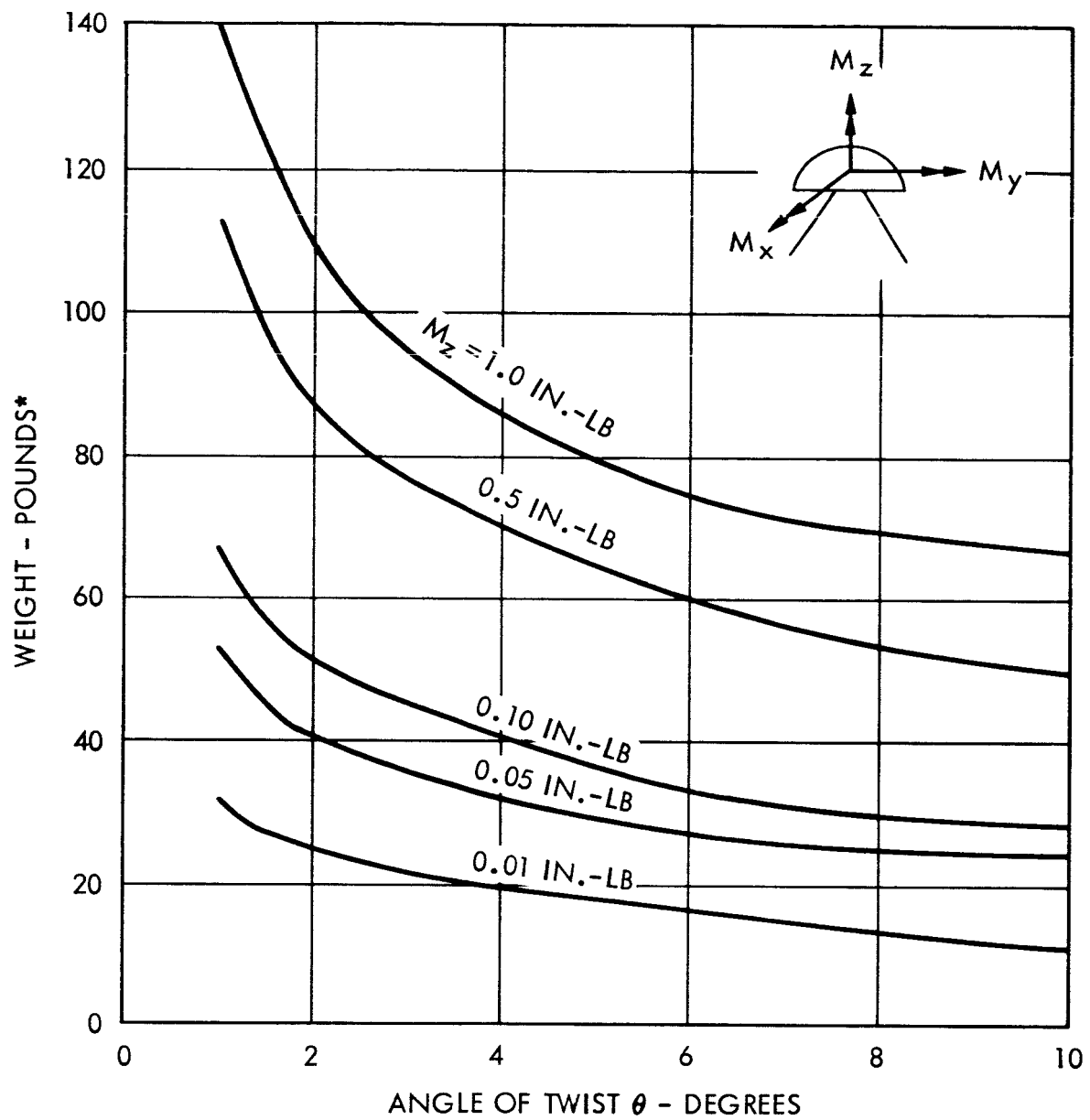


Figure 30. Design Parameters for Moment of Inertia Ratio of 6



* WEIGHT OF FOUR BOOMS, ALUMINUM WIRES,
AND 0.5-MIL PHOTOLYZABLE FILM

NOTE:
 $h = 410$ FT (SEE FIGURE 29)

Figure 31. Weight versus Angle of Twist of the Tetrapod

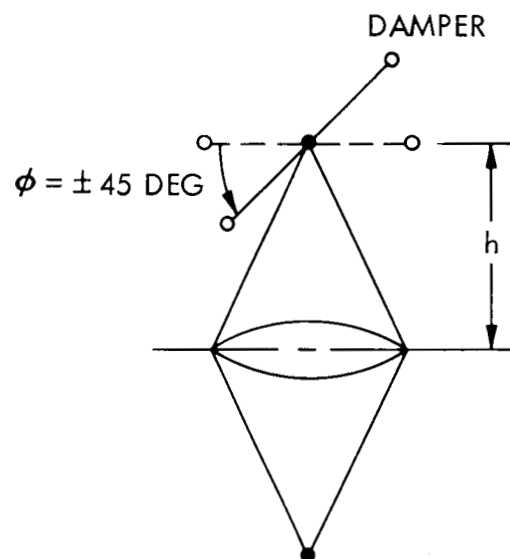
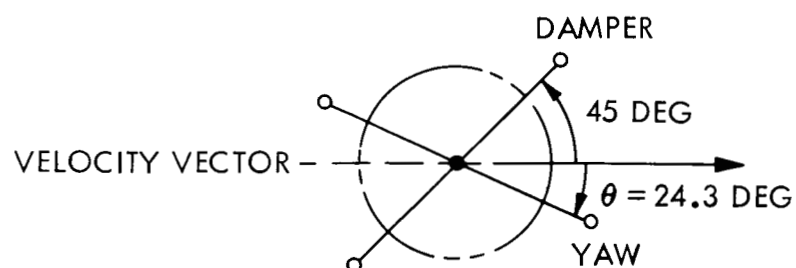


Figure 32. Geometry of Symmetrical Configuration Shown for Tumbling Calculations

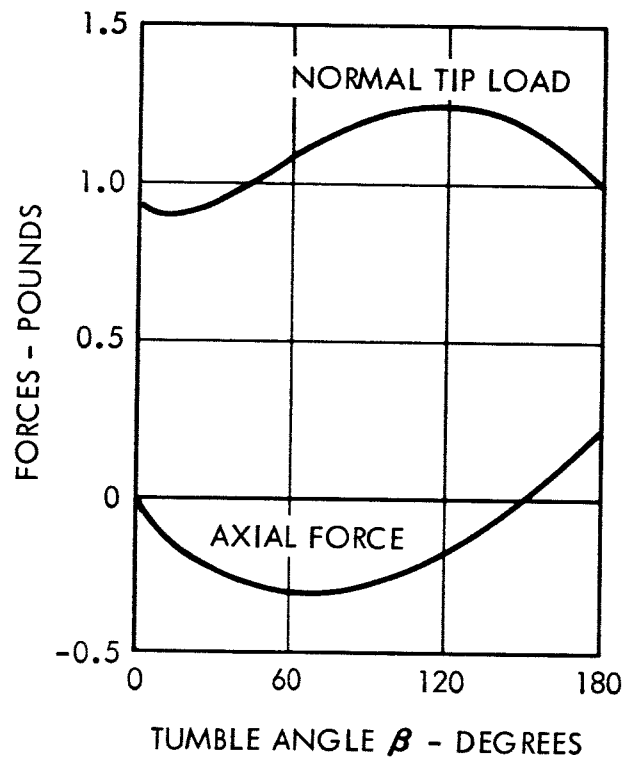


Figure 33. Tumbling - Loads on Yaw Boom
versus Tumble Angle

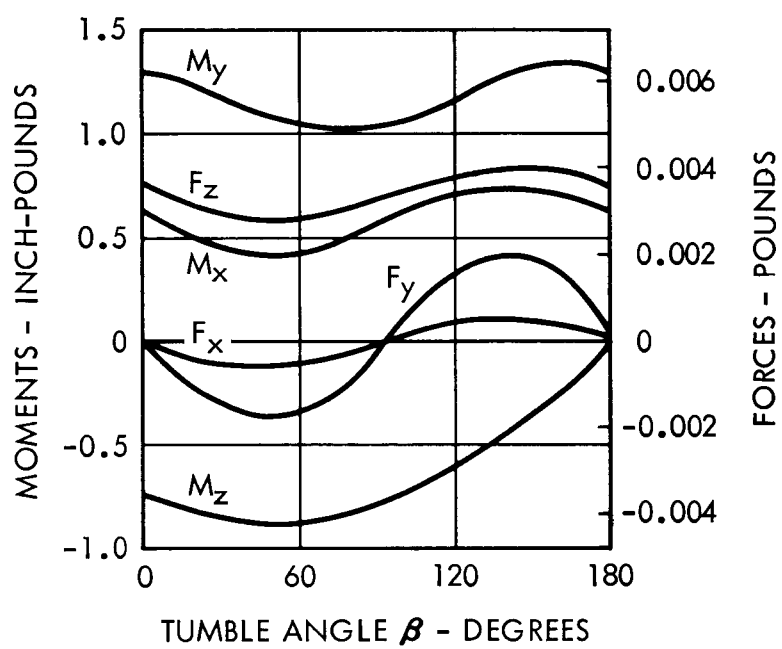


Figure 34. Tumbling Loads at Apex

| Stress (KSI) | Strain (in./in. $\times 10^3$) | Strain Energy (in.-lb/in. 3) | Recovery Energy (in.-lb/in. 3) |
|-----------------|------------------------------------|--|--|
| 3.0 | 0.3 | 0.45 | 0.45 |
| 3.5 | 0.4 | 0.775 | 0.613 |
| 4.0 | 0.55 | 1.340 | 0.800 |
| 4.5 | 0.60 | 2.400 | 1.013 |
| 5.0 | 1.25 | 4.540 | 1.250 |
| 5.5 | 2.4 | 10.58 | 1.513 |
| 6.0 | 4.60 | 23.23 | 1.800 |

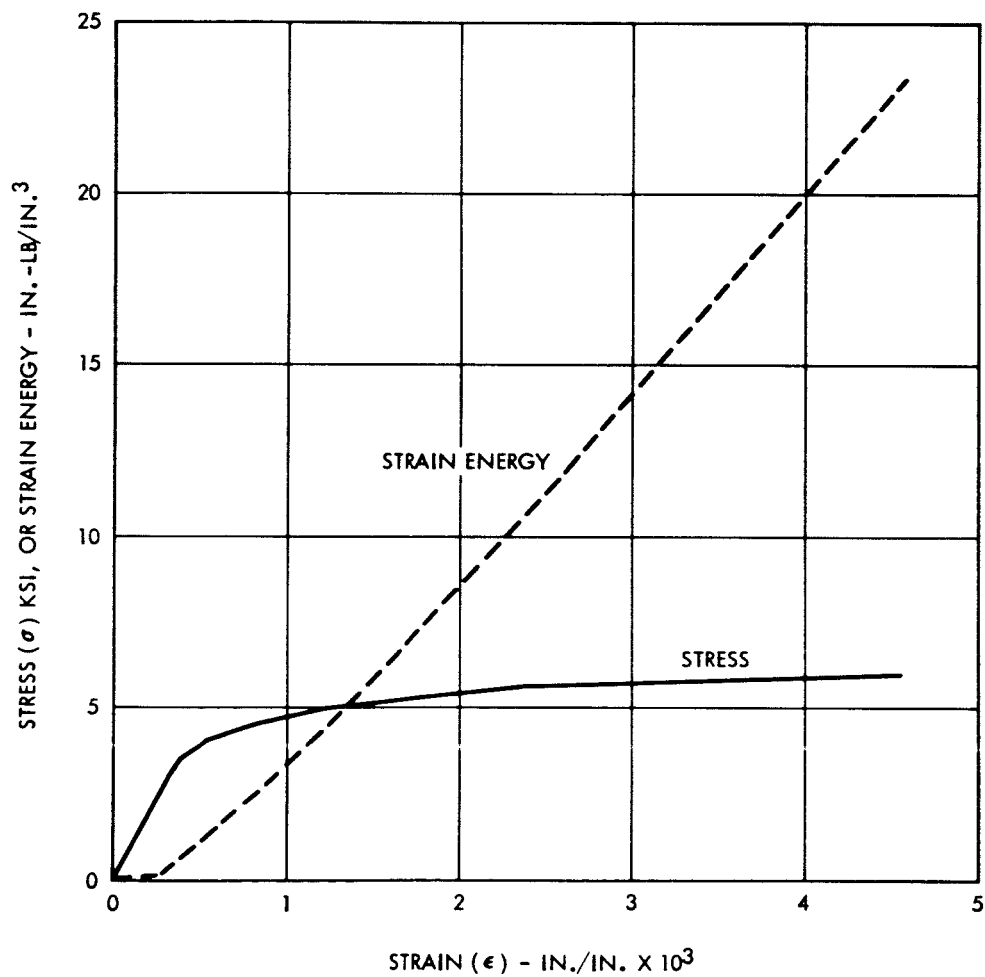


Figure 35. Stress and Strain Energy per Unit Volume versus Strain for 5.0 Mil Aluminum Wire

v_s = Separation velocity

v_R = Return velocity

w_s = Strain energy (total)

w_R = Recovery energy

$$\frac{v_R}{v_s} = \sqrt{\frac{w_R}{w_s}}$$

| σ | w_s | w_R | $\frac{w_R}{w_s}$ | $\sqrt{\frac{w_R}{w_s}}$ |
|----------|-------|-------|-------------------|--------------------------|
| 3,000 | 0.45 | 0.45 | 1.000 | 1.000 |
| 3,500 | 0.775 | 0.613 | 0.791 | 0.889 |
| 4,000 | 1.340 | 0.800 | 0.597 | 0.773 |
| 4,500 | 2.400 | 1.013 | 0.422 | 0.650 |
| 5,000 | 4.540 | 1.250 | 0.275 | 0.524 |
| 5,500 | 10.58 | 1.513 | 0.143 | 0.378 |
| 6,000 | 23.23 | 1.800 | 0.0775 | 0.278 |

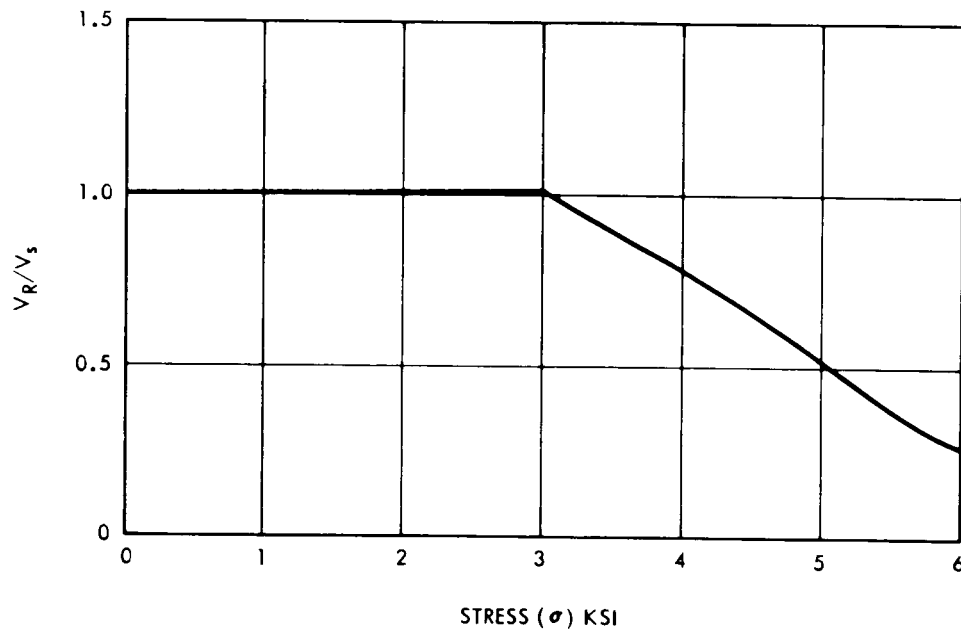


Figure 36. Separation-to-Return Velocity versus Stress Level in Axial Aluminum Wires of Tetrapod Booms of a Symmetric Satellite

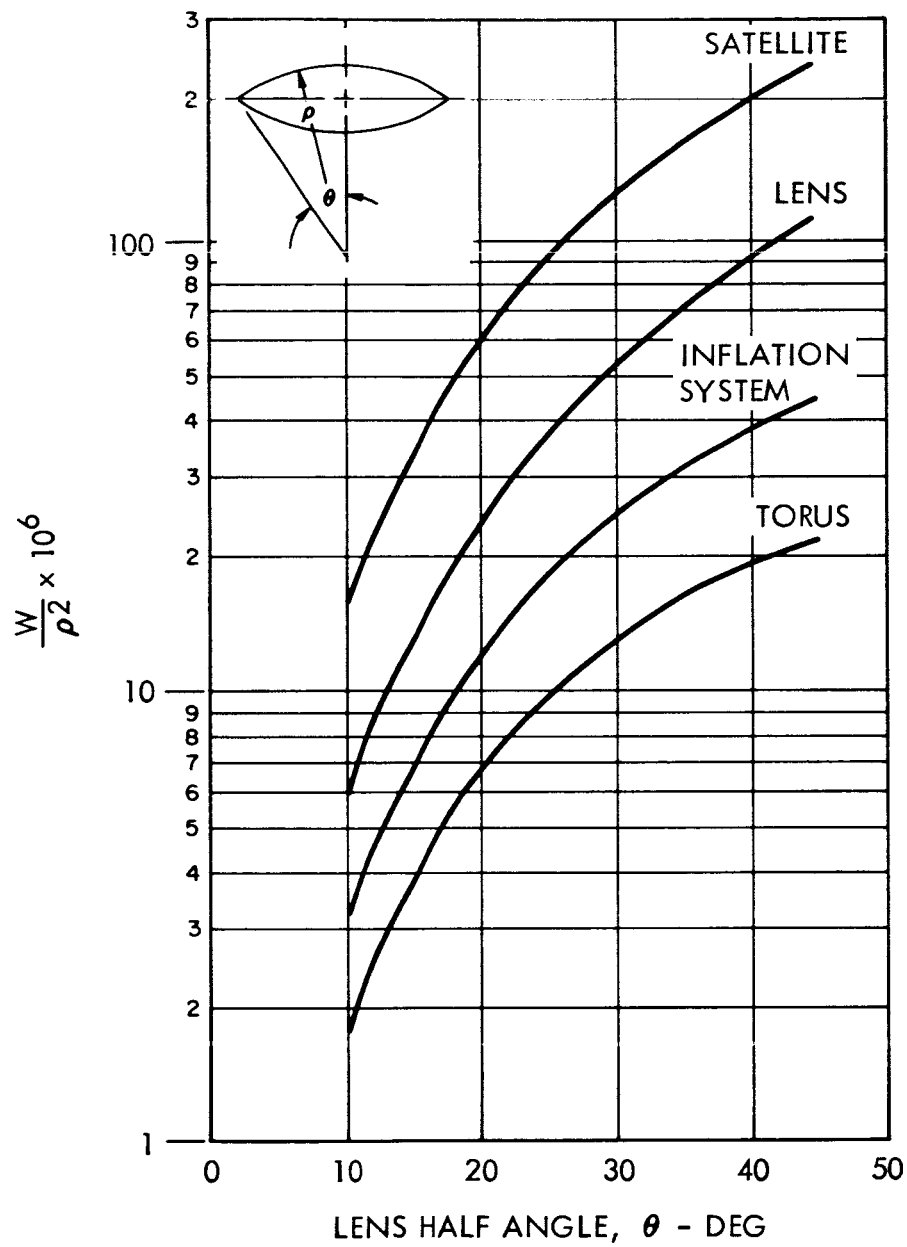


Figure 37. Weight Trade-Off

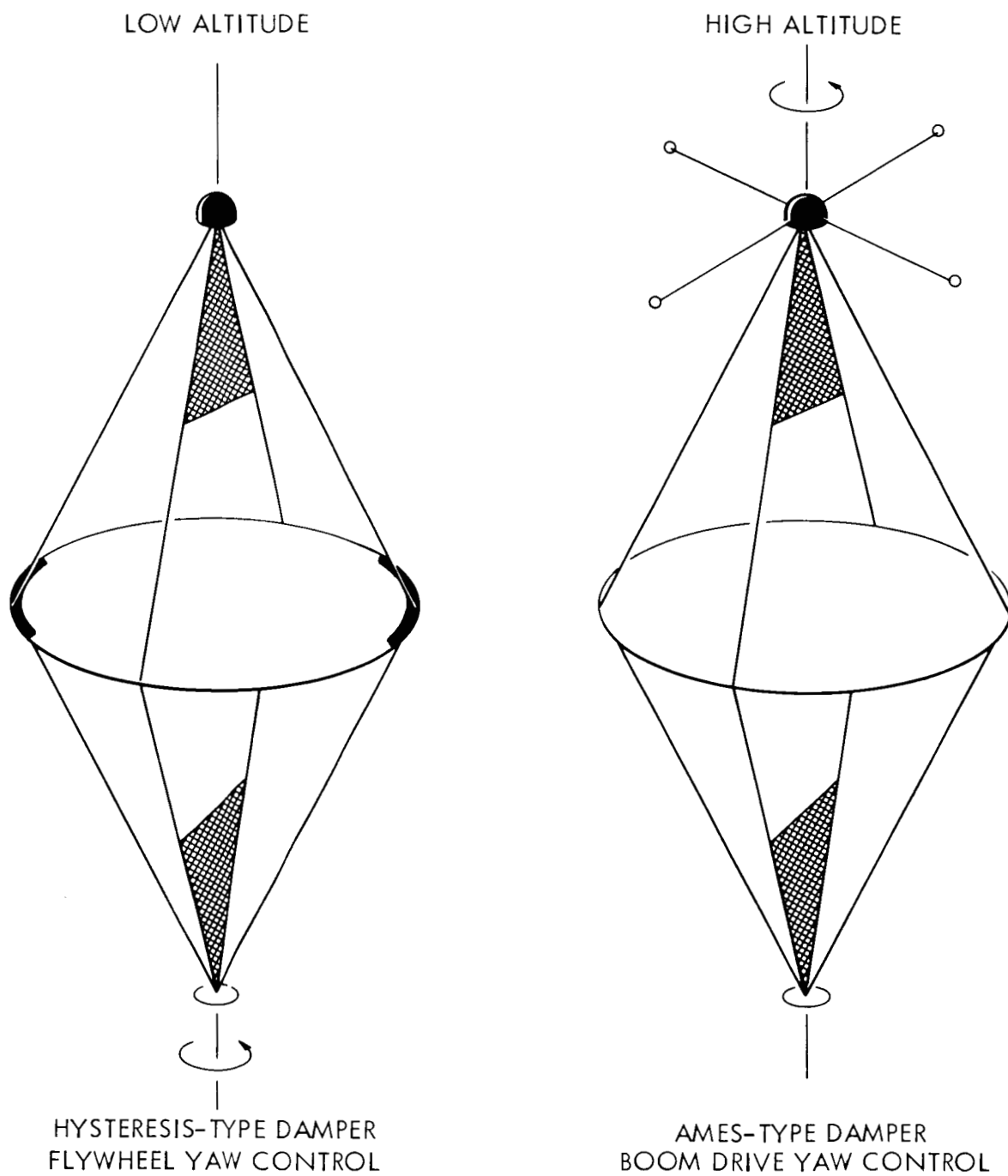


Figure 38. Recommended Configurations